DISSERTATION

GAIN-SATURATED REPETETIVE SOFT X-RAY LASERS WITH WAVELENGTHS SPANNING 9-30 NM AND LASING DOWN TO 7.4 NM

Submitted by

David Alan Alessi

Department of Electrical and Computer Engineering

In partial fulfillment of the requirements

For the Degree of Doctor of Philosophy

Colorado State University

Fort Collins, Colorado

Fall 2011

Doctoral Committee:

Advisor: Jorge J. Rocca

Siu Au Lee
Carmen S. Menoni
Mario C. Marconi

ABSTRACT

GAIN-SATURATED REPETETIVE SOFT X-RAY LASERS WITH WAVELENGTHS SPANNING 9-30 NM AND LASING DOWN TO 7.4 NM

This dissertation describes the development of table-top soft X-ray lasers with wavelengths ranging from 30 nm to 7.4 nm. The laser transisitons occur within collisionally excited states of nickel-like and neon-like ions which are created from laser ablation of solid targets. A Nd:glass slab laser system was developed to provide 20J (and then upgraded to 40J) of laser light at 527 nm for pumping a table-top chirped pulse amplification Ti:sapphire laser. With this increase in pump energy, the Ti:sapphire system is capable of producing 12J uncompressed laser pulses at a 1Hz repetition rate. Stretched and compressed pulses from this Ti:sapphire laser system operating near 800 nm are used to both ionize the material to a high degree and heat the free electrons in these plasmas to temperatures required for high gain. Simulations from a 1.5D hydrodynamic/atomic model indicate a peak gain of 90 cm^{-1} for the 8.8 nm laser transition in nickel-like lanthanum is reached with an electron temperature of ~850 eV and a density of 6×10^{20} cm^{-3}. By using the grazing incidence pumping geometry, gain saturated operation was demonstrated in the $2p^53p^1S_0\rightarrow2p^53s^1P_1$ transition of neon-like titanium (λ = 32.6 nm) and vanadium (λ = 30.4 nm), as well as in the $3d^94d^1S_0\rightarrow3d^94p^1P_1$ transition in nickel-like tellurium (λ = 10.9 nm) and lanthanum (λ = 8.8 nm). Strong

lasing was also demonstrated in the same neon-like transition in chromium ($\lambda = 28.6$ nm), as well as the same nickel-like transition in cerium ($\lambda = 8.5$ nm), praseodymium ($\lambda = 8.2$ nm), neodymium ($\lambda = 7.9$ nm) and samarium ($\lambda = 7.4$ nm). This is the first demonstration of the generation of bright gain-saturated sub-9-nm wavelengths with a table-top laser operating at 1-Hz repetition rate. The short wavelength, microjoule pulse energy, picosecond pulse duration and repetitive operation of these lasers will enable new applications such as sequential imaging of ultrafast nano-scale dynamic phenomena to be realized on a table top.

ACKNOWLEDGEMENTS

I would like to thank my adviser, Jorge J. Rocca for his guidance and motivation and my committee members, Siu Au Lee, Carmen Menoni and Mario Marconi for their support. I'd like to thank those whom I have worked with in the lab: Yong Wang, Brad Luther, Dale Martz, Miguel Larotonda, Francesco Pedaci, and Liang Yin. I would like to thank Mark Berrill for support for his hydrocodes and many useful discussions. I would like to acknowledge those who have helped me with these and other projects: Mike Grisham, Dinesh Patel, Brendan Reagan, Mark Woolston, Jorge Filevich, Fernando Brizuela, Sergio Carbajo, Dan Reinholz, Scott Heinbuch, Georgiy Vaschenko, Yanwei Liu, Eric Gullikson and Dennis Ross.

I would also like to acknowledge the support of my wife, Sarah Alessi, and each our families. I would like to thank my parents and grandparents for their support and encouragement throughout my entire education.

TABLE OF CONTENTS

CHAPTER 1

INTRODUCTION

1.1) Motivation

There has been great interest in the development of coherent soft x-ray (SXR) radiation for a vast array of applications since before the demonstration of the first SXR lasers in 1985 [1.1,1.2]. Recognition of the unique properties of coherent x-ray radiation has motivated the construction of numerous multi-user synchrotron facilities and a few free electron laser facilities worldwide [1.3]. However, the limited beamtime and high cost of these user facilities limit the use of coherent SXR light. The development of compact sources would make coherent soft x-ray light more widely accessible.

Figure 1.1 (from Attwood [1.3]) illustrates the extent of soft x-ray radiation in the electromagnetic spectrum. Herein both extreme ultraviolet (EUV) and soft x-ray (SXR) regions will be referred to as soft x-ray radiation. Early applications of coherent x-ray

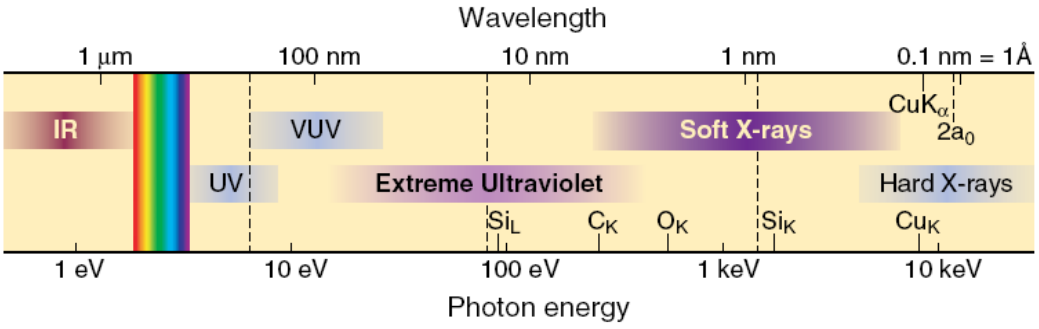

Figure 1.1: Illustration of various regions of the electromagnetic spectrum including: infrared (IR), visible, ultraviolet (UV), vacuum ultraviolet (VUV), extreme ultraviolet (EUV), soft X-rays (SXR), and hard X-rays. (From Attwood [1.3])

light were demonstrated using spatially filtered synchrotron light [1.4-1.7] as well as large, low repetition rate SXR laser facilities [1.3] and have motivated the development of smaller scale sources.

High harmonic generation (HHG) is an attractive method for generating coherent SXR light on a table-top due to the availability of femtosecond drive lasers. Sources with wavelengths as short as 13 nm have recently been made available commercially [1.8]. HHG is typically carried out by focusing a femtosecond duration Ti:Sapphire laser into a gas cell, gas jet, or waveguide. The tunnel ionization, acceleration, deceleration and recombination of electrons result in the generation of light at high order harmonic wavelengths. Recent advances in development of HHG have enabled table-top applications with wavelengths in the 13-30 nm range [1.9-1.13]. However the highest pulse energy reported to date below 10 nm is ~1 nJ (λ = 9.8 nm) [1.14].

Collisional SXR lasers, which are the subject of this dissertation, are capable of reaching higher pulse energies and higher average flux than HHG sources. For example, laser pulse energies up to 10 μJ have been generated in the 13 nm spectral regions by a table-top laser operating at 2.5Hz [1.15]. In addition, Chapter 5 describes a table-top collisionally pumped laser at 8.8 nm producing 2.7 μJ per pulse, an energy that is more than three orders of magnitude than reported using HHG at nearby wavelengths. Future advances in diode-pumped chirped pulse amplification (CPA) pump lasers [1.16-1.18] that have already reached 1 J energy output at 10-Hz repetition rate [1.16], promise to lead to the realization of high average power table-top lasers. There are various applications which require the high pulse energy or high average flux offered by SXR lasers. A few selected table-top applications are described below.

1.1.1) High Density Plasma Interferometry

Laser interferometry has been used for decades to obtain multi-dimensional electron density maps of a variety of plasmas [1.19, 1.20]. For this application, high brightness and a large pulse energy are needed to overcome bright plasma radiation. The density of the plasma being studied is limited by the wavelength of the laser used in the measurement due to refraction and absorption effects. The use of SXR lasers for plasma interferometry can allow for diagnostics of thicker, and higher density plasmas than visible and UV lasers. This makes SXR lasers an ideal source for the study of very high density plasmas, in particular those relevant to the fields of fusion and astrophysics. However this technique requires probing a plasma with a single, coherent, high-energy SXR light pulse with a duration shorter than the time scales of interest, making collisional SXR lasers a nearly ideal source.

High density plasma diagnostics using SXR laser interferometry was first demonstrated at Lawrence Livermore National Laboratory (LLNL) using the 15.5 nm Ne-like yttrium laser line pumped by the NOVA laser [1.21], and subsequently extended to experiments using the very compact capillary discharge laser [1.22-1.26] and the COMET laser [1.27, 1.28].

Figure 1.2a shows the experimental setup of the amplitude division interferometer used for studying dense plasmas with a compact SXR laser [1.22, 1.29]. In this interferometer the SXR laser impinges onto a diffraction grating where most of the

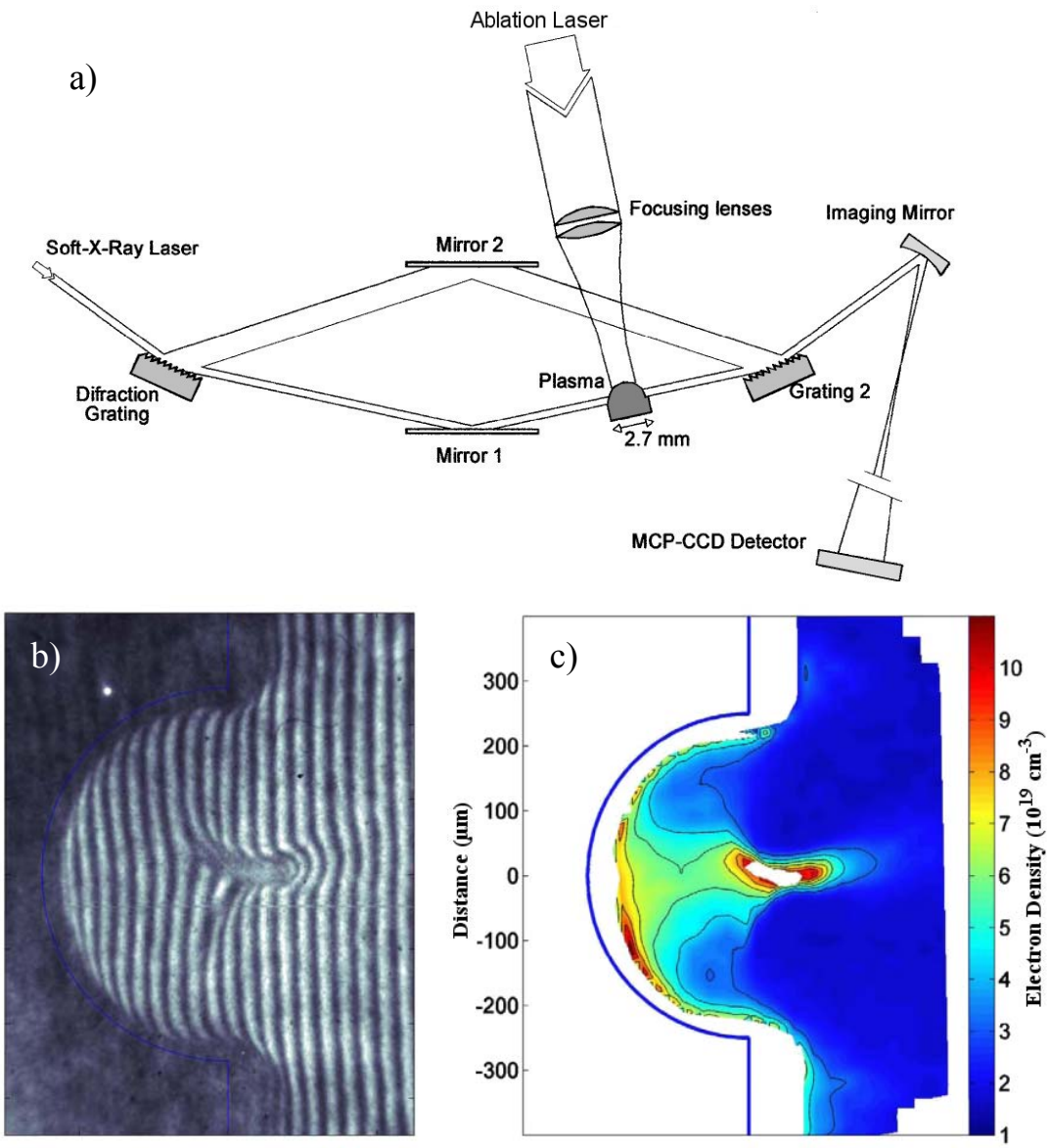

Figure 1.2: (a) Schematic diagram of the soft-x-ray amplitude-division grating interferometer and plasma diagnostics setup. The plasma to be studied is placed along one of the arms of the modified Mach-Zehnder interferometer. (from Filevich et al. [1.25]). (b) Soft x-ray laser interferrogram taken 2.6 ns after the peak of a 120 ps laser pulse incident from the right side. The large number of fringe shifts close to the axis of the groove is indicative of a high-density region created by the converging plasma (c) Measured electron density maps of the aluminum plasma corresponding to the interferograms of (b). (b and c from Purvis et al. [1.26])

energy is split equally between the first and zero diffraction orders. The plasma to be studied is placed in one arm of the interferometer before the beams are re-combined with a second grating. The interference pattern between the reference and probe beam is

imaged onto a MCP-CCD detector using near-normal incidence multilayer mirrors. Recent studies of index of refraction in highly ionized plasmas [1.28], colliding plasmas [1.24], and laboratory plasma jets [1.25, 1.26] have been done using table-top SXR lasers. Figure 1.2b shows a SXR laser interferrogram taken of a semi-cylindrical colliding plasma created by ablation of a 120 ps duration Ti:sapphire laser. The electron density map (figure 1.2c), determined from the displacement of the fringes, shows a high density region at the axis from a colliding plasma. Purvis et al. compared these results with 2D hydrodynamic simulations and showed that the combination of experimental data and simulations can be a powerful tool in studying dynamics of dense plasmas [1.24-1.26]. Development of high energy, shorter wavelength SXR lasers will allow for the study of longer length and higher density plasmas.

1.1.2) Nano-scale Imaging and Patterning

Applications in nanoscience and nanotechnology demand nanometer-scale spatial resolution imaging tools [1.30]. As the resolution of photon based imaging systems scales linearly with the source wavelength, reducing the wavelengths into the SXR region can enable imaging with nanoscale resolution. Several coherent and incoherent short wavelength sources have enabled imaging experiments [1.30-1.40]. Imaging with Fresnel zone plates and synchrotron radiation as shown in Figure 1.3 has achieved a record resolution of 15nm [1.41]. In this setup synchrotron radiation is spectrally filtered and focused onto the sample with a condenser zone plate, where a pinhole is used to spatially filter the source. An objective zone plate images the transmitted light from the sample onto a SXR sensitive CCD. In spite of the short wavelengths available with the

synchrotron source, the resolution of this system is limited in this case by the width of the outer-most zone of the objective zone plate. Recent progress has been made towards sub-10 nm imaging with the development of a new nanofabrication process for producing zone plates with smaller outer zone widths [1.42].

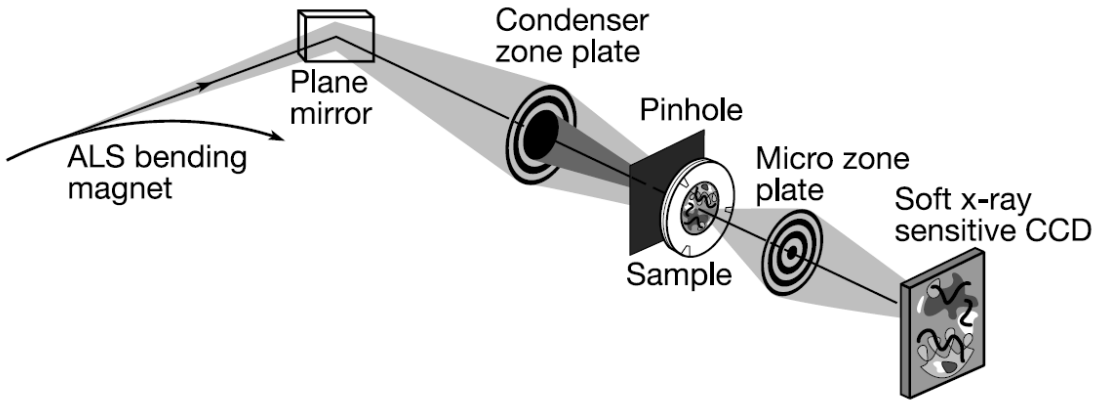

Figure 1.3: Soft X-Ray microscope (XM1) at the Advanced Light Source in Berkeley. (from Chao et al. [1.41])

The recent development of plasma-based table-top SXR laser sources [1.15,1.43,1.44] can make nano-scale microscopy more widely available. These sources also have the potential to capture events that occur on a picosecond time scale in a single-shot, which is not possible with incoherent sources. Record resolution (<38 nm) with a table-top source was obtained in 2006 with a 13.2 nm table-top SXR laser [1.30], a wavelength of interest for extreme ultraviolet lithography (EUVL). This experiment used the same setup as shown in Figure 1.3 where the source was a table-top SXR laser and the pinhole removed. The advantage of SXR lasers is the ability to take single shot images with zone plate optics. Recently single shot imaging of nanostructures with wavelength resolution [1.40] and imaging of nanoscale dynamics [1.45] were both demonstrated with a compact capillary discharge laser operating at 46.9 nm.

Microscopy with resolution of tens of nanometers will greatly benefit semiconductor manufacturing. Global semiconductor device sales exceeded $300 billion in the year 2010. The International Technology Roadmap for Semiconductors (ITRS) is aiming for introducing EUVL for the production of integrated circuits at the 22 nm node by 2013-2015 [1.46] and EUV/SXR sources are a critical component for enabling EUVL. The EUVL process uses an incoherent light source at the 13.5 nm reflection peak of Mo/Si multilayer mirrors to project light from a mask on to a photoresist. Testing of prototype EUVL mirrors has been done with at-wavelength interferometry using coherent 13.5 nm synchrotron radiation at the Advanced Light Source (ALS) Microfield Exposure Tool (MET) [1.47, 1.48]. Sub 15 nm resolution imaging of lithography masks was demonstrated at the Advanced Light Source (ALS) facility in Berkeley with synchrotron radiation and zone plate optics [1.41]. The current state of the art in zone plate manufacturing can produce outer most zone width of ~10 nm. While synchrotron radiation has been used to EUV image masks, the development of compact SXR light sources near 13.5 nm such as collisional SXR lasers will be necessary for in-situ inspection of these masks.

A recent increase in table-top SXR laser energy near 13 nm was demonstrated at CSU as part of work done related to this dissertation. A 13.2 nm SXR laser with several microwatts average power was demonstrated by laser ablation of a solid cadmium target with a high energy, 2.5 Hz repetition rate Ti:Sapphire laser. The Nd:glass slab laser system in section 2.2 provided the energy to pump the final amplification stage of this laser system. The high average power SXR laser was used in table-top actinic metrology of an EUVL mask using reflection mode setup of Figure 1.4a [1.49]. The SXR laser beam

is directed through a condenser zone plate to focus the light onto the EUVL mask. The reflected light is imaged onto a SXR sensitive CCD with the objective zone plate. Figure 1.4b shows the SXR image of a 180 nm half pitch absorption elbow in a bright field, showing the source intensity profile on the sample. The uniformity of the source was of high enough quality to allow for line edge roughness measurements of 175 nm half pitch gratings.

There have also been recent advances in imaging without zone plate optics (lensless imaging). This technique requires a coherent source as well as phase reconstruction algorithms. Recently lensless coherent imaging using a 29 nm HHG source generated with a table-top laser was demonstrated [1.50], and techniques have been developed to increase resolution capability [1.51] and determine 3D structure from a single view [1.52]. Single shot diffractive imaging was demonstrated using a HHG source at 32 nm and produced reconstructed images with a resolution of 119 nm [1.53]. Imaging with wavelengths below 13 nm in a single shot using HHG will require a significant increase in the pulse energy currently available. The high energy per pulse available from table-top collisional plasmas has enabled single-shot nano-scale holography at 13.9 nm [1.55], and has the potential to be demonstrated with shorter wavelengths.

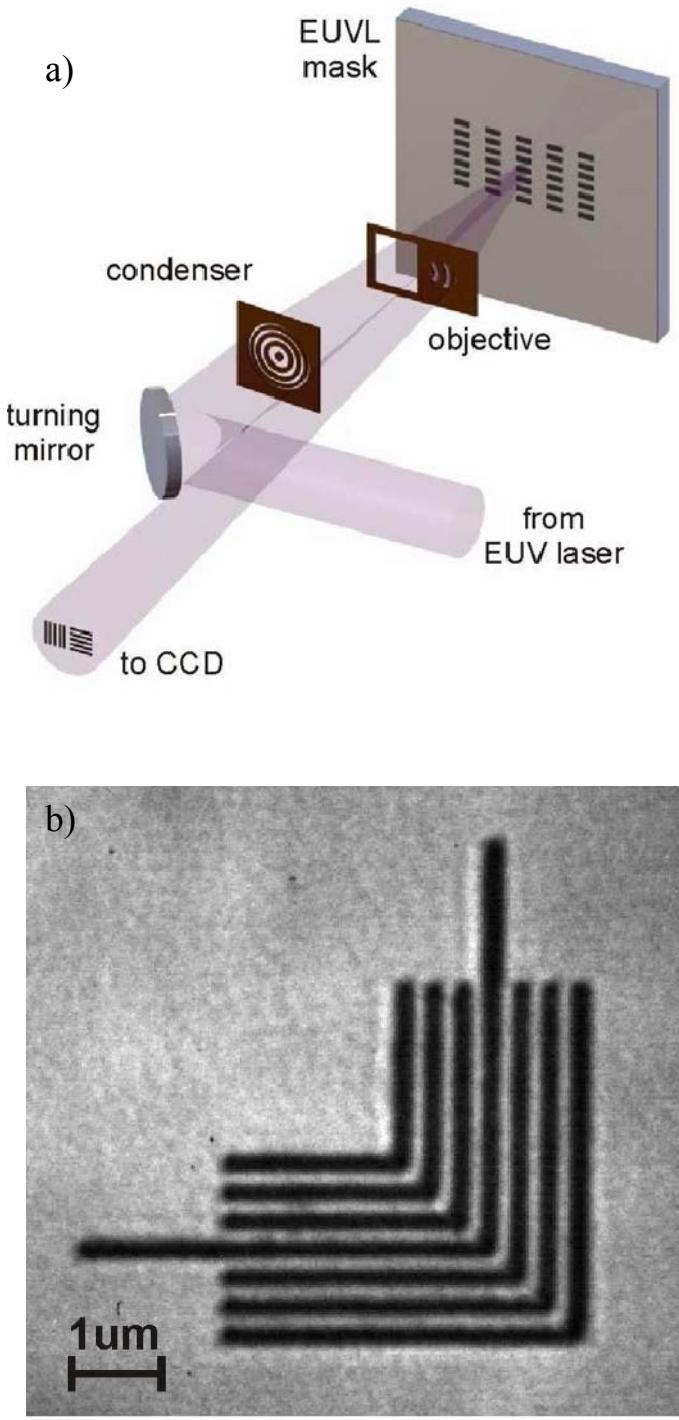

Figure 1.4: (a) Diagram of the microscope setup. The light from the laser is guided by a Mo/Si turning mirror onto a condenser zone plate which focuses the light onto the EUVL mask. The light reflected off the mask is collected by an off-axis zone plate which projects a magnified image onto an SXR-sensitive CCD. (b) SXR image of a 180 nm half-pitch absorption elbow pattern in a bright field obtained with an exposure of 90 seconds (From Brizuela et al. [1.49])

High average power coherent SXR light can also be used for generating periodic nano-structures. Inteferrometric techniques utilize the coherence of the source light to generate nano-scale intensity patterns onto photosensitive chemical resists [1.7, 1.56-1.59]. Figure 1.5a shows a SXR laser directed onto a Lloyd's mirror interferometer creating a sinusoidal illumination pattern in the sample plane. The period of the intensity pattern (d) is determined by the wavelength of the light source (λ) and the angle with respect to the Lloyd's mirror (θ) by the equation $d = \lambda/(2*\sin\theta)$. Nanoscale structures can be made by exposing a sample coated with a photosensitive resist such as poly-methyl methacrylate (PMMA) and chemically developing the exposed sample. Light from a synchrotron source has been used to print 38 nm period gratings onto PMMA [1.7]. More recently a technique to use second diffraction orders has been used to print 17.5 nm half-period gratings [1.56] and has the potential to scale to smaller half-periods.

While the process of using photolithography for high volume manufacturing of integrated circuits uses hundreds of watts of incoherent light, the development of coherent high average flux compact SXR sources can be used as a tool to for fabrication of low-cost custom manufactured nano-patterns. Recent progress has been made in coherent nano-patterning using compact SXR laser sources. Using a compact capillary discharge laser at 46.9 nm, gratings with a period of 55 nm were printed on PMMA[1.57]. Nano-pillers (Figure 1.5b) with 60 nm FWHM size and nano-holes were made with a Lloyd's mirror interferometer and making a second exposure with the sample rotated 90º [1.58]. Printing of periodic structures of arbitrary shape has been demonstrated with the 46.9 nm capillary discharge laser using the Talbot effect [1.59]. The feature size of these nanostructures is inherently limited by the source wavelength, so

the development of coherent shorter wavelength high average flux table-top SXR laser sources is of interest for printing smaller nanostructures.

a)

b)

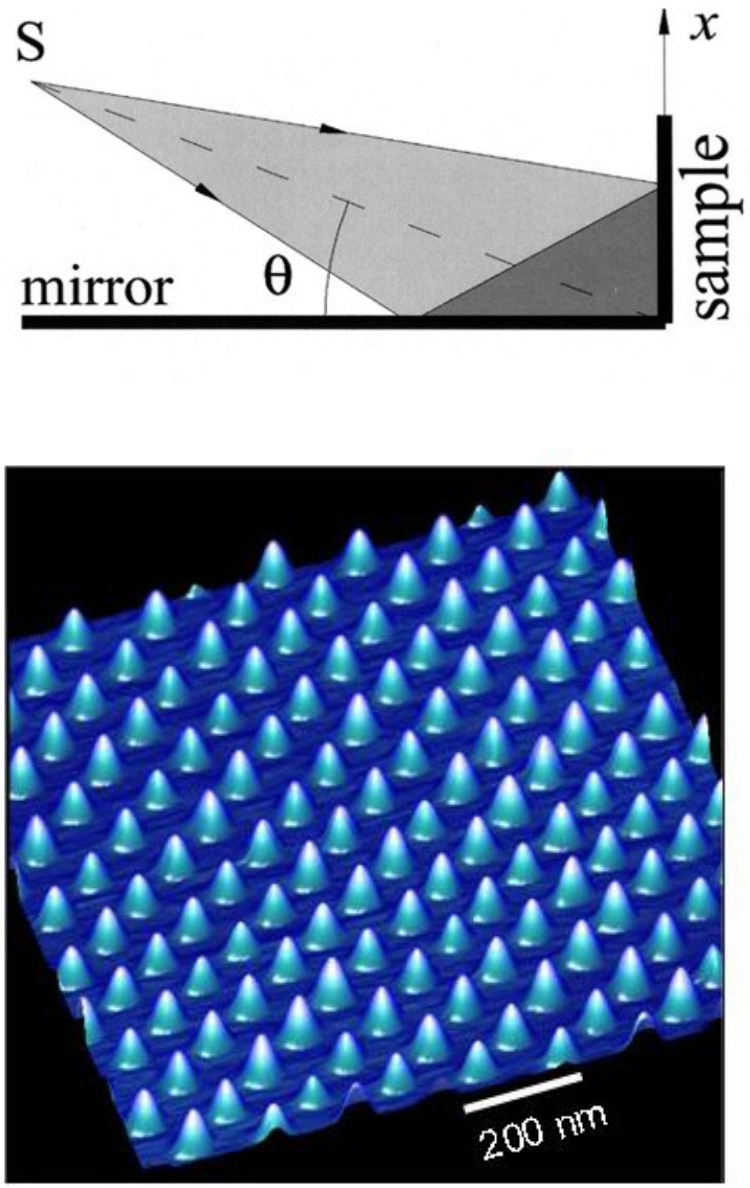

Figure 1.5: (a) Lloyd's mirror setup for printing lines, from Capeluto et al. [1.57]. (b) arrays of cone-shaped nano-dots patterned in PMMA by double exposure with a Lloyd's mirror configuration, from Wachulak et al. [1.58]

1.2) Previous Work in Collisional SXR Lasers

Collisional lasers are laser based on the generation of population inversion in atoms or ions excited by electron impact collisions. The argon ion laser [1.60, 1.61] is a common example, where a λ = 514 nm and a λ = 488 nm laser transition occurs in the Ar^{+} state and requires a plasma with electron temperature of ~5eV and a density of ~10^{14} cm^{-3} for significant gain. This plasma is created typically with an electrical discharge through an argon filled tube. The discharge tube is placed between two mirrors that form a stable optical resonator cavity. It was proposed in the 1980's that SXR wavelengths could be reached in dense, highly ionized Ne-like ions excited by collisions [1.62-1.68].

The first demonstration of a collisionally excited SXR laser was done in a large aspect ratio selenium plasma ionized to the neon-like state with a kilojoule laser in 1984 [1.1]. A single laser pulse was used to both generate a plasma with a significant fraction of Se ions in the Ne-like state (Se^{+24}) and heats the free electrons to temperatures suitable for exciting ions to the laser upper level through collisions. The λ = 21 nm laser transitions occurs between the 3p and 3s states where the laser upper level is populated by monopole excitation from the Ne-like ground state as well as from collisional de-excitation from higher excited states. The laser lower level is depopulated by fast radiative decay to the ground state.

In the first experiment, the plasma conditions (T_e ~ 1.0 keV, N_e ~ 1x10^{21} cm^{-3} [1.1]) allows for a population inversion to occur as a result of efficient pumping of electrons to the laser upper level and fast depletion of the laser lower level through rapid

radiative decay. The laser upper level population is not rapidly depleted due to the dipole forbidden nature of the $(2p^5_{1/2}\ 3p_{3/2})_2 \rightarrow (2s^2_0\ 2p^6_0)_0$ transition.

After the Ne-like Se SXR laser experiment, SXR lasing in Ni-like Eu (λ = 6.58nm, λ = 7.1nm), Yb (λ = 5.03, λ = 5.61) Ta (λ = 4.48) and W (λ = 4.32) plasmas was demonstrated [1.69, 1.70]. These experiments were also done with ~1ns duration pulses with kilojoule energy using the NOVA laser resulting in gains of 1-3 cm^{-1}. Figure 1.6 shows the energy level diagram for Ne-like Eu showing laser transitions at 6.58nm, 7.1nm, 10nm and 10.5nm. Collision rates to the laser upper levels are shown for plasma with a density of $2x10^{20}$ cm^{-3} and an electron temperature of 600eV. The upper levels have a potential energy of ~1.2keV (shown in parenthesis) above the ground state and the spontaneous emission rates are also shown in parenthesis.

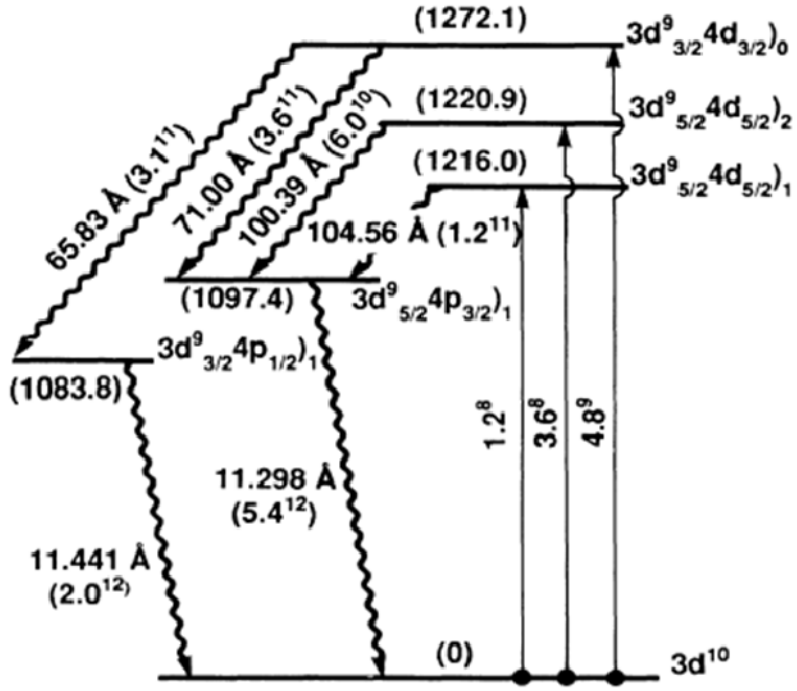

Figure 1.6: Simplified level diagram for Eu^{+35} showing the transitions of interest. The collision rates are given for ne = $2x10^{20}$ cm^{-3} and Te = 600 eV. Level energies and spontaneous emission rates are in parenthesis. (Figure from Macgowan et al. [1.69])

Investigation into SXR lasers in Ni-like ions followed from the recognition that using this sequence, shorter laser wavelengths could be accessed using plasmas with lower degree of ionization than the Ne-like sequence. Figure 1.7 shows the wavelengths of the $3p^1S_0 \rightarrow 3s^1P_1$ transition in Ne-like ions and the $4d^1S_0 \rightarrow 4p^1P_1$ transition in selected Ni-like ions. For example the Ne-like laser transition in Ru results in a laser transition at 13.3 nm requiring a large percentage of the ions to be in the +34 state. However, reaching the wavelength of ~13.2 nm using the Ni-like series only requires ionizing cadmium only 20 times due to the larger quantum efficiency of this transition. This reduction in the required degree of ionization corresponds to a significant reduction in pump energy.

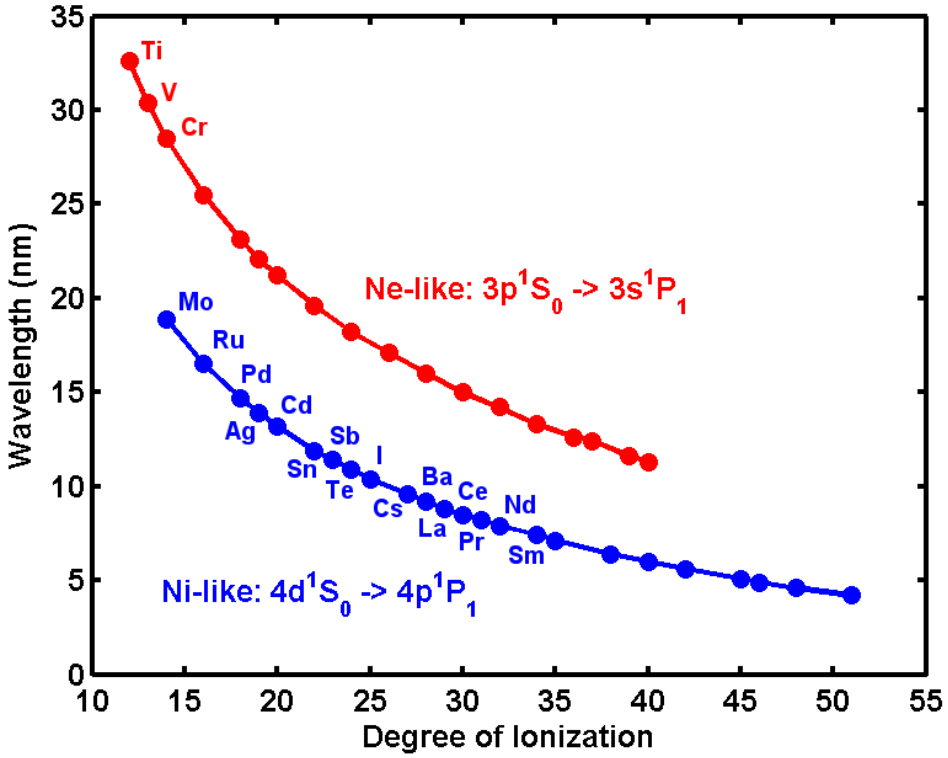

Figure 1.7: Soft X-ray laser wavelengths vs ion charge for the $3p^1S_0 \rightarrow 3s^1P_1$ transitions in Ne-like ions (red) and the $4d^1S_0 \rightarrow 4p^1P_1$ transition in Ni-like ions (blue). Materials in which SXR lasers have been demonstrated at CSU are labeled.

Lasing in Ni-like Ag, Te, La, Ce, Pr, Nd, Nd, Sm, Gd, Tb, and Dy ions was demonstrated using a multiple pulse pump scheme resulting in both a reduction of laser

pump energy and an increase in the gain-length product to ~8 [1.71, 1.72]. The initial pulses heat the plasma and allow for expansion and reduction of the density gradients in the region of optimal gain. This reduced density gradient results in less refraction of the amplified beam out of the gain region. Irregularities in the gain region can be smeared out by the plasma expansion [1.72]. Both of these effects can lead to higher gain-length product.

Gain-saturated lasing at wavelengths below 10 nm was achieved at 7.36 nm in a Ni-like Sm plasma and at 5.9 nm in a Ni-like Dy plasma using 150J of pump laser energy with a 75 ps duration from the VULCAN Nd:glass laser system in a two-target configuration [1.73, 1.74]. The SXR laser efficiency was increased by introducing a low intensity pre-pulse that was allowed to cool and expand on a timescale > 2 ns. The delay between the pre-pulse and main pulse results in lower density gradients in the gain region reducing refraction of the SXR laser. The reduced refraction allows for longer amplification lengths up to saturation.

These early demonstrations of SXR lasers were in the quasi-steady state regime as a result of the long (0.075-1 ns) pulse duration of the pump pulse as compared to the upper level lifetime (1-5 ps). Consequently, lasing occurs as long as optimal plasma conditions exist. Afanasiev and Shlyaptsev [1.75] recognized that gain coefficients are 1-2 orders of magnitude larger than those obtained for the same transition in the quasi-steady state regime can be produced for a short period of time by heating the plasma at a rate faster than the relaxation rate of the excited states [1.76]. Using this transient collisional scheme, gain-length products of 16.7 in Ne-like Te (λ = 32.6 nm) [1.77] and 18 in Ni-like Pd (λ = 14.7nm) [1.78] were demonstrated using chirped-pulse

amplification lasers capable of producing pump pulse durations of 0.5-8 ps and energies of 5-7J at a repetition rate of 1 shot every several minutes. However, widespread use of coherent x-ray light in numerous areas of science and technology remained relatively unexploited and requires the development of smaller scale sources capable of operating at higher repetition rates.

Motivated by the demonstrated and potential applications of SXR lasers significant effort has been placed in the development of compact high repetition rate SXR lasers [1.79-1.84]. Fast discharge excitation of capillary plasmas has produced extremely compact saturated SXR lasers emitting at 46.9 nm in Ne-like Ar at repetition rates of up to 10Hz [1.79]. Lasing was also achieved in Ne-like Cl at 53 nm [1.80]. Laser-driven optical field ionization lasers have produced saturated operation at 41.8 nm and 32.8 nm in Pd-like Xe and in Ni-like Kr, respectively [1.81, 1.82]. A remaining challenge is the demonstration of saturated high repetition rate table-top lasers at a variety of wavelengths with sufficient average power for applications. Different pumping configurations have recently been investigated to reduce the necessary pumping energy and enable operation at multi-hertz repetition rate. Transverse excitation of a Mo target with 150 fs, 300 mJ pulses impinging at 60° from normal incidence resulted in the appearance of the 18.9 and 22.6 nm laser lines of Ni-like Mo [1.85] however, gain saturated operation was not achieved. Longitudinal pumping at 10 Hz repetition rate produced non-saturated amplification at 18.9 nm in Ni-like Mo [1.86]. As described next, heating of plasmas with a picoseconds pulse, impinging at grazing incidence resulted in the demonstration of lasing [1.87] and the achievement of gain saturation using significantly reduced pump energy [1.43, 1.88, 1.89].

1.3) Efficient Pumping Using Grazing Incidence Geometry

The efficiency of transient laser pumped SXR lasers can be further improved by directing the pump pulse at a grazing incidence angle with respect to the target [1.87-1.89]. This pumping geometry takes advantage of the refraction of the pump beam in the electron density gradient of the precreated plasma to efficiently deposit energy into a plasma density region with optimum conditions for amplification. The process for creating the SXR lasers in the experiments using the grazing incidence pumping (GRIP) geometry consists in forming a plasma by typically directing a pulse at normal incidence onto a metal target (Figure 1.8a). The plasma undergoes expansion (Figure 1.8b) and subsequently is heated by a picosecond pulse directed at grazing incidence (Figure 1.8c). This rapidly heats the plasma to higher temperatures, resulting in significant gain and ASE laser output. The GRIP geometry results in saturated lasing at significantly reduced energies with respect to the normal incidence excitation scheme. It also overcomes the limitation in the maximum plasma length available for amplification that is associated with longitudinal pumping.

In the case of SXR laser plasmas heated by transverse normal incidence pumping, the majority of the energy of the heating pulse is absorbed near the critical density, which generates gain in a plasma region with strong refraction from a high density gradient as discussed below. This strong refraction ejects the amplified rays out of the gain medium [1.90]. Due to this refraction, effective amplification occurs at significantly lower densities, where the reduced density gradients allow for longer propagation lengths. However, in the normal incidence pumping geometry the low density plasma region is

inefficiently heated because its relatively low electron density only absorbs a small fraction of the pump radiation.

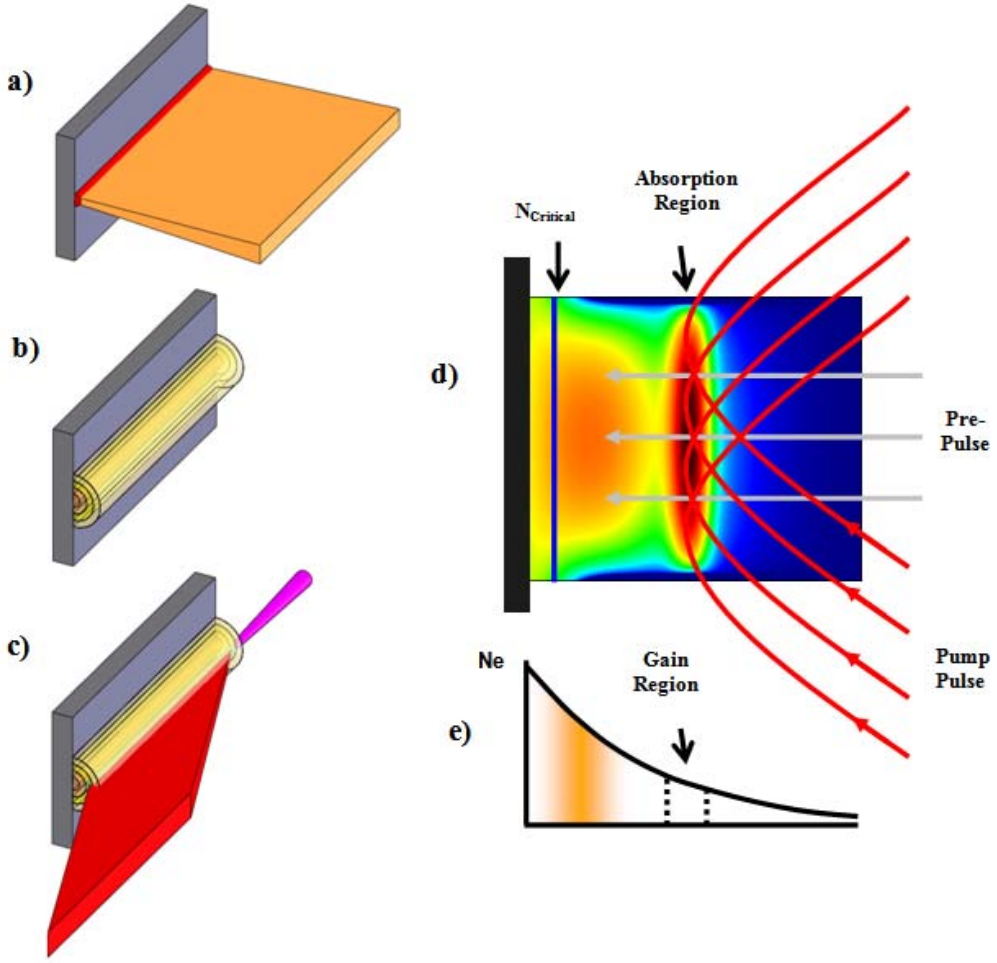

Figure 1.8: Illustration of grazing incidence pumping geometry with (a) normal incidence pre-pulse heating a solid target, (b) plasma expansion and (c) grazing incidence pump pulse with SXR laser output. Also shown with illustration of (d) refraction of pump beam into the gain region with (e) relaxed electron density gradient.

Typically only less than 10% of the laser pump energy is deposited in the amplification region and as a result a large amount of laser pump energy is required to heat the plasma to the high temperatures necessary for lasing. In contrast, the grazing incidence configuration takes advantage of the refraction of the pump beam to efficiently

deposit the energy of the pump beam into a region of the plasma with preselected electron density where the conditions are optimum for SXR amplification. In this preselected gain region the electron density and temperature are sufficiently high for the generation of a large population inversion by transient collisional excitation, yet the density gradient is small enough to allow for effective amplification of the soft x-rays thorough the entire length of the gain column. A remarkable property of refraction is that this electron density (n_e) is strictly defined by only two parameters, the grazing incidence angle (θ) and the laser pump wavelength (λ):

$$\sin\theta = \sqrt{\frac{n_e}{n_{cp}}} \tag{1}$$

where n_e is the maximum electron density within the amplification region and n_{cp} is the critical density at the wavelength of the pump. The critical density is the electron density at which the electron plasma frequency ω_p equals the laser frequency ω :

$$n_{cp} = \frac{\varepsilon_o m\omega^2}{e^2} \approx \frac{1.11\times10^{21} e/cm^3}{\lambda^2(\mu m)} \tag{2}$$

where m is the electron mass, e is the electron charge, and ε_o is the permittivity of free space. Hence, when the grazing angle is changed, different parts of the density profile formed by the pre-pulse are preferentially heated. For example, directing a λ = 800 nm pump laser at a grazing incidence angle of 23 degrees results in $n_e = 2.7\times10^{20}$ cm^{-3}, and a grazing incidence angle of 35 degrees results in $n_e = 5.7\times10^{20}$ cm^{-3}. At a given incidence angle the pump beam is reflected at the point where it encounters the corresponding selected density according to (1) (Figure 1.4d), significantly increasing the path length of the pump beam and therefore its absorption in the gain region. Hence, a large fraction of

the pump energy (typically 20% – 50%) can be selectively deposited into the gain region. In addition, the grazing incidence pumping configuration has the advantage of intrinsically providing a traveling wave for a range of incidence angles of interest, a fact that simplifies the experimental set up. The optimization of the amplification along the entire length of the medium requires that: a) refraction of the SXR laser radiation is minimized, and b) the mismatch between the traveling wave pump speed and the SXR laser photon speed is kept small compared to the gain lifetime. When the initial grazing angle is small, e.g., $\theta < 20^{\circ}$, this mismatch ~(L/c)×[1-cos(θ)] is also negligibly small. However, for larger angles it could reach substantial values. For example with a plasma column length of L = 1 cm and θ = 45° the mismatch is 10 ps, which could be comparable to transient gain lifetime which can be in the range 3–15 ps depending on the maximum electron density achieved (determined by the grazing angle) and the pump laser duration.

An example of the advantages of the GRIP scheme is illustrated in Fig. 1.9 by model simulation results for the specific case of the 14.7 nm Ni-like Pd laser [1.91]. These results were obtained using a 1.5D hydrodynamic/atomic physics code with multicell radiation transport and beam refraction developed by our group at Colorado State University [1.92]. The simulation compares the gain at normal incidence to the gain created by a 20º grazing incidence pump pulse. The plasma is created by a 350 mJ pre-pulse of 120 ps duration focused into an intensity of 2.4×10^{12} Wcm^{-2} impinging at normal incidence onto a 4 mm long target. The plasma is subsequently heated by a 1 J pulse 8 ps in duration focused to an intensity of 8×10^{13} Wcm^{-2}. In the case of normal incidence

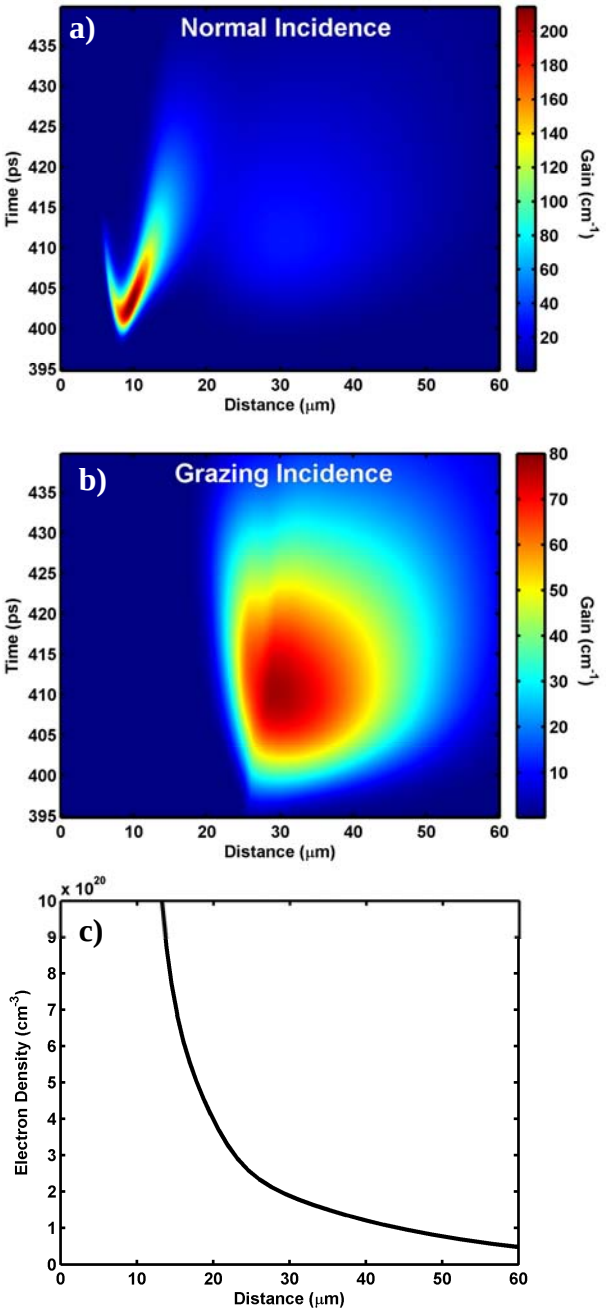

Figure 1.9: Simulated gain and electron density for a Ni-like Pd 14.7 nm laser at the moment of peak gain for: a) gain coefficient for normal incidence irradiation, b) gain coefficient for 20 degree grazing incidence irradiation c) lineout of the electron density profile at the time of the peak of the short pulse. At normal incidence the region of large gain coefficient coincides with large density gradients that rapidly refract the beam out of the narrow gain region. For a pump angle of 20 degrees the beam heats the plasma where n_e = 2 x 10^{20} cm^{-3}, creating large gain in a region where reduced refraction allows the beam to effectively propagate and amplify. The plasma is assumed to be created by a 120 ps normal incidence pre-pulse with an intensity of 2.4 x 10^{12} W cm^{-2}, and heated after a 400 ps delay by a 8 ps duration, 800 nm wavelength, 1 J pulse focused to an intensity of 8 x 10^{13} W cm^{-2}, both line foci are 30 μm × 4 mm FWHM. (From Luther et al. [1.91])

pumping the picosecond pulse rapidly heats the region near the critical density, generating a transient gain with a peak gain coefficient of about 200 cm^{-1} at a distance of 10 μm from the target, where the value of the electron density is close to 2×10^{21} cm^{-3}. However in this region the amplified soft X-rays refract out of the high gain region in only a few hundred micrometers, inhibiting amplification to large intensities. In contrast, at 20° grazing incidence angle the pump beam energy is coupled into the region of the plasma with $n_e = 2.0\times10^{20}$ cm^{-3}, where the peak small signal gain is computed to be 80 cm^{-1} and the refraction length (L_r) is larger than the 4 mm target length, allowing amplification to intensities that exceed the gain saturation intensity.

The simulations show that for the case of the grazing incidence pumped lasers the fraction of the pump energy deposited into the gain region is of the order of 20% – 30%, significantly greater than the 5% – 8% corresponding to the normal incidence pumping case. This significantly reduces the amount of pump energy required for lasing in the gain-saturated regime, making possible the development of high repetition rate table-top lasers.

Several high repetition rate SXR lasers have been demonstrated with the grazing incidence pumping geometry. Pumping of the 18.9 nm line of Ni-like Mo with 150 mJ of total pumping energy from a 10 Hz laser was reported to generate a gain length product of ~ 14 [1.87]. In work related to this dissertation, the use of 1 J heating pulses resulted in 5 Hz operation of Ni-like Mo, Ru, Pd, Ag and Cd at wavelengths of 18.9 nm, 16.5 nm, 14.7 nm, 13.9 nm, 13.2 nm in the gain-saturated regime [1.43, 1.44, 1.88, 1.89, 1.91, 1.93] with amplification at wavelengths as low as 10.9 nm in Ni-like Te [1.43] (figure 1.10). This geometry was also applied to the Ne-like isoelectronic sequence to

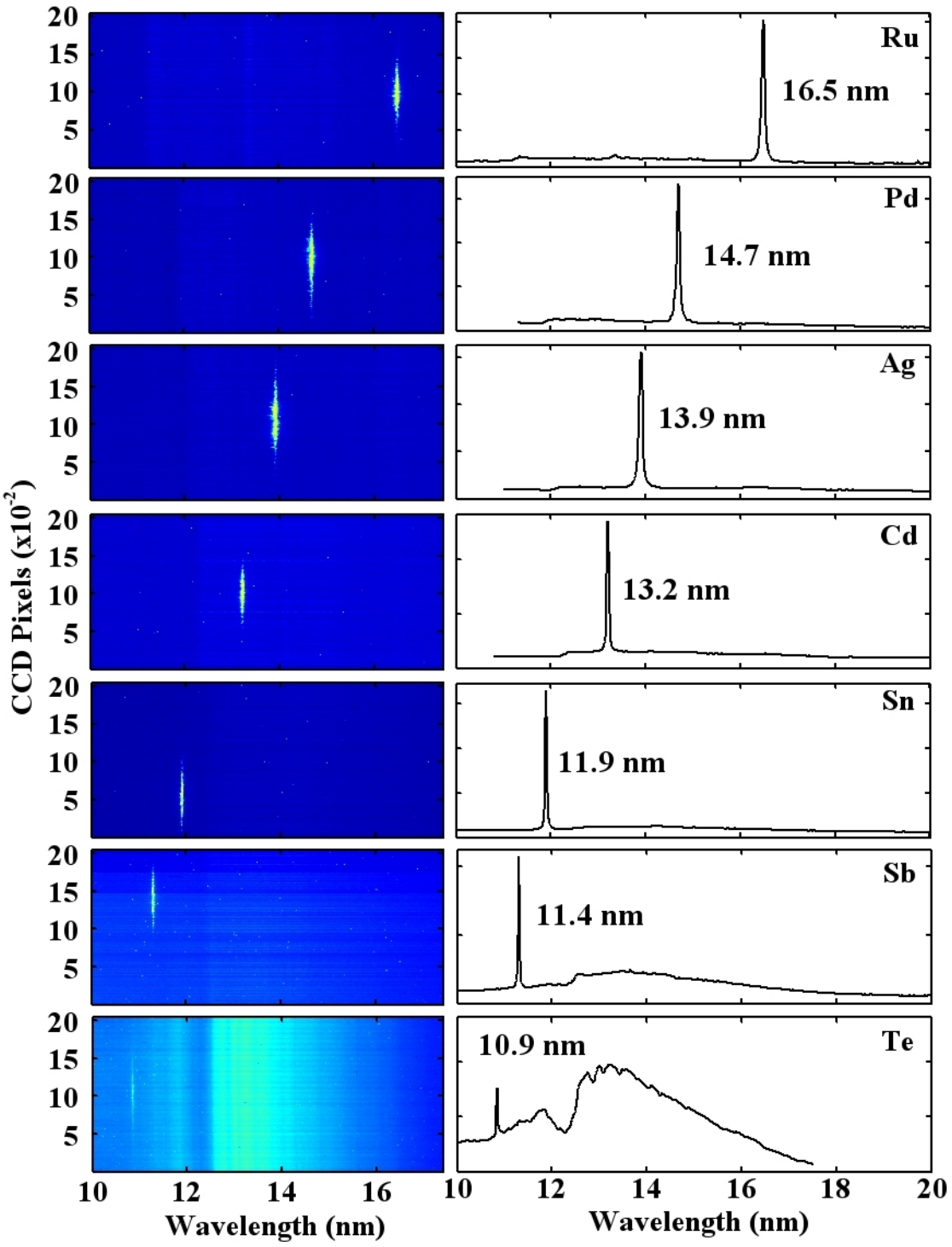

Figure 1.10: On axis spectra showing SXR lasers in the Ni-like $4d^1S_0 - 4p^1P_1$ isoelectronic sequence pumped by a picosecond 1J grazing incidence 800nm laser pulse.

demonstrate saturated amplification of Ti (32.6nm) and V (30.4) at a 5 Hz repetition rate as well as lasing in nearby Cr (28.6 nm) [1.89] (figure 1.11). This reduction in required pump energy to obtain gain-saturated lasing in this wavelength range has led to the demonstration of several similar lasers at other facilities [1.94-1.98].

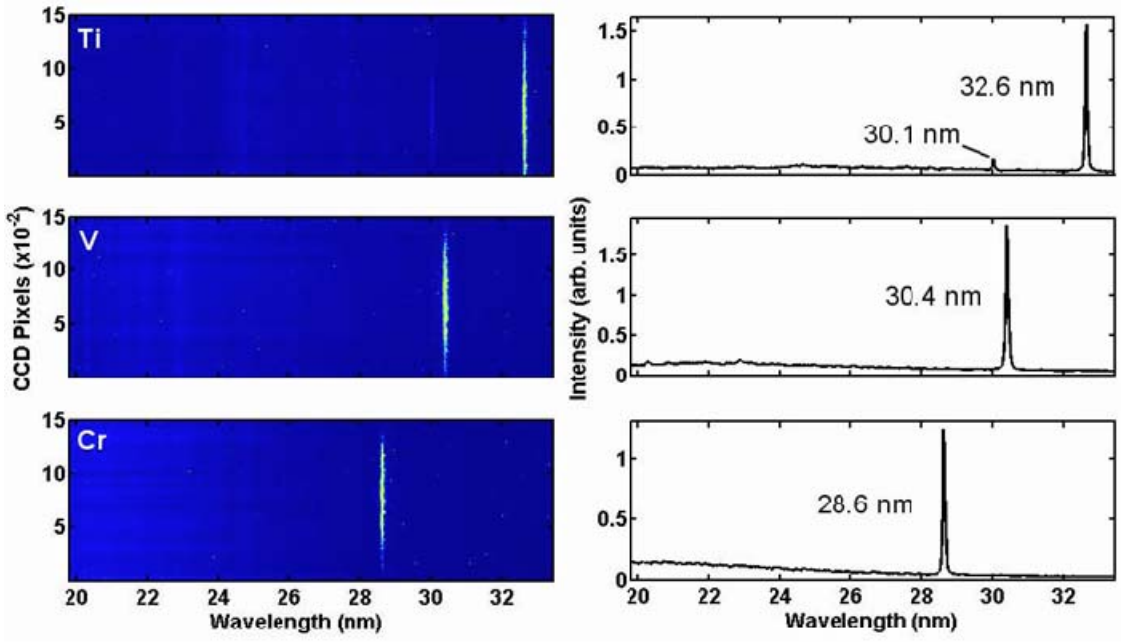

Figure 1.11: Single shot on-axis spectra of 4 mm long line focus plasmas showing lasing in the $2p^5\ 3p^1S_0 \rightarrow 2p^5\ 3s^1P_1$ transition of Ne-like Ti, V and Cr ions.

As discussed in subsequent chapters recent progress in table-top SXR lasers has been made at CSU using an increase of Ti:sapphire pump energy from the installation of the frequency doubled Nd:glass slab laser systems described in section 2.2 and 2.3 as well as a novel grazing incidence line focusing system that allows for more uniform pumping along the target length (section 5.5). This upgrade has resulted in demonstration of a significant increase in energy and average power of a 13.9 nm SXR laser [1.15]. Figure 1.12 shows a single shot on-axis spectrum of this laser as well as shot-to-shot pulse energy fluctuation while being operated at 2.5 Hz, with a short pulse pump energy

of ~2.7 J directed at a 23 deg grazing incidence angle onto a pre-created Ag plasma. The resulting average power was ~20 μW, where single shot operation reached energies of 10 μJ. Applying these same pumping conditions to cadmium targets resulted in sufficient flux to demonstrate table-top EUV mask metrology in reflection mode [1.49], a process previously was only performed using synchrotron light. Demonstration and characterization of SXR lasers from 10.9nm down to 7.4 nm are presented in Chapters 3 and 4 of this dissertation.

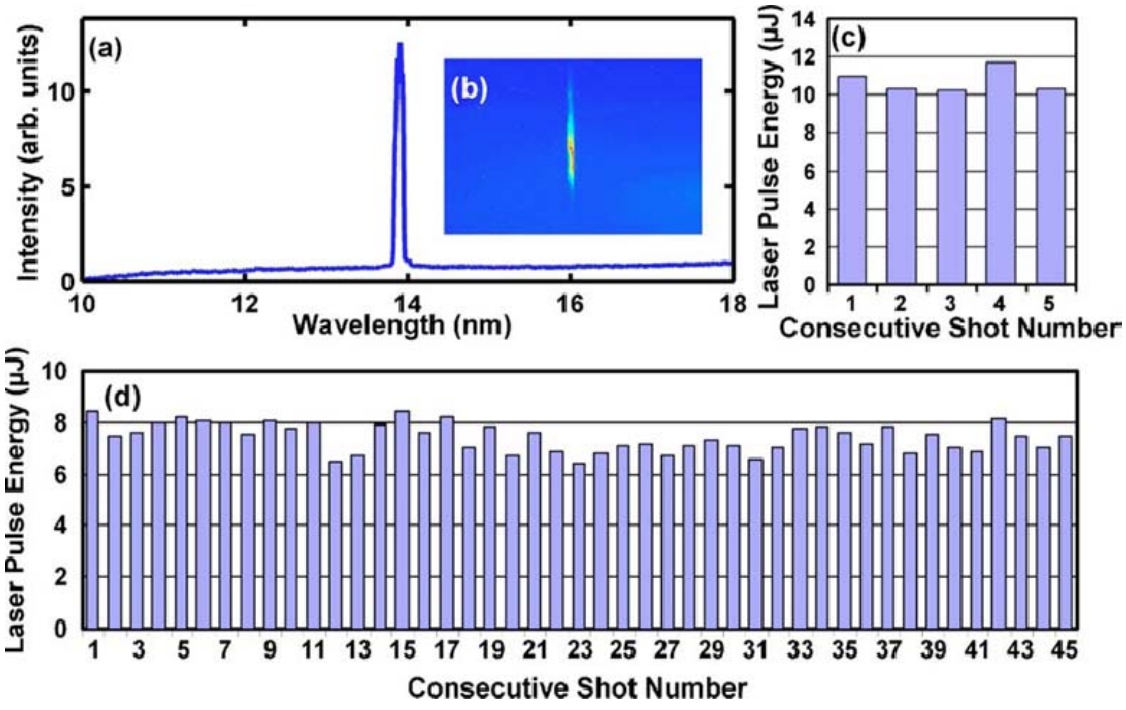

Figure 1.12: (a) Spectra of the Ni-like Ag plasma amplifier, showing highly monochromatic laser emission at =13.9 nm. (b) Spectrally resolved CCD image of the laser output. (c) Laser output pulse energy of the =13.9 nm laser operating at 0.5 Hz and (d) 2.5 Hz SXR laser operation with an average energy of 7.4 μJ with a shot-to-shot laser pulse energy variation of σ =7%.

1.4) Phase Coherent Injection Seeded Collisional Soft X-ray Lasers

The beams produced by amplified spontaneous emission in these amplifiers are characterized by relatively large beam divergence (5–15 mrad) [1.43, 1.44, 1.96, 1.98, 1.99], highly speckled patterns (Fig. 1.13(a) and [1.83]), and limited spatial [1.100] and temporal coherence [1.101, 1.102]. Previous work by Tanaka et al. demonstrated a significantly reduced far-field divergence and increased spatial coherence using an injection technique scheme that makes use of two SXR plasma amplifiers [1.103]. However the pulses did not have full temporal coherence. Injection seeding of SXR amplifiers with high harmonic (HH) pulses is a promising technique for improving the characteristics of SXR lasers that has additional advantages [1.104-1.111]. Figure 1.13a shows the experimental setup used by Wang [1.108]. The plasma amplifier is generated with a normal incidence pre-pulse and a grazing incidence short pulse. Part of the Ti:Sapphire pump laser is compressed, in a separate grating compressor, to a 50 fs pulse duration and focused into a gas cell with a 5m focal length lens. A toroidal mirror images the HHG beam onto a ~100 μm spot on the SXR plasma amplifier. Two BK7 substrates are placed at a grazing angle of 9º to attenuate the transmitted visible light and transmit the SXR beam. The seeded SXR beam is directed onto a spectrometer, where a double slit is placed in the beam to measure spatial coherence. Figure 1.13b-c shows a comparison of the far field beam profiles for an unseeded and seeded 13.9 nm Ni-like Ag laser. In addition to a reduced beam divergence [1.107, 1.110] and providing full spatial coherence (Figure 1.13d) [1.107], this technique can generate intense SXR laser pulses with full temporal coherence [1.54], shorter pulse width [1.109], and defined polarization

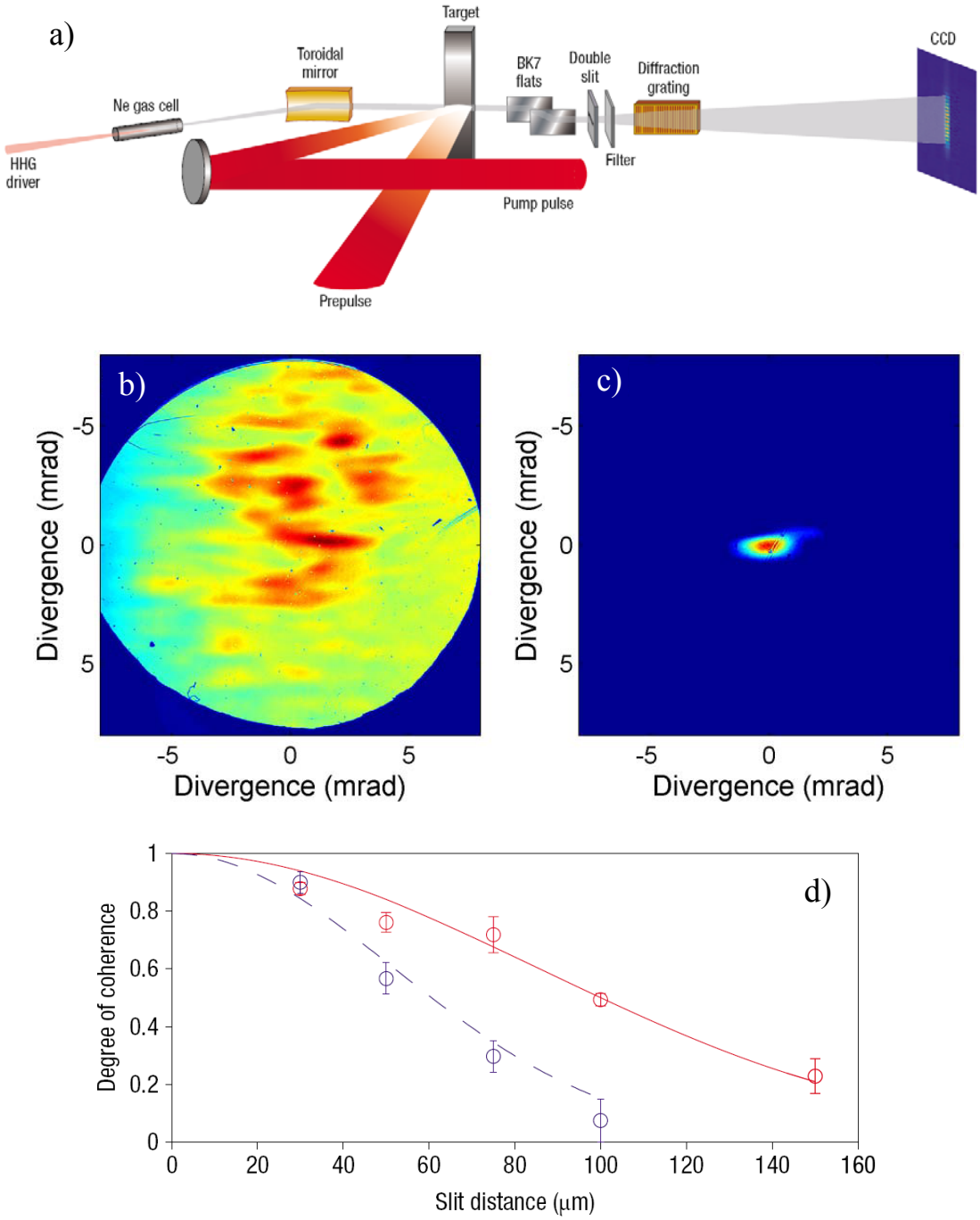

Figure 1.13: (a) Setup for injection seeding of a solid target plasma amplifier with a HHG beam. Comparison of the far field from (b) an unseeded 13:9 nm Ni-like Ag amplifier and (c) the same amplifier seeded by HHG pulses. Injection seeding results in an ~10× decrease of the beam divergence. The circular aperture in (b) is from a filter frame. (d) Degree of coherence as a function of slit separation for the injection-seeded (solid line) and unseeded (dashed line) laser. It is important to note that the laser beam diameters at this location are 80–100 mm and ~1 mm for the seeded and unseeded lasers, respectively, as presented by Wang et al. [1.108]

[1.105]. The seeding of broad bandwidth solid-target SXR laser amplifiers with HHG pulses has the potential of generating femtosecond SXR laser pulses [1.105, 1.109]. Simulations predict that seeding of the Ni-like lanthanum laser (λ = 8.8 nm) described in Chapter 5 would result in pulse durations of 500-700 fs, and energies of ~100 nJ.

1.5) References

[1.1] D. L. Matthews, P. L. Hagelstein, M. D. Rosen, M. J. Eckart, N. M. Ceglio, A. U. Hazi, H. Medecki, B. J. MacGowan, J. E. Trebes, B. L. Whitten, E. M. Campbell, C. W. Hatcher, A. M. Hawryluk, R. L. Kauffman, L. D. Pleasance, G. Rambach, J. H. Scofield, G. Stone, and T. A. Weaver, "*Demonstration of a Soft X-Ray Amplifier*," Phys. Rev. Lett. **54**, 110 (1985)

[1.2] S. Suckewer, C. H. Skinner, H. Milchberg, C. Keane, and D. Voorhees, "*Amplification of Stimulated Soft-X-Ray Emission in a Confined Plasma Column*," Phys. Rev. Lett. **55**, 1753 (1985).

[1.3] D. T. Attwood, *Soft X-Rays and Extreme Ultraviolet Radiation: Principles and Applications* (Cambridge University Press, Cambridge, England, 1999). Linac Coherent Light Source: http://lcls.slac.stanford.edu. Free Electron Laser in Hamburg http://flash.desy.de

[1.4] M. R. Howells and M. A. Iarocci and J. Kirz, *"Experiments in x-ray holographic microscopy using synchrotron radiation,"* J. Opt. Soc. Am. A **3**, 2171 (1986)

[1.5] Harald Ade, Janos Kirz, Steven L. Hulbert, Erik D. Johnson, Erik Anderson, and Dieter Kern, *"X-ray spectromicroscopy with a zone plate generated microprobe,"* Appl. Phys. Lett. **56**, 1841 (1990)

[1.6] C. Jacobsen, S. Williams, E. Anderson, M.T. Browne, C.J. Buckley, D. Kern, J. Kirz, M. Rivers and X. Zhang, *"Diffraction-limited imaging in a scanning transmission X-ray microscope,"* Optics Communications **86**, 351-364 (1991)

[1.7] H. H. Solak, D. He,W. Li, S. S. Gasson, S. S. Cerrina, B. H. Sohn, X. M. Yang, and P. Nealey, *"Exposure of 38 nm period grating patterns with extreme ultraviolet interferometric lithography,"* Appl. Phys. Lett. **75**, 2328–2330 (1999)

[1.8] KM Labs XUUS. http://www.kmlabs.com/extreme.htm

[1.9] Etienne Gagnon, Predrag Ranitovic, Xiao-Min Tong, C. L. Cocke, Margaret M. Murnane, Henry C. Kapteyn, and Arvinder S. Sandhu, *"Soft X-ray-driven femtosecond molecular dynamics."* Science **317**, 1374–1378 (2007)

[1.10] Arvinder S. Sandhu, Etienne Gagnon, Robin Santra, Vandana Sharma, Wen Li, Phay Ho, Predrag Ranitovic, C. Lewis Cocke, Margaret M. Murnane, and Henry C. Kapteyn *"Observing the creation of electronic Feshbach resonances in soft X-ray-induced O2 dissociation."* Science **322**, 1081–1085 (2008)

[1.11] L. Miaja-Avila, G. Saathoff, S. Mathias, J. Yin, C. La-o-vorakiat, M. Bauer, M. Aeschlimann, M. M. Murnane, and H. C. Kapteyn, "*Direct measurement of core-level relaxation dynamics on a surface-adsorbate system."* Phys Rev Lett **101**, 046101 (2008)

[1.12] Xiaoshi Zhang, Amy L. Lytle, Tenio Popmintchev, Xibin Zhou, Henry C. Kapteyn, Margaret M. Murnane and Oren Cohen, *"Quasi-phase-matching and quantum-path control of highharmonic generation using counterpropagating light."* Nat Phys **3**, 270–275. (2007)

[1.13] Xibin Zhou, Robynne Lock, Wen Li, Nick Wagner, Margaret M. Murnane, and Henry C. Kapteyn, *"Molecular recollision interferometry in high harmonic generation,"* Phys Rev Lett **100**, 073902 (2008)

[1.14] Eiji J. Takahashi, Yasuo Nabekawa, Hiroki Mashiko, Hirokazu Hasegawa, Akira Suda, and Katsumi Midorikawa, *"Generation of Strong Optical Field in Soft X-Ray Region by Using High-Order Harmonics,"* IEEE J. Sel. Topics Quantum Electron. **10**, 1315 (2004)

[1.15] D. H. Martz, D. Alessi, B. M. Luther, Y. Wang, D. Kemp, M. Berrill and J. J. Rocca, *"High Energy 13.9 nm Table-top Soft X-ray Laser at 2.5 Hz Repetition Rate Excited by a Slab-pumped Ti:sapphire Laser,"* Optics Letters **35**, 1632 (2010)

[1.16] F. Furch, B. Reagan, B. Luther, A. Curtis, S. Meehan, and J.J. Rocca, *"Demonstration of an all-diode-pumped soft x-ray laser,"* Optics Letters **34**, 3352 (2009)

[1.17] J. Tümmler, R. Jung, H. Stiel, P. V. Nickles, and W. Sandner, *"High-repetition-rate chirped-pulse-amplification thin-disk laser system with joule-level pulse energy,"* Optics Letters, **34**, 1378-1380 (2009)

[1.18] A. H. Curtis, B. A. Reagan, K. A. Wernsing, F. J. Furch, B. M. Luther, and J. J. Rocca, *"Demonstration of a compact 100 Hz, 0.1 J, diode-pumped picosecond laser,"* Opt. Lett. **36**, 2164-2166 (2011)

[1.19] D. T. Attwood, D. W. Sweeney, J. M. Auerbach, and P. H. Y. Lee, *"Interferometric Confirmation of Radiation-Pressure Effects in Laser-Plasma Interactions,"* Phys. Rev. Lett. **40**, 184 (1978)

[1.20] M. D. Rosen, P. L. Hagelstein, D. L. Matthews, E. M. Campbell, A. U. Hazi, B. L. Whitten, B. MacGowan, R. E. Turner, R. W. Lee, G. Charatis, G. E. Bush, C. L. Shepard, and P. D. Rockett, *"Exploding-Foil Technique for Achieving a Soft X-Ray Laser,"* Phys. Rev. Lett. **54**, 106 (1985)

[1.21] L. B. Da Silva, T. W. Barbee, Jr., R. Cauble, P. Celliers, D. Ciarlo, S. Libby, R. A. London, D. Matthews, S. Mrowka, J. C. Moreno, D. Ress, J. E. Trebes, A. S. Wan, and F. Weber, *"Electron Density Measurements of High Density Plasmas Using Soft X-Ray Laser Interferometry"* Phys. Rev. Lett. **74**, 3991 (1995)

[1.22] J. Filevich, K. Kanizay, M. C. Marconi, J. L. A. Chilla, and J. J. Rocca, *"Dense plasma diagnostics with an amplitude-division soft-x-ray laser interferometer based on diffraction gratings,"* Opt. Lett. **25**, 356 (2000);

[1.23] J. J. Rocca, E. C. Hammarsten, E. Jankowska, J. Filevich, M. C. Marconi, S. Moon and V. N. Shlyaptsev, "*Application of extremely compact capillary discharge soft x-ray lasers to dense plasma diagnostics*," Physics of Plasmas **10**, 2031 (2003)

[1.24] Mike Purvis, Jonathan Grava, Jorge Filevich, Mario C. Marconi, James Dunn, Stephen J. Moon, Vyacheslav N. Shlyaptsev, Elizabeth Jankowska, and Jorge J. Rocca, *"Dynamics of converging laser-created plasmas in semicylindrical cavities studied using soft x-ray laser interferometry,"* Phys. Rev. E **76** 046402 (2007)

[1.25] Jonathan Grava, Michael A. Purvis, Jorge Filevich, Mario C. Marconi, Jorge J. Rocca, James Dunn, Stephen J. Moon, and Vyacheslav N. Shlyaptsev, *"Dynamics of a dense laboratory plasma jet investigated using soft x-ray laser interferometry,"* Phys. Rev. E **78** 016403 (2008)

[1.26] Michael A. Purvis, Jonathan Grava, Jorge Filevich, Duncan P. Ryan, Stephen J. Moon, James Dunn, Vyacheslav N. Shlyaptsev, and Jorge J. Rocca, *"Collimation of dense plasma jets created by low-energy laser pulses and studied with soft x-ray laser interferometry"* Phys. Rev. E **81**, 036408 (2010)

[1.27] R. F. Smith, J. Dunn, J. Nilsen, V. N. Shlyaptsev, S. Moon, J. Filevich, J. J. Rocca, M. C. Marconi, J. R. Hunter, and T. W. Barbee, Jr., *"Picosecond X-Ray Laser Interferometry of Dense Plasmas,"* Phys. Rev. Lett. **89**, 065004 (2002)

[1.28] J. Filevich, J. J. Rocca, and M. C. Marconi, S. J. Moon, J. Nilsen, J. H. Scofield, J. Dunn, R. F. Smith, R. Keenan, and J. R. Hunter and V. N. Shlyaptsev, *"Observation of a Multiply Ionized Plasma with Index of Refraction Greater than One,"* Phys. Rev. Lett. **94**, 035005 (2005)

[1.29] Juan L. A. Chilla, Jorge J. Rocca, Oscar E. Martinez, and Mario C. Marconi*, "Soft-x-ray interferometer for single-shot laser linewidth measurements,"* Opt. Lett. **21**, 955-957 (1996)

[1.30] G. Vaschenko, C. Brewer, F. Brizuela, Y. Wang, M. A. Larotonda, B. M. Luther, M. C. Marconi, J. J. Rocca, C. S. Menoni, E. H. Anderson, W. Chao, B. D. Harteneck, J. A. Liddle, Y. Liu, and D. T. Attwood, *"Sub-38 nm resolution tabletop microscopy with 13 nm wavelength laser light,"* Opt. Lett. **31**, 1214–1216 (2006).

[1.31] J. A. Trail and R. L. Byer, *"Compact scanning soft-x-ray microscope using a laser-produced plasma source and normal-incidence multilayer mirrors,"* Opt. Lett. **14**, 539 (1989).

[1.32] D. S. DiCicco, D. Kim, R. Rosser, and S. Suckewer, *"First stage in the development of a soft-x-ray reflection imaging microscope in the Schwarzschild configuration using a soft-x-ray laser at 18.2 nm,"* Opt. Lett. **17**, 157 (1992).

[1.33] L. B. Da Silva, J. E. Trebes, S. Mrowka, T. W. Barbee, Jr., J. Brase, J. A. Koch, R. A. London, B. J. MacGowan, D. L. Matthews, D. Minyard, G. Stone, T. Yorkey, E.

Anderson, D. T. Attwood, and D. Kern, *"Demonstration of x-ray microscopy with an x-ray laser operating near the carbon K edge,"* Opt. Lett. **17**, 754 (1992).

[1.34] M. Wieland, C. Spielmann, U. Kleineberg, T. Westerwalbesloh, U. Heinzmann, and T. Wilhein, *"Toward time-resolved soft X-ray microscopy usingpulsed fs-high-harmonic radiation,"* Ultramicroscopy **102**, 93 (2005).

[1.35] A. R. Libertun, X. Zhang, A. Paul, D. Raymondson, E. Gershgoren, E. Gagnon, S. Backus, M. M. Murnane, H. C. Kapteyn, R. A. Bartels, Y. Liu, and D. T. Attwood, in Conference on Lasers and Electro-Optics, Vol. **96** of OSA Trends in Optics and Photonics (Optical Society of America, 2004), paper JMD4.

[1.36] M. Kishimoto, M. Tanaka, R. Tai, K. Sukegawa, M. Kado, N. Hasegawa, H. Tang, T. Kawachi, P. Lu, K. Nagashima, H. Daido, Y. Kato, K. Nagai, and H. Takenaka, *"Development of soft X-ray microscopy System using X-ray laser in JAERI Kansai,"* J. Phys. IV **104**, 141 (2003).

[1.37] G. Vaschenko, F. Brizuela, C. Brewer, M. Grisham, H. Mancini, C. S. Menoni, M. Marconi, and J. J. Rocca, *"Nanoimaging with a compact extreme-ultraviolet laser,"* Opt. Lett. **30**, 2095 (2005).

[1.38] I. A. Artioukov, A. V. Vinogradov, V. E. Asadchikov, Y. S. Kasyanov, R. V. Serov, A. I. Fedorenko, V. V. Kondratenko, and S. A. Yulin, *"Schwarzschild soft-x-ray microscope for imaging of nonradiating objects,"* Opt. Lett. **20**, 2451 (1995).

[1.39] M. Berglund, L. Rymell, M. Peuker, T. Wilhein, and H. M. Hertz, "Compact water-window transmission X-ray microscopy," J. Microsc. (Oxford) **197**, 268 (2000).

[1.40] Courtney A. Brewer, Fernando Brizuela, Przemyslaw Wachulak, Dale H. Martz, Weilun Chao, Erik H. Anderson, David T. Attwood, Alexander V. Vinogradov, Igor A. Artyukov, Alexander G. Ponomareko, Valeriy V. Kondratenko, Mario C. Marconi, Jorge J. Rocca, and Carmen S. Menoni, *"Single-shot extreme ultraviolet laser imaging of nanostructures with wavelength resolution,"* Opt. Lett. **33**, 518 (2008)

[1.41] Weilun Chao, Bruce D. Harteneck, J. Alexander Liddle, Erik H. Anderson and David T. Attwood, *"Soft X-ray microscopy at a spatial resolution better than 15 nm,"* Nature **435**, 1210-1213 (2005)

[1.42] W. Chao, J. Kim, S. Rekawa, P. Fischer, E.H. Anderson, *"Demonstration of 12 nm Resolution Fresnel Zone Plate Lens based Soft X-ray Microscopy,"* Optics Letters **17**, 17669 (2009)

[1.43] Y. Wang, M. A. Larotonda, B. M. Luther, D. Alessi, M. Berrill, V. N. Shlyaptsev, and J. J. Rocca, "*Demonstration of high-repetition-rate tabletop soft-x-ray lasers with saturated output at wavelengths down to 13.9 nm and gain down to 10.9 nm*," Phys. Rev. A **72**, 053807 (2005)

[1.44] J. J. Rocca, Y. Wang, M. A. Larotonda, B. M. Luther, M. Berrill, and D. Alessi, "*Saturated 13.2 nm high-repetition-rate laser in nickellike cadmium*," Opt. Lett. **30**, 2581 (2005)

[1.45] S. Carbajo, I. D. Howlett, F Brizuela, K. S. Buchanan, M. C. Marconi, W. Chao, E. H. Anderson, I Artioukov, A. Vinogradov, J. J. Rocca and C. S. Menoni, *"Movies of nanoscale dynamic interactions with a table-top soft X-ray laser,"* Nature Photonics (submitted 2011)

[1.46] The International Technology Roadmap for Semiconductors: http://www.itrs.net/

[1.47] Patrick P. Naulleau, Jason P. Cain, and Kenneth A. Goldberg, "*Lithographic characterization of the spherical error in an extreme-ultraviolet optic by use of a programmable pupil-fill illuminator*," Applied Opitcs **20**, 1957 (2006)

[1.48] Kenneth A. Goldberg, Patrick P. Naulleau, Paul E. Denham, Senajith B. Rekawa, Keith Jackson, Erik H. Anderson, and J. Alexander Liddle, "*At-wavelength alignment and testing of the 0.3 NA MET optic*," J. Vac. Sci. Technol. B **22**, 2956 (2004)

[1.49] F. Brizuela, S. Carbajo, A. Sakdinawat, D. Alessi, D. Martz, Y. Wang, B. Luther, K. A. Goldberg, I. Mochi, D. T. Attwood, B. La Fontaine, J. J. Rocca, and C. S. Menoni, *"Extreme Ultraviolet Laser-based Table-Top Aerial Image Metrology of Lithographic Masks,"* Optics Express **18**, 14467 (2010)

[1.50] Richard L. Sandberg, Ariel Paul, Daisy A. Raymondson, Steffen Hädrich, David M. Gaudiosi, Jim Holtsnider, Ra'anan I. Tobey, Oren Cohen, Margaret M. Murnane, and Henry C. Kapteyn, Changyong Song and Jianwei Miao,Yanwei Liu and Farhad Salmassi, *"Lensless Diffractive Imaging Using Tabletop Coherent High-Harmonic Soft-X-Ray Beams,"* Phys. Rev. Lett. **99**, 098103 (2007)

[1.51] S. Marchesini et al, *"Massively parallel X-ray holography,"* Nat. Photonics **2**, 560 (2008)

[1.52] Kevin S. Raines, Sara Salha, Richard L. Sandberg, Huaidong Jiang, Jose A. Rodríguez, Benjamin P. Fahimian, Henry C. Kapteyn, Jincheng Du, and Jianwei Miao, *"Three-dimensional structure determination from a single view,"* Nature **463**, 214 (2010)

[1.53] A. Ravasio et al., *"Single-Shot Diffractive Imaging with a Table-Top Femtosecond Soft X-Ray Laser-Harmonics Source,"* Phys. Rev. Lett. **103**, 028104 (2009)

[1.54] L. M. Meng, D. Alessi, O. Guilbaud, Y. Wang, M. Berrill, B. M. Luther, S. R. Domingue, D. H. Martz, D. Joyeux, S. De Rossi, J.J. Rocca, and A. Klisnick, *"Temporal coherence and spectral linewidth of an injection-seeded transient collisional soft x-ray laser,"* Optics Express **19**, 12087 (2011)

[1.55] H. T. Kim, I. J. Kim, C. M. Kim, T. M. Jeong, T. J. Yu, S. K. Lee, J. H. Sung, J. W. Yoon, H. Yun, S. C. Jeon, I. W. Choi, and J. Lee, *"Single-shot nanometer-scale holographic imaging with laser-driven x-ray laser,"* Applied Physics Letters **98**, 121105 (2011)

[1.56] Artak Isoyan, A. Wüest, John Wallace, Fan Jiang, and Franco Cerrina, *"4X reduction extreme ultraviolet interferometric lithography,"* Opt. Express **16**, 9106-9111 (2008)

[1.57] Maria G. Capeluto, Georgiy Vaschenko, Michael Grisham, Mario C. Marconi, S. Ludueña, L. Pietrasanta, Yunfeng Lu, Bruce Parkinson, Carmen S. Menoni and J. J. Rocca, *"Nanopatterning With Interferometric Lithography Using a Compact λ = 46.9 nm Laser,"* IEEE Transactions on Nanotechnology **5**, 3 (2006)

[1.58] P. W. Wachulak, M. G. Capeluto, M. C. Marconi, C. S. Menoni, and J. J. Rocca, *"Patterning of nano-scale arrays by table-top extreme ultraviolet laser interferometric lithography,"* Opt. Express **15**, 3465-3469 (2007)

[1.59] A. Isoyan, F. Jiang, Y. C. Cheng, F. Cerrina, P. Wachulak, L. Urbanski, J. Rocca, C. Menoni, and M. Marconi, *"Talbot lithography: Self-imaging of complex structures,"* J. Vac. Sci. Technol. B **27**, 2931 (2009)

[1.60] W. B. Bridges, *"Laser oscillation in singly ionized argon in the visible spectrum,"* Appl. Phys. Lett. **4**, 128-130 (1964)

[1.61] W. R. Bennett, J. W. Knutson, G. N. Mercer, and J. L. Detch, *"Super-radiance, excitation mechanisms, and quasi-cw oscillation in the visible Ar+ laser,"* Appl. Phys. Lett. **4**, 180 (1964)

[1.62] A. G. Molchanov, *"Lasers in the vacuum ultraviolet and in the x-ray regions of the spectrum,"* Sov. Phys. Usp. **15**, 124 (1972)

[1.63] R. C. Elton, *"Extension of 3p→ 3s Ion Lasers into the Vacuum Ultraviolet Region,"* Appl. Opt. **14**, 97 (1975)

[1.64] A. N. Zherikin, K. N. Koshelev, and V. S. Letokhov, *"Gain in the far vacuum ultraviolet region due to transitions in multiply charged ions,"* Sov. J. Quantum Electron. **6**, 82 (1976)

[1.65] A. V. Vinogradov, I. I. Sobel'man, and E. A. Yukov, *"Population inversion of transitions in neon-like ions,"* Sov. J. Quantum Electron. **7**, 32 (1977)

[1.66] L. A. Vainshtein, A. V. Vinogradov, V. I. Safranova, and I. Vu. Skolev, *"Stimulated emission in far ultraviolet due to transitions in multiply charged neon-like ions,"* Sov. J. Quantum Electron. **8**, 239 (1978)

[1.67] A. V. Vinogradov and V. N. Shlyaptsev, *"Calculations of population inversion due to transitions in multiply charged neon-like ions in the 200–2000 Å range,"* Sov. J. Quantum Electron. 10, 754 (1980)

[1.68] A. V. Vinogradov and V. N. Shlyaptsev, *"Gain in the 100–1000 Å range in a homogeneous stationary plasma,"* Sov. J. Quantum Electron. 13, 303 (1983)

[1.69] B. J. MacGowan, S. Maxon, P. L. Hagelstein, C. J. Keane, R. A. London, D. L. Matthews, M. D. Rosen, J. H. Scofield, and D. A. Whelan, "*Demonstration of soft x-ray amplification in nickel-like ions*," Phys. Rev. Lett. **59**, 2157 (1987)

[1.70] B. J. MacGowan, S. Maxon, L. B. Da Silva, D. J. Fields, C. J. Keane, D. L. Matthews, A. L. Osterheld, J. H. Scofield, G. Shimkaveg, and G. F. Stone, *"Demonstration of X-Ray Amplifiers near the Carbon K Edge,"* Phys Rev Lett **65**, 420 (1990)

[1.71] H. Daido, Y.Kato, S.Ninomiya, R. Kodame, G.Yuan, M.Takagi, H.Takabe, *"Efficient soft x-ray lasing at 6-8 nm in nickel-like lanthanides",* Phys.Rev. Lett. **75** 1074, (1995)

[1.72] H. Daido, S. Ninomiya, T. Imani, R. Kodama, M. Takagi, Y. Kato, K. Murai, J. Zhang, Y. You, Y. Gu, *"Nickellike soft-x-ray lasing at the wavelengths between 14 and 7.9 nm,"* Optics Letters **21**, 958-960 (1996)

[1.73] J. Zhang, A. G. MacPhee, J. Lin, E. Wolfrum, R. Smith, C. Danson, M. H. Key, C. L. S. Lewis, D. Neely, J. Nilsen, G. J. Pert, G. J. Tallents, J. S. Wark, *"A Saturated X-ray Laser Beam at 7 Nanometers,"* Science **276**, 1097 (1997)

[1.74] R. Smith, G. J. Tallents, J. Zhang, G. Eker, S. McCabe, G. J. Pert, and E. Wolfrum, "*Saturation behavior of two x-ray lasing transitions in Ni-like Dy*," Phys. Rev. A **59**, R47 (1999)

[1.75] Afanasiev and Shlyaptsev*, "Formation of a population inversion of transitions in Ne-like ions in steady-state and transient plasmas,"* Sov. J. Quantum Electron. **19**, 1606 (1989)

[1.76] J. J. Rocca, *"Table-top soft x-ray lasers,"* Review of Scientific Instruments **70**, 3799 (1999)

[1.77] M. P. Kalachnikov, P. V. Nickles, M. Schnürer, W. Sandner, V. N. Shlyaptsev, C. Danson, D. Neely, E. Wolfrum, J. Zhang, A. Behjat, A. Demir, G. J. Tallents, P. J.

Warwick, and C. L. S. Lewis, *"Saturated operation of a transient collisional x-ray laser,"* Phys. Rev. A **57**, 4778 (1998)

[1.78] J. Dunn, Y. Li, A. L. Osterheld, J. Nilsen[1], J. R. Hunter, and V. N. Shlyaptsev, "*Gain Saturation Regime for Laser-Driven Tabletop, Transient Ni-Like Ion X-Ray Lasers*," Phys. Rev. Lett. **84**, 4834 (2000)

[1.79] B. R. Benware, C. D. Macchietto, C. H. Moreno, and J. J. Rocca, "*Demonstration of a High Average Power Tabletop Soft X-Ray Laser,*" Phys. Rev. Lett. **81**, 5804 (1998); C. D. Macchietto, B. R. Benware, and J. J. Rocca, "*Generation of millijoule-levelsoft-x-ray laser pulses at a 4-Hz repetitionrate in a highly saturated tabletop capillary dischargeamplifier*," Opt. Lett. **24**, 1115 (1999)

[1.80] M. Frati, M. Seminario, and J. J. Rocca, *"Demonstration of a 10-μJ tabletop laser at 52.9 nm in neonlike chlorine,"* Opt. Lett. **25**, 1022-1024 (2000)

[1.81] S. Sebban, R. Haroutunian, Ph. Balcou, G. Grillon, A. Rousse, S. Kazamias, T. Marin, J. P. Rousseau, L. Notebaert, M. Pittman, J. P. Chambaret, A. Antonetti, D. Hulin, D. Ros, A. Klisnick, A. Carillon, P. Jaeglé, G. Jamelot, and J. F. Wyart, "*Saturated Amplification of a Collisionally Pumped Optical-Field-Ionization Soft X-Ray Laser at 41.8 nm*," Phys. Rev. Lett. **86**, 3004 (2001)

[1.82] S. Sebban, T. Mocek, D. Ros, L. Upcraft, Ph. Balcou, R. Haroutunian, G. Grillon, B. Rus, A. Klisnick, A. Carillon, G. Jamelot, C. Valentin, A. Rousse, J. P. Rousseau, L. Notebaert, M. Pittman, and D. Hulin, *"Demonstration of a Ni-Like Kr Optical-Field-Ionization Collisional Soft X-Ray Laser at 32.8 nm,"* Phys. Rev. Lett. **89**, 253901 (2002)

[1.83] D. V. Korobkin, C. H. Nam, S. Suckewer, and A. Goltsov, "*Demonstration of Soft X-Ray Lasing to Ground State in Li III*," Phys. Rev. Lett. **77**, 5206 (1996)

[1.84] K. A. Janulewicz, A. Lucianetti, G. Priebe, W. Sandner, and P. V. Nickles, "*Saturated Ni-like Ag x-ray laser at 13.9 nm pumped by a single picosecond laser pulse*," Phys. Rev. A **68**, 051802 (2003)

[1.85] Riccardo Tommasini, Joseph Nilsen, Ernst E. Fill, "*Investigations on 10-Hz sub-Joule fs-laser pumped neon- and nickel-like x-ray lasers*," Soft X-Ray Lasers and Applications IV; Ernst E. Fill, Jorge J. Rocca; Eds. Proc. SPIE **4505**, 85 (2001)

[1.86] T. Ozaki, R. A. Ganeev, A. Ishizawa, T. Kanai, and H. Kuroda, "*Highly Directive 18.9 nm Nickel-like Molybdenum X-Ray Laser Operating at 150 mJ Pump Energy*," Phys Rev. Lett. **89**, 253902 (2002); R. Li and Z. Z. Xu, "*Highly efficient transient collisional excitation X-ray laser in Ni-like Mo ions*," J. Phys. IV **11**(PR2), 27 (2001) Proc. 7th Int. Conf. X-Ray Lasers, Vol 11, G. Jamelot, C. Moller, and A Klishnick, Eds., Saint-Malo, France, 2001, pp. 27-34

[1.87] R. Keenan, J. Dunn, P. K. Patel, D. F. Price, R. F. Smith, and V. N. Shlyaptsev, "*High-Repetition-Rate Grazing-Incidence Pumped X-Ray Laser Operating at 18.9 nm*," Phys. Rev. Lett. **94**, 103901 (2005); Roisin Keenan, James Dunn, Vyacheslav N. Shlyaptsev, Raymond F. Smith, Pravesh K. Patel, Dwight F. Price, "*Efficient pumping schemes for high average brightness collisional x-ray lasers*," Soft X-Ray Lasers and Applications V; Ernst E. Fill, Szymon Suckewer; Eds. Proc. SPIE **5197**, 213 (2003)

[1.88] B. M. Luther, Y. Wang, M. A. Larotonda, D. Alessi, M. Berrill, M. C. Marconi, V. N. Shlyaptsev, J. J. Rocca, "*Saturated high-repetition-rate 18.9-nm tabletop laser in nickellike molybdenum*," Opt. Lett. **30**, 165 (2005)

[1.89] D. Alessi, B.M. Luther, Y. Wang, M.A. Larotonda, M. Berrill, and J.J. Rocca, *"High repetition rate operation of saturated table-top soft x-ray lasers in transitions of neon-like ions near 30 nm,"* Optics Express **13**, 2093 (2005)

[1.90] R. A. London, "*Beam optics of exploding foil plasma x-ray lasers*," Phys. Fluids **31**, 184 (1988).

[1.91] B.M. Luther, Y. Wang, M.A. Larotonda, D. Alessi, M. Berrill, J.J. Rocca, J. Dunn, R. Keenan, and V.N. Shlyaptsev, "High Repetition Rate Collisional Soft X-Ray Lasers Based on Grazing Incidence Pumping," IEEE Journal of Quantum Electronics **42**, 4 (2006)

[1.92] Mark A. Berrill, Thesis: "*A Computer Model to Simulate Laser Created Plasmas used for the Generation of Extreme Ultraviolet Radiation*," Colorado State University, Department of Electrical and Computer Engineering, Summer 2006.

[1.93] M.A. Larotonda, B.M. Luther, Y. Wang, Y. Liu, D. Alessi, M. Berrill, A. Dummer, F. Brizuela, C.S. Menoni, M.C. Marconi, V.N. Shlyaptsev, J. Dunn, and J.J. Rocca, "Characteristics of a Saturated 18.9-nm Tabletop Laser Operating at 5-Hz Repetition Rate," IEEE Journal of selected topics in Quantum Electronics **10**, 1363 (2004)

[1.94] K. Cassou, S. Kazamias, D. Ros, F. Plé, G. Jamelot, A. Klisnick, O. Lundh, F. Lindau, A. Persson, C.-G. Wahlström, S. de Rossi, D. Joyeux, B. Zielbauer, D.

Ursescu, and T. Kühl, *"Optimization toward a high-average-brightness soft-x-ray laser pumped at grazing incidence,"* Opt. Lett. **32**, 139-141 (2007)

[1.95] S. Kazamias, K. Cassou, D. Ros, F. Plé, G. Jamelot, A. Klisnick, O. Lundh, F. Lindau, A. Persson, C.-G. Wahlström, S. de Rossi, D. Joyeux, B. Zielbauer, D. Ursescu, and T. Kühl, *"Characterization of a transient collisional Ni-like molybdenum soft-x-ray laser pumped in grazing incidence,"* Phys. Rev. A **77**, 033812 (2008)

[1.96] H. T. Kim, I. W. Choi, N. Hafz, J. H. Sung, T. J. Yu, K.-H. Hong, T. M. Jeong, Y.-C. Noh, D.-K. Ko, K. A. Janulewicz, J. Tümmler, P. V. Nickles, W. Sandner, and J. Lee, *"Demonstration of a saturated Ni-like Ag x-ray laser pumped by a single profiled laser pulse from a 10-Hz Ti:sapphire laser system,"* Phys. Rev. A **77**, 023807 (2008)

[1.97] Jürg E. Balmer, Christoph Imesch, and Felix Staub, "Gain saturation in Ni-like lasers," Proc. SPIE **7451**, 74510O (2009)

[1.98] Daniel Zimmer, Bernhard Zielbauer, Moana Pittman, Olivier Guilbaud, Jamil Habib, Sophie Kazamias, David Ros, Vincent Bagnoud, and Thomas Kuehl, *"Optimization of a tabletop high-repetition-rate soft x-ray laser pumped in double-pulse single-beam grazing incidence,"* Opt. Lett. **35**, 450-452 (2010)

[1.99] D. Alessi, D. H. Martz, Y. Wang, M. Berrill, B. M. Luther and J. J. Rocca, *"Gain-saturated 10.9 nm tabletop laser operating at 1 Hz repetition rate,"* Optics Letters **35**, 414 (2010)

[1.100] Y. Liu, Y. Wang, M. A. Larotonda, B. M. Luther, J. J. Rocca, and D. T. Attwood, *"Spatial coherence measurements of a 13.2 nm transient nickel-like cadmium soft x-ray laser pumped at grazing incidence",* Optics Express **14**, 12872-12879 (2006)

[1.101] A. Klisnick, O. Guilbaud, D. Ros, K. Cassou, S. Kazamias, G. Jamelot, J. C. Lagron, D. Joyeux, D. Phalippou, Y. Lechantre, M. Edwards, P. Mistry, G.J. Tallents, *"Experimental study of the temporal coherence and spectral profile of the 13.9nm transient X-ray laser",* JQRST **99,** 370-380 (2006).

[1.102] R. Smith, J. Dunn, J. Hunter, and J. Nilsen, S. Hubert, S. Jacquemot, C. Remond, R. Marmoret, M. Fajardo, P. Zeitoun, L. Vanbostal, C. Lewis, M. Ravet, F. Delmotte, *"Longitudinal coherence measurements of a transient collisional x-ray laser,"* Opt. Lett. **23**, 2291-2263 (2003).

[1.103] Momoko Tanaka, Masaharu Nishikino, Tetsuya Kawachi, Noboru Hasegawa, Masataka Kado, Maki Kishimoto, Keisuke Nagashima, Yoshiaki Kato, *"X-ray laser beam with diffraction-limited divergence generated with two gain media,"* Opt. Lett. **28**, 1680-1682 (2003).

[1.104] T. Ditmire, M. H. R. Hutchinson, M. H. Key, ' C. L. S. Lewis, A. MacPhee, I. Mercer, D. Neely, M. D. Perry, R. A. Smith, J. S. Wark and M. Zepf, *"Amplification of XUV harmonic radiation in a gallium amplifier,"* Phys. Rev. A **51**, R4337–R4340 (1995).

[1.105] Ph. Zeitoun, G. Faivre, S. Sebban, T. Mocek, A. Hallou, M. Fajardo, D. Aubert, Ph. Balcou, F. Burgy, D. Douillet, S. Kazamias, G. de Lachèze-Murel, T. Lefrou, S. le Pape, P. Mercère, H. Merdji, A. S. Morlens, J. P. Rousseau, C. Valentin, *"A high-*

intensity highly coherent soft X-ray femtosecond laser seeded by a high harmonic beam", Nature **431**, 426 (2004).

[1.106] T. Mocek, S. Sebban, G. Maynard, Ph. Zeitoun, G. Faivre, A. Hallou, M. Fajardo, S. Kazamias, B. Cros, D. Aubert, G. de Lachèze-Murel, J. P. Rousseau, and J. Dubau, *"Absolute Time-Resolved X-Ray Laser Gain Measurement",* Phys. Rev. Letters **95**, 173902 (2005)

[1.107] Y. Wang, E. Granados, M.A. Larotonda, M. Berrill, B. M. Luther, D. Patel, C. S. Menoni, J. J. Rocca, *"High-Brightness Injection-Seeded Soft-X-Ray-Laser Amplifier Using a Solid Target"*, Phys. Rev. Lett. **97**, 123901 (2006).

[1.108] Y. Wang, E. Granados, F. Pedaci, D. Alessi, B. M. Luther, M. Berrill, J. J. Rocca, *"Phase-coherent, injection-seeded, table-top soft-X-ray lasers at 18.9 nm and 13.9 nm,"* Nature Photonics **2**, 94-98 (2008)

[1.109] Y. Wang, M. Berrill, F. Pedaci, M. M. Shakya, S. Gilbertson, Z. Chang, E. Granados, B. M. Luther, M. A. Larotonda, J. J. Rocca, *"Measurement of 1-ps soft-x-ray laser pulses from an injection-seeded plasma amplifier",* Phys. Rev. A **79**, 023810 (2009)

[1.110] M. Berrill, D. Alessi, Y. Wang, S. R. Domingue, D. H. Martz, B. M. Luther, Y. Liu and J. J. Rocca, *"Improved beam characteristics of solid-target soft x-ray laser amplifiers by injection-seeding with high harmonics,"* Optics Letters **35**, 2317 (2010)

[1.111] F. Pedaci, Y. Wang, M. Berrill, B. Luther, E. Granados, J. J. Rocca, *"Highly coherent injection-seeded 13.2 nm tabletop soft x-ray laser",* Opt. Lett. **33**, 491 (2008).

CHAPTER 2

SLAB-PUMPED TI:SAPPHIRE LASER PUMP SYSTEM FOR GENERATING SOFT X-RAY LASERS

2.1) Ti:Sapphire Laser System

The experiments were conducted using a Ti:sapphire pump laser system (shown in Figure 2.1) consisting of a mode-locked oscillator and three to four stages of chirped-pulse amplification. The oscillator (Kapteyn-Murnane Labs model TS) is Kerr lens mode locked and operates at 86 MHz with an output of 5-6 nJ per pulse, a pulse duration of 30 fs and a center wavelength of 800 nm. This crystal is pumped continuously with a 5 W, diode pumped, single longitudinal mode, frequency doubled, Nd:YVO_4 laser (Coherent Inc Verdi) operating at 532 nm. The output of the oscillator is chirped by a grating pulse stretcher resulting in pulse broadening to 210 ps and it is then electro-optically sampled at 10Hz with a pockels cell and polarizer. The stretched beam is then amplified to 2 mJ with the first stage 8 pass amplifier. The 1st stage amplifier Ti:Sapphire crystal (10 mm diameter cut at Brewster angle) is pumped by 130 mW from an 8 W, q-switched, frequency Doubled Nd:YAG laser (Spectra Physics QuantaRay PRO 270) operating at 10 Hz.

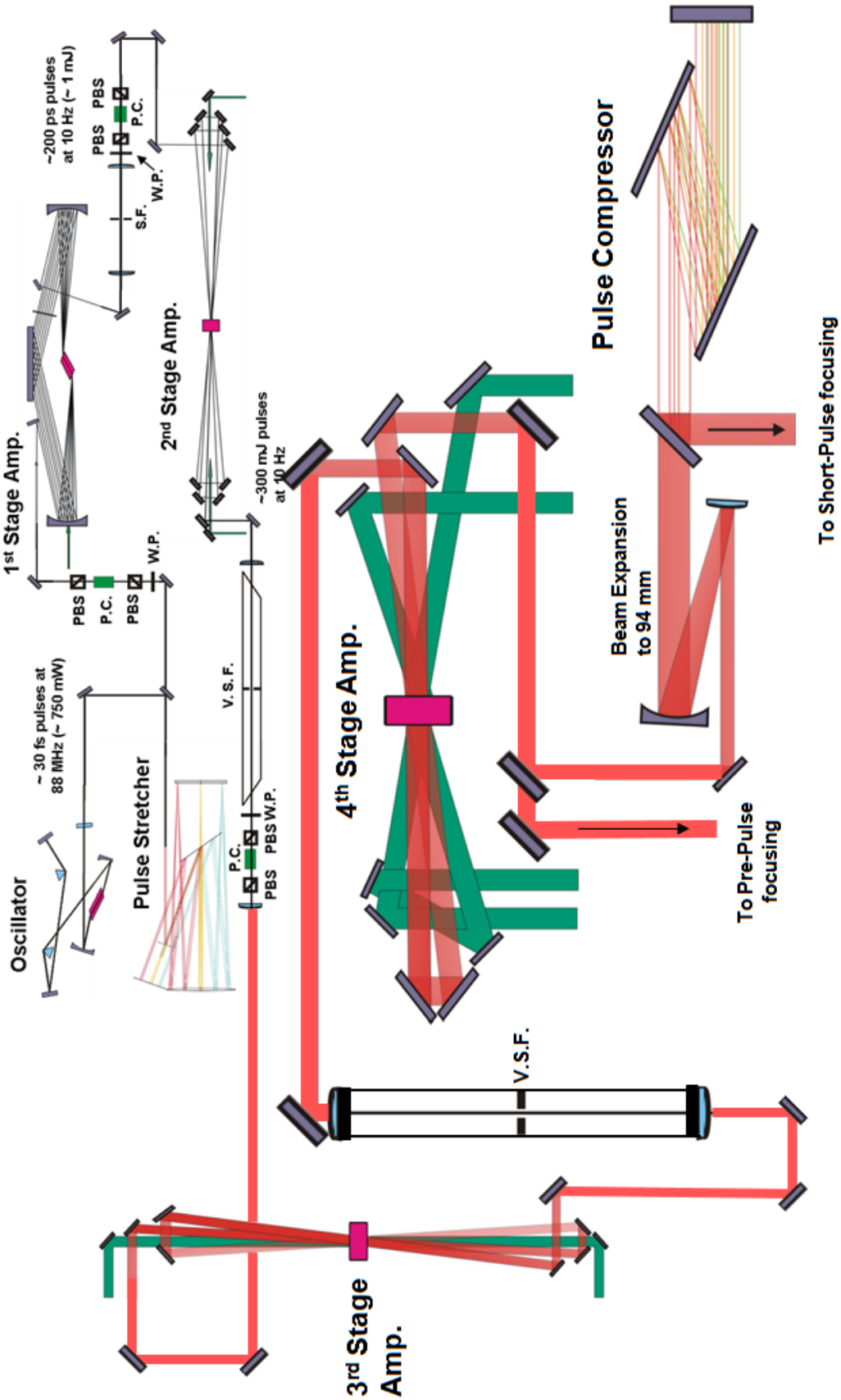

Figure 2.1: Diagram of the Ti:Sapphire Laser system used to generate Soft X-Ray Lasers

The 1st stage output is then spatially filtered and the spurious pre-pulse is removed by a pockels cell and polarizer combination. The laser is then amplified to ~280 mJ with a 2nd stage 5 pass Ti:Sapphire (15 mm diameter) bowtie amplifier. Each side of the amplifier is pumped by the remaining 7 W (390 mJ/pulse) of the 8 W doubled Nd:YAG laser. Figure 2.2 shows a cross correlation of the 2nd stage laser pulse fit to a gaussian shape with a 140 ps FWHM rising edge and a 240 ps FWHM falling edge. Following the 2nd stage amplifier, the laser is again spatially filtered and any pre-pulse is removed with a pockels cell and polarizer set.

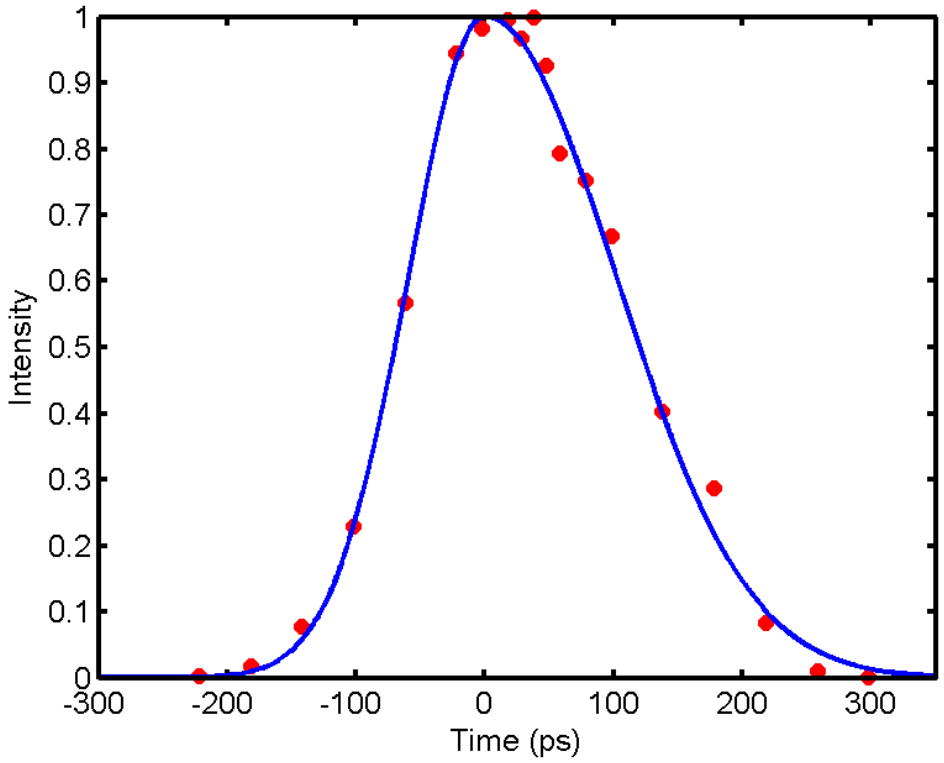

Figure 2.2: Cross correlation (data points) of the 2nd stage amplified uncompressed laser pulse fit to a gaussian shape (line) with a 140ps FWHM rising edge and a 240ps FWHM falling edge

The 3rd stage amplifier consists of a Ti:Sapphire crystal pumped at normal incidence on both faces by a frequency doubled Nd:glass laser system. In the experiments

obtaining saturated operation of a 10.9 nm Ni-like Te laser at 1Hz (Chapter 3) the 3rd stage is the final amplifier stage and is pumped by two 10 J beams (λ = 527 nm) from a Q-switched frequency doubled Nd:glass slab laser system described in section 2.2. Using this pump laser system, this Ti:Sapphire laser is capable of producing an uncompressed energy of ~7.5 J with a beam diameter of ~30 mm. An additional upgrade was completed for obtaining saturated operation of an 8.8 nm laser and observation of lasing down to 7.36 nm (Chapter 4). In this upgrade the 3rd and 4th stage amplifiers were pumped by a total of four 10 J (λ = 527 nm) beams from a Q-switched frequency doubled Nd:glass slab laser system described in section 2.3. Using this latest increase in pump energy, the Ti:Sapphire laser system can produce uncompressed laser pulses with ~12 J of energy at a 1 Hz repetition rate.

To conduct the SXR laser experiments, part of the uncompressed Ti:sapphire beam was directed to the pre-pulse arm with a beam splitter and the remaining energy was expanded to a beam diameter of 94 mm and compressed to 1-3 ps with a 1740 lines/mm grating compressor to form the main heating pulse. A waveplate and polarizer combination was added to the pre-pulse arm to divert a small fraction of the pre-pulse energy into an additional optional pre-pulse that precedes the main pulse by 5 ns. This pulse that precedes the main pre-pulse is responsible for creating the ion density profile. The addition of this pulse increased the 10.9 nm Ni-like Te SXR laser output, but did not have a significant effect on the generation of the 8.8 nm Ni-like La SXR laser.

2.2) 20J Slab Laser System for Pumping a Ti:Sapphire Laser

This section describes the Nd:glass slab laser system that was developed for pumping the Ti:Sapphire laser described in Section 2.1.With this pump configuration the Ti:sapphire system had 3 amplification stages and the 20 J of pump energy from this slab system was used for pumping the 3rd stage amplifier. Using this pump laser resulted in 7.5J of uncompressed laser energy which was capable of firing at a 2.5 Hz repetition rate. This increase in pump energy resulted in advancements in both high average power (and high energy) table-top SXR lasers near 13 nm and progress towards shorter wavelength table-top SXR lasers.

The following discussion is from the journal article titled: "High-energy 13.9 nm table-top soft-x-ray laser at 2.5 Hz repetition rate excited by a slab-pumped Ti:sapphire laser."

Published in: Optics Letters, Vol. 35, pp. 1632-1634 © 2010 Optical Society of America

Author List: D. H. Martz, D. Alessi, B. M. Luther, Y. Wang, D. Kemp, M. Berrill, and J. J. Rocca

The chirped pulse amplification Ti:sapphire system consists of a mode-locked oscillator and three multipass amplifiers. The third amplification stage is pumped by up to 20 J of 527 nm light from the frequency-doubled output of a Nd:glass zig-zag slab

laser developed in house. This dual-arm pump laser configuration (Fig. 2.3) was designed to operate at repetition rates of several hertz. It has long been recognized that the slab geometry has advantages that can overcome some of the limitations imposed by the more commonly used rod configuration [2.1,2.2]. The optical propagation along a zig-zag path, confined to the slab by total internal reflection, eliminates first-order thermal and stress-induced focusing. It also reduces stress-induced birefringence and allows for high repetition-rate, high-average-power operation limited only by stress-induced fracture of the laser glass [2.3]. The slab geometry has been previously used to amplify 1.053 μm nanosecond pulses to energies up to 25 J [2.4, 2.5]. More recently, a picosecond chirped pulse amplification laser based on Nd:glass slab amplifiers has been used to pump SXR lasers at a repetition rate of 0.1 Hz, producing pulse energies up to ~1 μJ [2.6, 2.7].

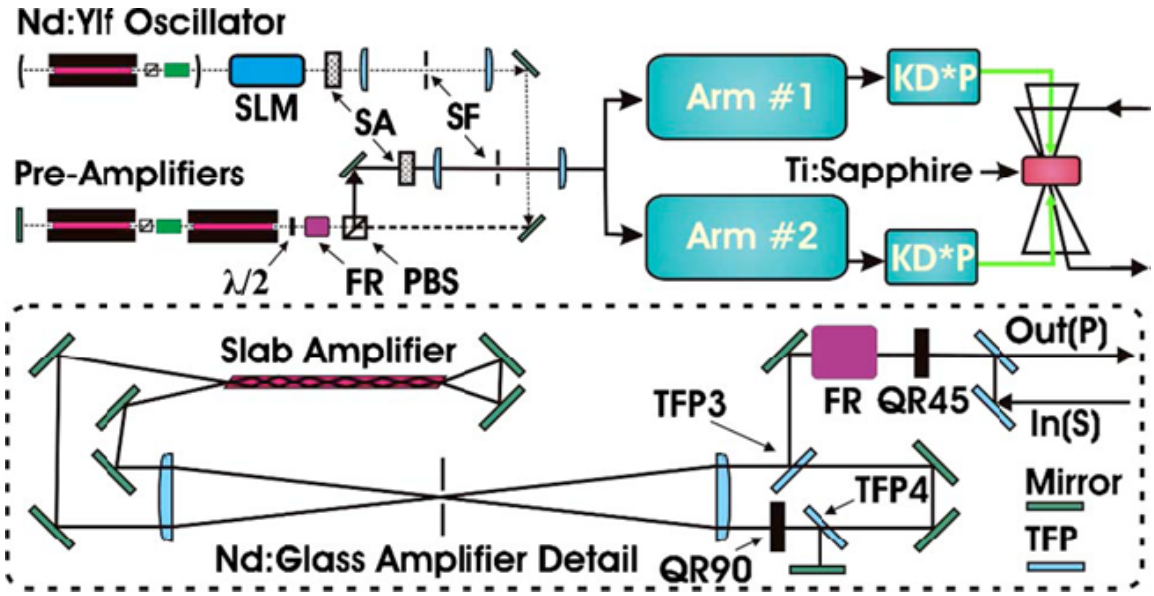

Figure 2.3: Top, block diagram of the third amplification stage of the Ti:sapphire pump laser system and associated slab amplifier laser system used in SXR laser experiments. Bottom, schematic diagram of the eight-pass Nd:glass slab amplifier. Labeled components shown are: spatial light modulator (SLM), serrated aperture (SA), spatial filter (SF), faraday rotator (FR), polarizing beam splitter (PBS), 45 degree quarts rotator (QR45), thin film polarize (TFP), 90 degree quartz rotator (QR90), potassium dideuterium phosphate crystal (KD*P).

As previously discussed, in our Ti:sapphire laser system, pulses from a Kerr lens mode-locked oscillator are stretched to 210 ps FWHM with a grating stretcher. The first two amplifier stages are pumped by a commercial 10 Hz frequency-doubled 800 mJ Q-switched Nd:YAG laser, resulting in 800 nm laser pulses with ~200 mJ energy, and the third multipass amplifier is pumped by the Nd:glass slab amplifiers.

The front end of the slab laser consists of a Q-switched Nd:YLF oscillator and a sequence of pre-amplifier Nd:YLF rods. The oscillator cavity consists of an 80% reflective output coupler with a radius of curvature of 3 m and a high reflector with a 10 m radius of curvature placed 0.58 m from the output coupler. The oscillator is q-switched with a pockels cell and polarizer combination. An iris is placed in the oscillator and closed to a diameter of about ~1 mm which prevents the preferential lasing of higher order spatial modes. The polarizer arrangement allows for lasing only perpendicular to the c-axis resulting in a central wavelength of 1053 nm. It produces 1 mJ pulses of ~19 ns FWHM at a 5 Hz repetition rate in a TEM_{00} gaussian mode.

The pulses from the oscillator are directed through an active liquid crystal spatial light modulator (SLM) and are relay imaged onto a serrated aperture (SA) and then spatially filtered to produce a beam with a super-Gaussian intensity profile. The beam is then imaged into a preamplifier consisting of two 7 mm diameter Nd:YLF rods arranged in a double-pass configuration to yield pulse energies of ~120 mJ. The double pass amplification is accomplished by using a polarizing beam splitter (PBS) cube, a Faraday rotator (FR) and a half-wave plate $\lambda/2$ combination. The output of the preamplifier is imaged onto a second serrated aperture and spatial filter (SF) pair to obtain a flat-top beam profile. This profile is relay imaged throughout the rest of the system. The beam is

subsequently stretched onto an oval of 8 mm × 120 mm dimension through a pair of cylindrical anamorphic imaging telescopes (not shown in Fig. 2.3) to conform to the 10 mm × 140 mm cross section of the slab amplifiers shown in figure 2.4. The resulting beam is split into two identical arms by a 50% beam splitter, and each beam is amplified

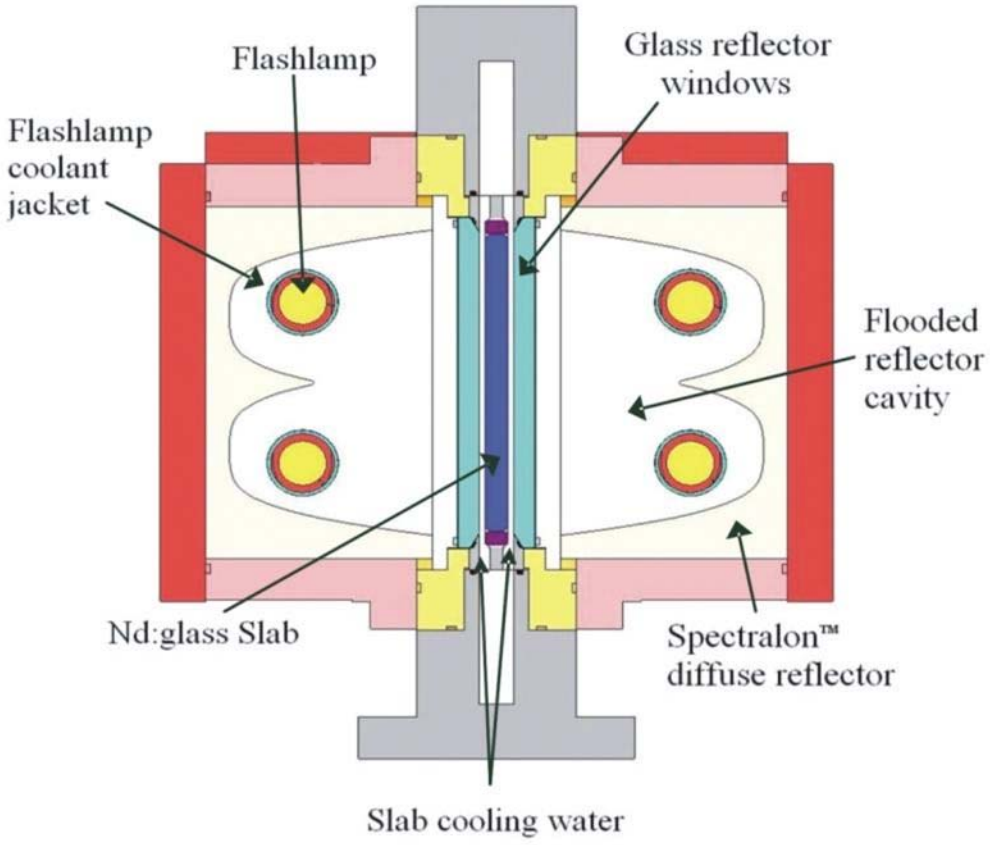

Figure 2.4: Cross sectional view of slab head showing 10 x 140 x 400 mm slab, flashlamps, reflector cavity, and water flow channels.

by eight passes through the 400 mm long slab amplifiers. The slabs were pumped by four Xe flashlamps, which were driven with a 300 μs electrical pulse, depositing ~700 J of electrical energy per lamp. Each arm operates in the following fashion. The input (S-polarized) beam reflects off a thin film polarizer (TFP) pair and travels through a 45° quartz rotator (QR45)/FR combination. The beam remains S polarized and is then injected into an eight-pass amplifier cavity by a third TFP (TFP3). With a relay imaging

telescope, the pulses are directed into the slab for two passes of amplification. The same telescope images the beam back through a 90° quartz rotator (QR90), changing the polarization to P, resulting in transmission through TFP4. The beam is then reinjected along the path of the input beam (passing through TFP3) for an additional two passes through the slab. After a total of four passes the beam again passes through QR90, restoring the polarization to S, thereby causing it to be ejected by TFP4 to a normal incidence mirror. The mirror directs the beam back on itself, reversing the process for a total of eight passes before being sent back through the QR45/FR pair, resulting in P polarization and ejection by the input TFP.

Each slab amplifier arm generates pulses with an energy of up to 18 J that are frequency doubled in a pair of KD*P crystals to produce up to 10 J of λ =527 nm light in each arm. Both beams are reshaped to 30 mm diameter and imaged into the 30-mm-thick third-stage Ti:sapphire amplifier rod. A near flat-top pump beam is achieved by adjusting the input beam's intensity profile by using the SLM. Three-pass amplification of the λ=800 nm 200 mJ laser pulses through the third stage Ti:sapphire amplifier produces pulse energies up to 7.5 J at a 2.5 Hz repetition rate with a typical spatial profile shown in Fig. 2.5(b). Figure 2.5(a) shows a series of consecutive laser shots acquired while operating the amplifier at 1 Hz repetition rate. The shot-to-shot energy variation was measured to be ~1%.

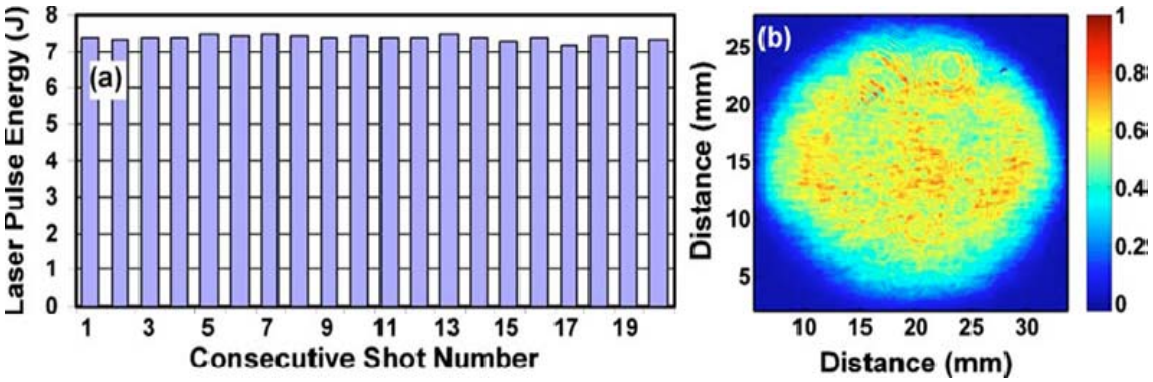

Figure 2.5: (a) Shot-to-shot variation of amplified λ=800 nm Ti:sapphire laser pulse energy measured at a 1 Hz repetition rate. The average laser pulse energy is 7.4 J, and the standard deviation σ=1%. (b) Typical intensity profile of the amplified λ =800 nm beam.

2.3) 40J Slab Laser System for Pumping a Ti:Sapphire Laser

To make further progress in the development of shorter wavelength table-top soft x-ray lasers, considerably more excitation laser energy is needed due to the steep scaling as a function of shorter wavelength. This increase in Ti:sapphire laser energy was accomplished by adding a 4th amplification stage and developing a flashlamp Nd:glass slab laser system capable of producing both 5 J to pump the third stage amplifier and 35 J (@ 527 nm) to pump the 4th stage amplifier. This Nd:glass laser system is similar to the one described in Chapter 2.2. The most significant difference between the two systems is the use of a slab pre-amplifier and the replacement of the 8-pass slab amplification scheme with a double-pass arrangement. Figure 2.6 shows the output pulse energy resulting from double pass amplification through one of the Nd:glass slab as a function of seed energy. Seeding a single slab with a 1.75 J beam results in a double pass output of 12 J. The resulting beam was split into four equal 3J beams to seed each of the two pass 4 slab amplifiers. This resulted in four 18 J beam. This arrangement has several advantages. Thermal and stress induced aberrations from the slab and spherical aberrations from

multiple passes through a relay image telescope are reduced resulting in an increase in doubling efficiency and a more uniformly distributed pump profile. The double-pass arrangement does not allow for an unintentional laser cavity to be formed as in the 8-pass system which can result in an increase of inter-cavity energy. The double-pass system is easier to align which reduces the chance of edge diffraction in the high energy laser beam, facilitating its day-to-day use. The double-pass system does not require the extensive use of expensive, custom large-area optics such as the faraday rotators, thin film polarizers and 7" diameter achromat lenses.

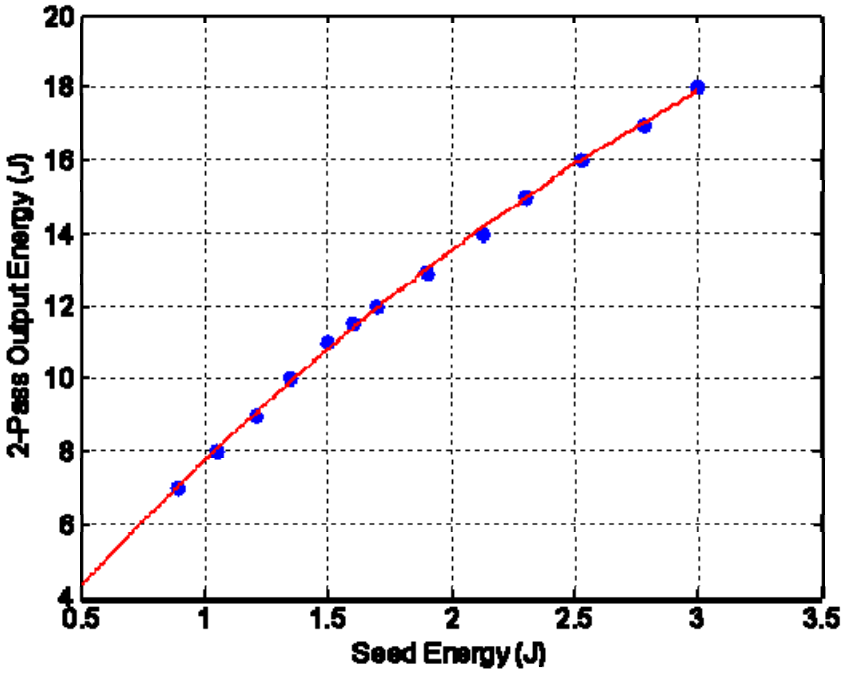

Figure 2.6: Double-pass output energy of a flashlamp pumped Nd:glass amplifier as a function of seed energy

The front end of the 40 J slab system consists of an Nd:YLF oscillator (identical to that used in Chapter 2.2) and a sequence of pre-amplifier Nd:YLF rods shown in figure 2.7. Pulses from the oscillator with an energy of 5 mJ are relay imaged and expanded

onto a serrated aperture and spatial filter combination to produce super-gaussian spatial profile pulses of 280 mJ after amplification in two passes through two 7 mm diameter Nd:YLF rods. A pockels cell and polarizer are placed between the 1st and 2nd passes to reduce ASE. The pulses pass through an optical isolator consisting of a polarizer, faraday rotator, waveplate and additional polarizer to prevent back reflections from travelling through the system.

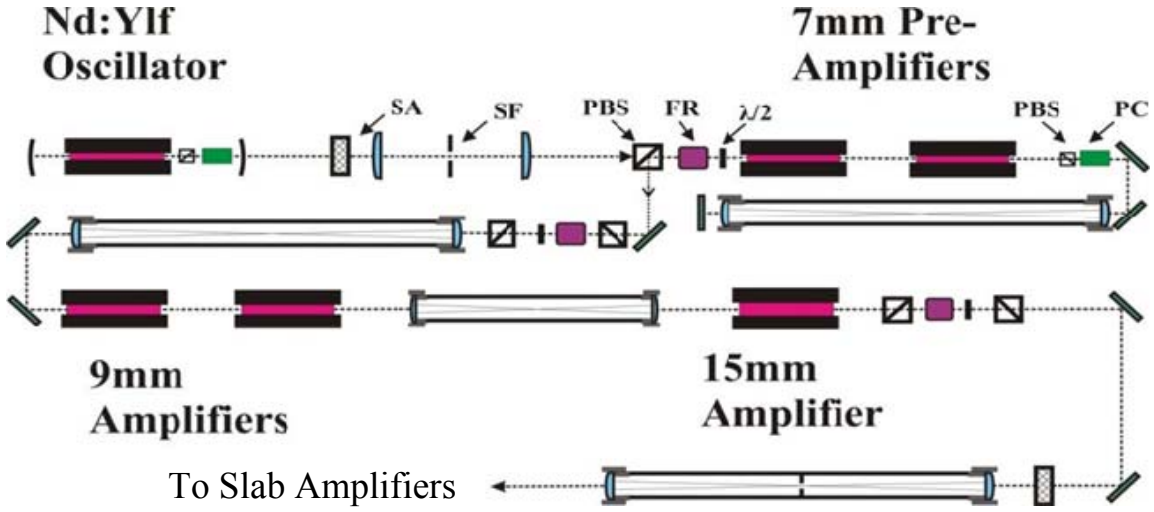

Figure 2.7: Diagram of Nd:YLF oscillator front end and and pre-amplifiers for the slab laser system. Labeled components are: serrated aperture (SA), spatial filter (SF), polarizing beam splitter (PBS), faraday rotator (FR), pockels cell (PC),

After relay imaging and single pass amplification in two 9mm diameter Nd:YLF rods the pulses reach an energy of 1.1 J. The pulses are relay imaged and amplified by a single pass through a 15 mm diameter Nd:YLF rod reaching an energy of 2.5 J. An anamorphic telescope expands the beam to an 8 mm x 120 mm oval to fit the 10 mm x 140 mm aperture of the same slab amplifiers used in Chapter 2.2. A serrated edge and horizontal slit aperture (in vacuum) are used in this up telescope to allow for defining the 8mm width of the beam and allowing for slight adjustment to prevent clipping by the edges of the slab faces.

The pre-amplified pulses are injected into the slab amplification system shown in figure 2.8. Seed pulses are double-passed through a single Nd:glass slab reaching 12 J energy per pulse. The beam is subsequently relay-imaged and split into four 3 J beams, each used to seed additional double-pass slabs resulting in four 18J beams. To limit depolarization of the beam thin film polarizing mirrors are used after each slab, but are not necessary between the first and second passes. Four KD*P doubling crystal pairs similar to those used in the pump laser described in section 2.2 are used in this system with a doubling efficiency of ~ 55% to produce four 10 J beams at the 2nd harmonic wavelength of 527 nm. Half of the energy of one arm (~5 J) is directed to the 3rd stage Ti:sapphire amplifier to produce Ti:Sapphire pulses of 1.9 J and the remaining 30-35 J is used for pumping of the 4th stage amplifier. Figure 2.9(a) shows the output energy of the fourth Ti:sapphire stage as a function of pump energy. Uncompressed laser pulses with up to 12 J of energy are obtained at a 1 Hz repetition rate with a good quality spatial profile (Figure 2.9b) when the 4th stage is pumped with ~34 J.

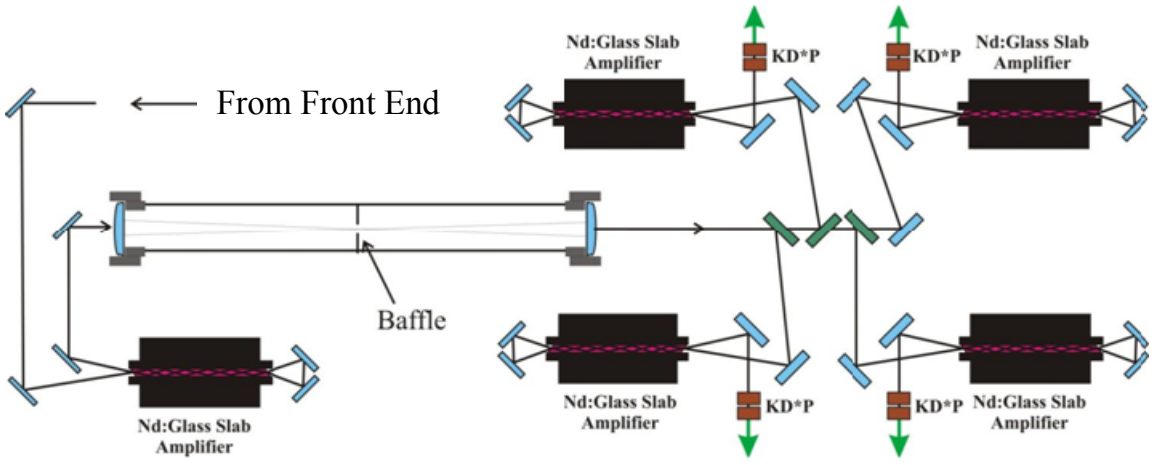

Figure 2.8: Diagram of Nd:glass slab amplifier system consisting of a double-passed seed slab and four double pass slabs producing a total of four 10 J, $\lambda = 527$ nm laser pulses.

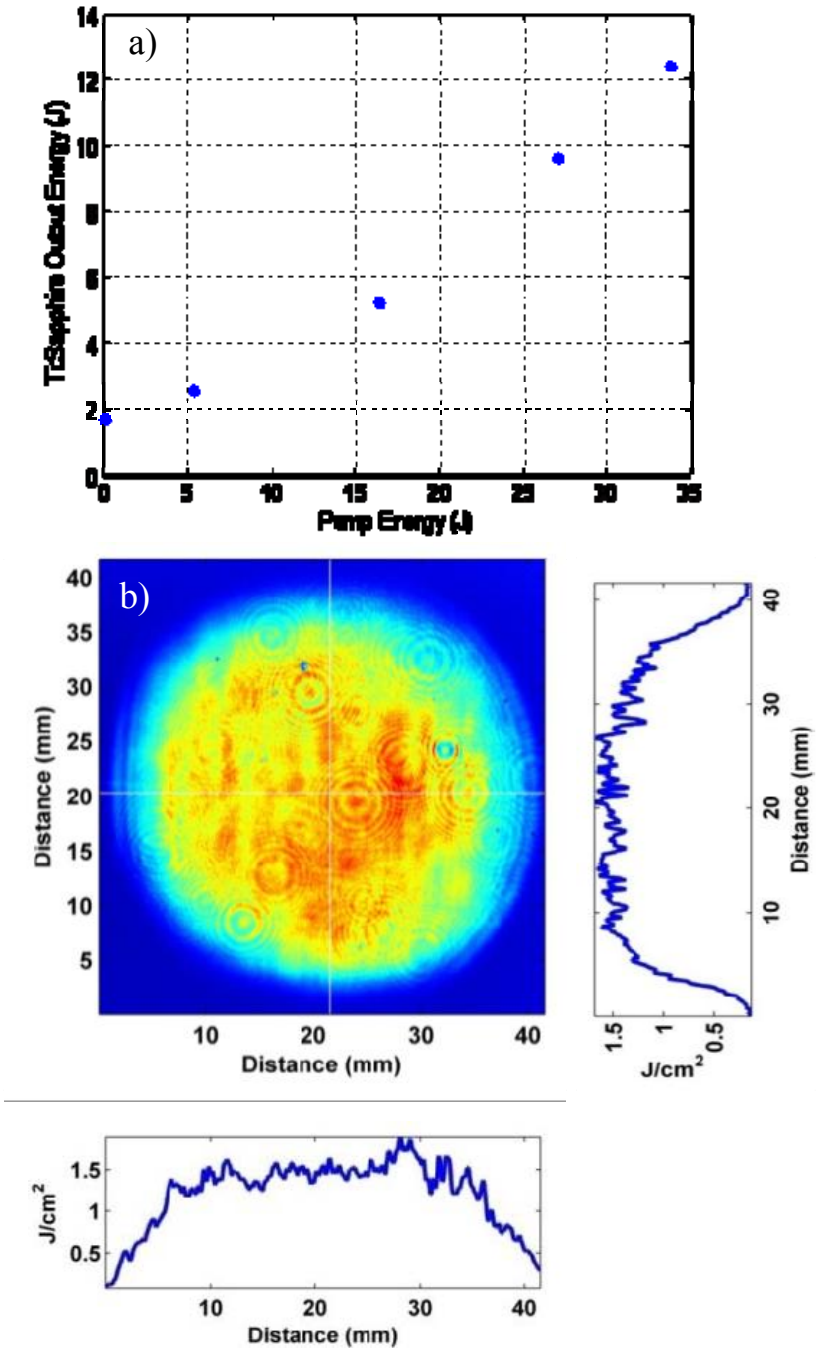

Figure 2.9: (a) Output of the 4th stage of the Ti:Sapphire laser system as a function of green pump laser energy. (b) Spatial profile and cuts of a 12J uncompressed Ti:Sapphire laser pulse.

2.4) References

[2.1] W. S. Martin and J. P. Chernoch, *"Multiple Internal Reflection Face-Pumped Laser,"* U.S. Patent 3,633,126 (January 4, 1972).

[2.2] J. Eggleston, T. Kane, K. Kuhn, J. Unternahrer, and R. Byer, *"The slab geometry laser-Part I: Theory,"* IEEE J. Quantum Electron. **20**, 289 (1984).

[2.3] T. Kane, J. Eggleston, and R. Byer, *"The slab geometry laser-II: Thermal effects in a finite slab,"* IEEE J. Quantum Electron. **21**, 1195 (1985).

[2.4] C. B. Dane, L. E. Zapata, W. A. Neuman, M. A. Norton, and L. A. Hackel, *"Design and operation of a 150 W near diffraction-limited laser amplifier with SBS wavefront correction,"* IEEE J. Quantum Electron. **31**, 148 (1995).

[2.5] M. J. Shoup, J. H. Kelly, and D. L. Smith, *"Design and testing of a large-aperture, high-gain, Brewster's angle zigzag Nd:glass slab amplifier,"* Appl. Opt. **36**, 5827 (1997).

[2.6] Y. Ochi, N. Hasegawa, T. Kawachi, and K. Nagashima, *"Development of a chirped pulse amplification laser with zigzag slab Nd:glass amplifiers dedicated to x-ray laser research,"* Appl. Opt. **46**, 1500 (2007).

[2.7] Y. Ochi, T. Kawachi, N. Hasegawa, M. Nishikino, T. Ohba, M. Tanaka, M. Kishimoto, T. Kaihori, K. Nagashima, and A. Sugiyama, *"Demonstration of SubmicroJoule, Spatially Coherent Soft-X-ray Laser Pumped by 0.1 Hertz, 10 Joule, Picosecond Laser,"* Jpn. J. Appl. Phys. **48**, 120212 (2009).

CHAPTER 3

HIGH REPETITION RATE OPERATION OF SATURATED TABLETOP SOFT X-RAY LASERS IN TRANSITIONS OF NEON-LIKE IONS NEAR 30 NM

This chapter presents the first demonstration of grazing incidence laser pumping in Ne-like SXR lasers. Average powers exceeding 1 microwatt in laser transitions of Ne-like ions at wavelengths near 30 nm were demonstrated. Gain-saturated operation was obtained at a repetition rate of 5 Hz by exciting solid targets with Ti:sapphire pump pulses of ~1 J energy and 8 ps duration impinging at grazing incidence of 20 degrees. Gain-length products of about 20 were obtained in the 30.4 nm and 32.6 nm transitions of Ne-like V and Ne-like Ti respectively. Strong lasing was also observed in Ne-like Cr at 28.6 nm and in the 30.1 nm line of Ne-like Ti. This average power makes these table-top sources suitable for applications.

Published in: Optics Express, Vol. 13, No. 6, pp. 2093-2095 © 2005 Optical Society of America

Author List: D. Alessi, B. M. Luther, Y. Wang, M. A. Larotonda, M. Berrill, and J. J. Rocca

3.1) Introduction

There is much interest in the development of compact soft x-ray lasers capable of generating high average powers for applications. This requires operation of the soft x-ray amplifiers in the gain-saturated regime at high repetition rate. The first soft x-ray lasers to achieve high average powers used collisional electron impact excitation of Ne-like ions in a capillary discharge plasma [3.1,3.2]. Capillary discharge excitation has produced average powers of a few mW in the 46.9 nm line of Ne-like Ar. Collisional optical-field-ionization lasers operating at 10 Hz repetition rate in Pd-like Xe at 41.8 nm [3.3,3.4] and in Ni-like Kr at 32.8 nm [3.5] have also been reported to reach gain saturation. Saturated soft x-ray amplification in transitions of Nelike and Ni-like ions excited by transient collisional electron excitation was also obtained but only at repetition rates of one shot every several minutes in plasmas heated by picoseconds duration pulses of 3-7 J energy [3.6-3.8]. In recent work the energy necessary to pump transient collisional soft x-ray lasers has been significantly reduced using a grazing incidence pumping geometry that increases the absorption of the pump beam in the gain region [3.9-3.12]. This pumping geometry significantly increases the energy deposition efficiency of the pump beam into the gain region by taking advantage of refraction to increase the path length of the pump rays through this region of the plasma. Excitation of Mo plasmas at a grazing incidence angle has resulted in gain saturated operation in the 18.9 nm line of Ni-like Mo at 5-10 Hz repetition rate [3.9-3.11]. Most recently saturated laser operation at 5 Hz repetition rate was obtained in several transitions of Ni-like ions with wavelengths ranging from 16.4 nm to 13.9 nm by grazing incidence heating of plasmas with 8 picosecond pulses of

1 J energy [3.12]. It is of significant interest to extend these results to other isoelectronic sequences, as different applications require access to different wavelengths. For example, the characterization of extreme ultraviolet optics for solar coronal studies would significantly benefit from compact high repetition lasers with wavelengths between 30 and 37 nm that includes both the HeII 30.4 nm line and strong lines of FeXI-XVI [3.13].

Herein we report the extension of gain saturated high repetition rate laser-pumped transient soft x-ray lasers to transitions in Ne-like ions using grazing incidence pumping. High average power soft x-ray laser operation was obtained for the first time to our knowledge in the $2p^5 3p\,^1S_0 \rightarrow 2p^5 3s\,^1P_1$ transitions of Ne-like Ti and V at 32.6 nm and 30.4 nm respectively. We also observed strong lasing in the corresponding line in Ne-like Cr at 28.6 nm, and in the 30.1 nm $2p^5 3d\,^1P_1 \rightarrow 2p^5 3p\,^1P_1$ line of Ne-like Ti which inversion relies on strong re-absorption of the 2.335 nm resonant transition linking the $3d\,^1P_1$ laser upper level to the ion ground state [3.14].

3.2) Experimental Setup

The pump beam geometry is similar to the one used in recent experiments with Ni-like ions [3.10-3.12]. The targets were 4 mm wide polished slabs with a thickness of 2 mm for Ti and V and 1mm for Cr. They were irradiated with pulses from a Ti:sapphire laser system operating at a center wavelength of 800 nm consisting of a mode-locked oscillator and three stages of chirped-pulse amplification. A beam splitter was placed at the exit of the third amplifier stage to direct a fraction of the energy of the uncompressed laser pulses (120 ps duration) into the pre-pulse arm. The rest of the laser energy was compressed to 8 ps to form the main heating pulse. Pre-pulses of 0.35 J for Ti and 0.5 J

for V and Cr, were used to form a plasma by irradiating the target at normal incidence. This pre-pulse was preceded by a 10 mJ pre-pulse about 5 ns before. The pre-pulses were focused into a 4.1 mm long × 30 μm wide line using the combination of a spherical and a cylindrical lens. The plasma was allowed to expand to reduce the density gradient and it was subsequently rapidly heated by the 8 ps duration pulse with ~ 1 J of energy impinging at a selected grazing incidence angle onto the target. The short pulse was focused into a line of the same size utilizing an f = 76.2 cm parabolic mirror placed at 7 degrees from normal incidence. The normal to the target surface was tilted from the axis defined by the pre-pulse beam to form grazing incidence angles of 17, 20 or 23 degrees with respect to the axis of the short pulse beam. The plasma emission was attenuated with calibrated Al filters and a set of metallic meshes of measured transmissivity. The soft x-ray laser beam was monitored using a flat field spectrograph composed of a 1200 l/mm gold coated variably spaced spherical grating and a 1 square inch back-illuminated CCD detector array placed in the image plane of the grating.

3.3) Experimental Results

Figure 3.1 shows on-axis spectra corresponding to 4 mm long plasmas of Ti, V and Cr irradiated at a grazing incidence angle of 20 degrees. In the Ti experiment the energy of the picosecond pulse was 1 J. In the V and Cr experiments the energy of the main pre-pulse was increased to 0.52 J at expense of the energy of the picosecond pulse, which in these cases was ~ 0.9 J. In all cases, the $3p^1S_0 \rightarrow 3s^1P_1$ line of the Ne-like ions is observed to clearly dominate the spectra. In the case of Ti, lasing was also observed in

the 30.1 nm $3d^1P_1 \rightarrow 3p^1P_1$ line of the Ne-like ion, but its intensity of was weaker for the range of pump parameters investigated.

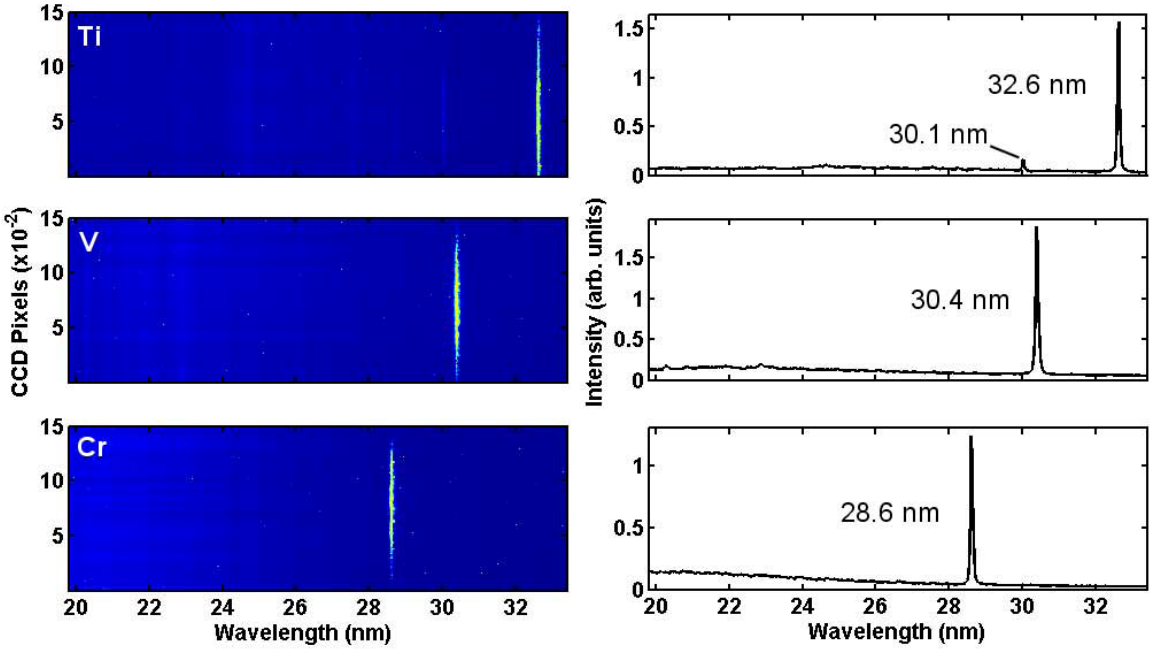

Figure 3.1: Single shot on-axis spectra of 4 mm long line focus plasmas showing lasing in the $2p^53p^1S_0$-$2p^53s^1P_1$ transition of Ne-like Ti, V and Cr ions. In all three cases, this laser-line dominates the spectrum.

Figure 3.2 shows the variation of the soft x-ray laser output intensity as a function of the angle of incidence of the short pulse beam for all three lasers. At an incidence angle of 17 degrees lasing was observed for the $3p^1S_0$-$3s^1P_1$ lines of the Ne-like ions of all three species (see Fig. 3.2). However, at this angle the pump beam is deposited in a region where the electron density is lower than the optimum value for maximum soft x-ray laser output intensity. The output intensity of all three lasers was observed to increase significantly for an angle of 20 degrees, for which refraction helps to couple the pump beam into a region of higher electron density ($2x10^{20}$ cm^{-3}). At the steeper angle of incidence of 23 degrees a significant fraction of the beam energy is absorbed in a higher density region where the electron density gradients are too steep for optimum

amplification. Also contributing to a lower laser output at this angle is the shorter duration of the gain and the increased mismatch between the velocity of the traveling wave of the pump and the speed of light in the plasma.

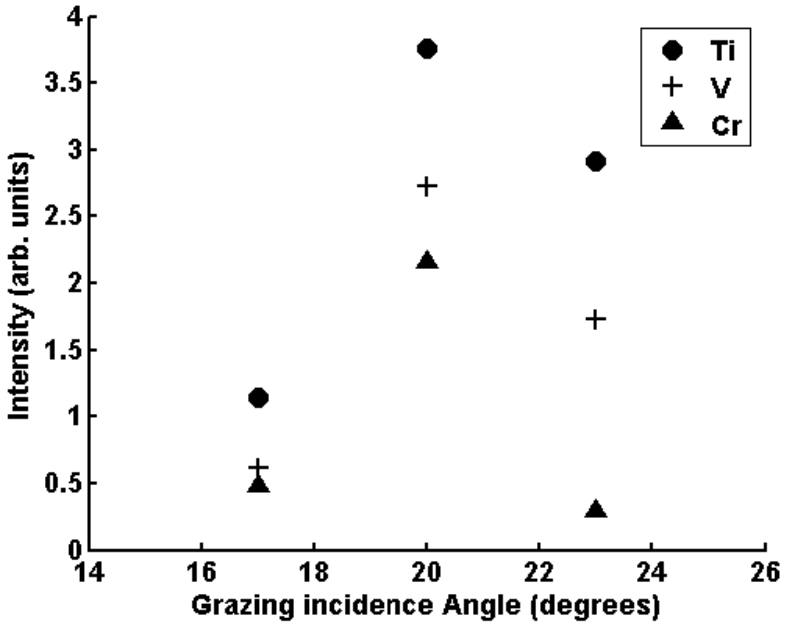

Figure 3.2: Variation of output laser intensity as a function of grazing incidence angle for Ne-like Ti, V and Cr. Each point represents the mean of 15 or more consecutive laser shots. In all three cases the laser operates best at 20 degrees. At this angle the standard deviation of each data set ranges from 14% to 38% of the mean.

Figure 3.3 shows the output intensity of the 30.4 nm line of Ne-like V as a function of time delay between the main pre-pulse and the short pulse for a grazing incidence angle of 20 degrees. Strong lasing was observed to occur over a wide range of time delays. The optimum delays were observed to be approximately 600 ps for Ne-like Ti and 450 ps for Ne-like V and Cr. This result, which follows the same trend observed for lasing in Ni-like ion transitions [3.12], is related to the fact that a more highly ionized pre-plasma is required for lasing at higher Z, allowing less time for plasma cooling during expansion and recombination. The maximum intensity of the 30.1 nm line of Ne-

like Ti occurs at a delay of 520 ps, an earlier time than the optimum for the 32.6 nm line. At this delay the intensity of the 30.1 nm line is typically half that of the 32.6 nm line.

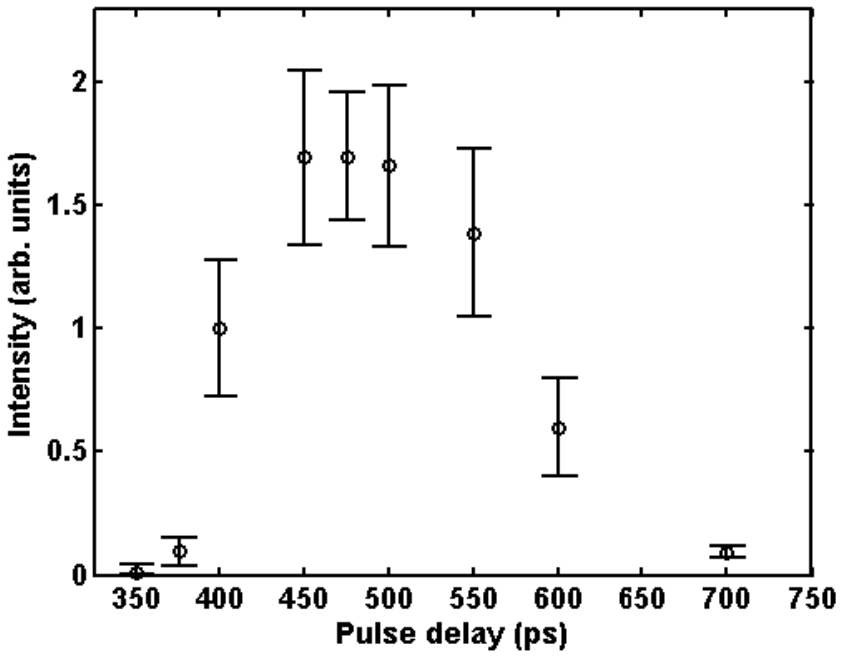

Figure 3.3: Laser output intensity of the 30.4 nm line of Ne-like V as a function of time delay between the main pre-pulse and the short pulse. Lasing is strong for delays ranging from 400 ps to 600 ps. Each point is the average of 10 or more laser shots; the error bars correspond to ± the standard deviation of the set.

Figure 3.4 shows the variation of the laser intensity of the 30.4 nm line of the Ne-like V as a function of plasma length. The solid line represents a fit of the data with the expression derived by Tallents et al. for the variation of the laser intensity with plasma length taking into account gain saturation [3.15].

For short plasma lengths the laser output intensity is observed to increase exponentially with a small signal gain coefficient of g = 72 cm-1, until saturation is reached. The gain-length product reaches 21.7 for a 4 mm target, which exceeds the gain-length product value of ~ 15 at which most collisionally excited soft x-ray lasers have been observed to reach gain saturation. A similar measurement for the 32.6 nm line of

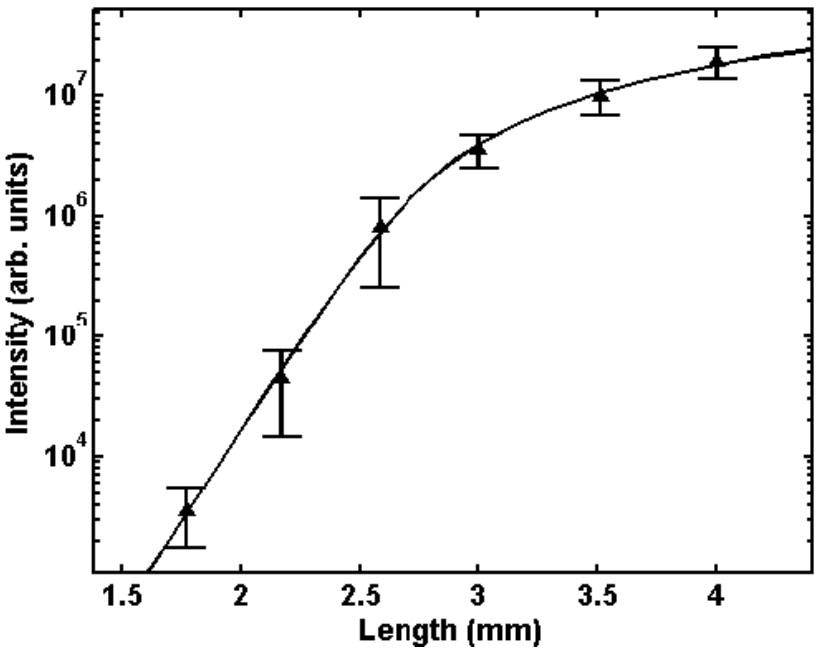

Figure 3.4: Intensity of the 30.4 nm line of Ne-like V as a function of plasma length. Each point is the average of 10 or more shots. A fit of the data results in a gain coefficient of 72 cm-1 and a gain-length product of 21.7. Each point is the average of 10 or more laser shots; the error bars correspond to ± the standard deviation of the set.

Ne-like Ti yielded a comparable gain-length product, gxl= 18.4. The gain-length product for the 28.6 nm line of Ne-like Cr was not measured, but the laser output intensity was lower than for the other two elements.

Operation at 5 Hz repetition rate was demonstrated for both Ne-like Ti and V moving the targets at a constant velocity of 40 μm per shot. Figure 3.5 illustrates a series of 250 contiguous laser shots at this repetition rate for the 30.4 nm line of Ne-like V. The 250 consecutive shots have a distribution characterized by a standard deviation which is 35% of the mean. Operation at 5 Hz repetition rate yielded laser pulses with an energy of up to 540 nJ, estimated from the counts on the CCD taking into account the quantum efficiency of the detector and the losses. The average pulse energy was 300 nJ corresponding to an average output power of about 1.5 μW. For the 32.6 nm line of Ne-

like Ti the maximum soft x-ray laser pulse energy observed was estimated to be 780 nJ. The average energy for this line was 530 nJ, corresponding to an average output power of about 2.6 μW. This is to our knowledge the first report of laser average powers in excess of 1 microwatt in this region of the spectrum.

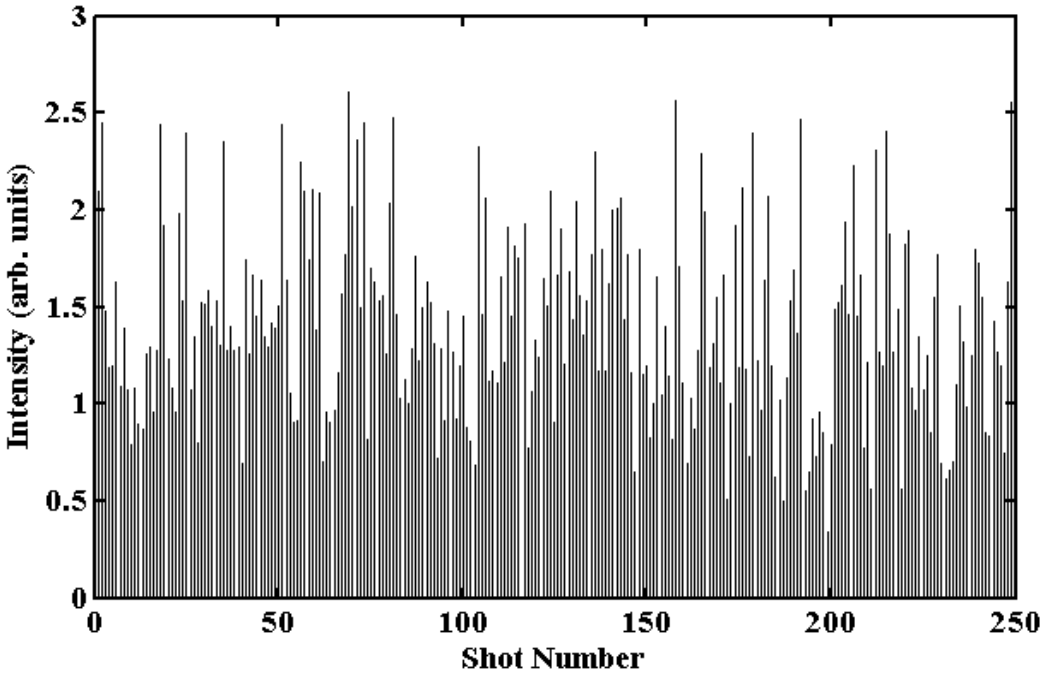

Figure 3.5: Shot-to-shot variation of the intensity of the 30.4 nm Ne-like V laser line at 5 Hz repetition rate. The 250 consecutive shots have a distribution characterized by a standard deviation which is 35% of the mean.

3.4 Conclusions

In summary, microwatt average power laser-pumped Ne-like ion lasers were demonstrated for the first time to our knowledge. This demonstration of saturated high repetition rate table-top lasers in Ne-like Ti and Ne-like V and its possible extension to other isoelectronic lines will significantly increase the diversity of soft x-ray laser wavelengths available for applications requiring high average powers.

3.5) References

[3.1] B. R. Benware, C. D. Macchietto, C. H. Moreno, and J. J. Rocca, *"Demonstration of a High Average Power Tabletop Soft X-Ray Laser,"* Phys. Rev. Lett. **81**, 5804-5807 (1998).

[3.2] M. Frati, M. Seminario, J. J. Rocca, *"Demonstration of a 10-μJ tabletop laser at 52.9 nm in neonlike chlorine,"* Opt. Lett. **25**, 1022-1024 (2000).

[3.3] S. Sebban, R. Haroutunian, P. Balcou, G. Grillon, A. Rousse, S. Kazamias, T. Marin, J. P. Rousseau, L. Notebaert, M. Pittman, J. P. Chambaret, A. Antonetti, D. Hulin, D. Ros, A. Klisnick, A. Carillon, P. Jaegle, G. Jamelot, J. F. Wyart, *"Saturated Amplification of a Collisionally Pumped Optical-Field-Ionization Soft X-Ray Laser at 41.8 nm,"* Phys. Rev. Lett. **86**, 3004-3007 (2001).

[3.4] A. Butler, A. J. Gonsalves, C.M. McKenna, D. J. Spence, S. M. Hooker, S. Sebban, T. Mocek, and I. Bettaibi, and B. Cros*, "Demonstration of a Collisionally Excited Optical-Field-Ionization XUV Laser Driven in a Plasma Waveguide,"* Phys. Rev. Lett. **91**, Art. 205001 (2003).

[3.5] S. Sebban, T. Mocek, D. Ros, L. Upcraft, P. Balcou, R. Haroutunian, G. Grillon, B. Rus, A. Klisnick, A. Carillon, G. Jamelot, C. Valentin, A. Rousse, J. P. Rousseau, L. Notebaert, M. Pittman, D. Hulin, *"Demonstration of a Ni-Like Kr Optical-Field-Ionization Collisional Soft X-Ray Laser at 32.8 nm,"* Phys. Rev. Lett. **89**, Art. 253901 (2002).

[3.6] P. V. Nickles, V. N. Shlyaptsev, M. Kalachnikov, M. Schnürer, *"Short Pulse X-Ray Laser at 32.6 nm Based on Transient Gain in Ne-like Titanium,"* Phys. Rev. Lett. **78**, 2748-2751 (1997).

[3.7] J. Dunn, Y. Li, A. L. Osterheld, J. Nilsen, J. R. Hunter, V. N. Shlyaptsev, *"Gain Saturation Regime for Laser-Driven Tabletop, Transient Ni-Like Ion X-Ray Lasers,"* Phys. Rev. Lett. **84**, 4834-4837 (2000).

[3.8] K. A. Janulewicz, A. Lucianetti, G. Priebe, W. Sandner, P. V. Nickles, *"Saturated Ni-like Ag x-ray laser at 13.9 nm pumped by a single picosecond laser pulse,"* Phys. Rev. A **68**, Art. 051802 (2003).

[3.9] R. Keenan, J. Dunn, V. N. Shlyaptsev, R. Smith, P. K. Patel, D. F. Price, *"Efficient pumping schemes for high average brightness collisional x-ray lasers,"* in Soft X-Ray Lasers and Applications V, E. E. Fill, S. Suckewer, eds., Proc. SPIE **5197**, 213-220 (2003), and R. Keenan, J. Dunn, P. K. Patel, D. F. Price, R. F. Smith, V. N. Shlyaptsev, *"High repetition rate grazing incidence pumped X-ray laser operating at 18.9 nm,"* Phys. Rev. Lett. **94**, 103901 (2005)

[3.10] B. M. Luther, Y. Wang, M. A. Larotonda, D. Alessi, M. Berrill, M. C. Marconi, V. N. Shlyaptsev, J. J. Rocca, *"Saturated high-repetition-rate 18.9-nm tabletop laser in nickellike molybdenum,"* Opt. Lett. **30**, 165- 167 (2005).

[3.11] M. A. Larotonda, B. M. Luther, Y. Wang, Y, Liu, D. Alessi, M. Berrill, A. Dummer, F. Brizuela, C. S. Menoni, M. C. Marconi, V. N. Shlyaptsev, J. Dunn, and J. J. Rocca, *"Characteristics of a Saturated 18.9-nm Tabletop Laser Operating at 5-Hz Repetition Rate,"* IEEE J. Select. Topics Quantum Elecron. **10**, 1363-1367 (2004)

[3.12] Y. Wang, M. A. Larotonda, B. M. Luther, D. Alessi, M. Berrill, V. N. Shlyaptsev, and J. J. Rocca, *"Demonstration of saturated high repetition rate tabletop soft x-ray lasers at wavelengths down to 13.9 nm and gain down to 10.9 nm,"* Phys. Rev. A **72**, 053807 (2005)

[3.13] R.J. Thomas and J. M. Davila. *"EUNIS: a solar EUV normal incidence spectrometer,"* in UV/EUV and Visible Space Instrumentation for Astronomy and Solar Physics, O. H. W. Siegmund, S. Fineschi, M. A. Gummin, eds., Proc. SPIE **4498**, 161-172 (2001).

[3.14] J. Nilsen, *"Analysis of a picosecond-laser-driven Ne-like Ti x-ray laser,"* Physical Review A **55**, 3271-3274 (1997).

[3.15] G. J. Tallents, Y. Abou-Ali, M. Edwards, R. E. King , G. J. Pert, S. J. Pestehe, F. Strati, R. Keenan, C. L. S. Lewis, S. Topping, O. Guilbaud, A. Klisnick, D. Ros, R. Clarke, D. Neely, and M. Notley, *"Saturated and Short Pulse Duration X-Ray Lasers,"* in X-Ray Lasers:2002, J. J. Rocca, J. Dunn, and S. Suckewer, eds., AIP Conf. Proc. **641**, 291-297 (2002).

CHAPTER 4

GAIN-SATURATED 10.9 NM TABLETOP LASER OPERATING AT 1 HZ REPETITION RATE

This chapter discusses the demonstration of a gain-saturated 10.9 nm table-top soft x-ray laser operating at 1 Hz repetition rate. Lasing occurs by collisional electron impact excitation in the $4d^1S_0 \rightarrow 4p^1P_1$ transition of nickel-like Te in a line-focus plasma heated by a chirped pulse amplification Ti:sapphire laser. With an average power of 1 microwatt and pulse energy up to ~2 microjoules this laser extended the ability to conduct table-top laser experiments to a shorter wavelength. These results were obtained using the Ti:sapphire pump system described in section 2.2.

Published in: Optics Letters, Vol. 35, Issue 3, pp. 414-416 © 2010 Optical Society of America

Author List: D. Alessi, D. H. Martz, Y. Wang, M. Berrill, B. M. Luther and J. J. Rocca

4.1) Introduction

There is great interest in extending tabletop soft x-ray lasers to shorter wavelengths for applications. Of particular interest is the development of gain-saturated lasers that can be fired repetitively, producing the average power required for many applications. Both capillary discharges and laser-created plasmas have been successfully used to demonstrate gain-saturated collisionally excited tabletop lasers that operate at wavelengths between 46.9 and 13.2 nm at repetition rates of several hertz [4.1-4.10]. However, the steep wavelength scaling of the energy necessary to pump such lasers imposes a challenge to the demonstration of gain-saturated high-repetitionrate lasers at shorter wavelengths. As a result, the use of tabletop soft x-ray lasers in applications has been limited to wavelengths above 13 nm. The shortest wavelength tabletop laser used in applications is a gain-saturated 13.2 nm nickel-like Cd laser that enabled the implementation of broad area microscopes with spatial resolution down to 38 nm [4.11].

Herein we report the demonstration of a gain saturated tabletop 10.9 nm laser in the 4d $^1S_0$->4p $^1P_1$ transition of nickel-like Te that operates at 1 Hz repetition rate. Lasing in nickel-like Te was first demonstrated using 520 J of laser pump energy to heat a collisionally pumped plasma [4.12]. More recently gain in this transition was obtained in a tabletop setup using 1 J pulses of 8 ps duration impinging at a grazing angle of 23 deg to heat a precreated plasma [4.4]. However, the output laser intensity was weak and far from saturation, producing an insufficient photon flux for applications. Model computations conducted using a 1.5 dimension hydrodynamic/atomic physics code developed in house [4.13] suggest that gain-saturated lasing in the λ=10.9 nm $4d^1S_0 \rightarrow 4p^1P_1$ transition of nickel-like Te can be generated by irradiation of a solid Te

target with a sequence of pulses from a chirped pulse amplification laser with a total energy of less than 4 J. Figure 4.1 shows the simulated evolution of the plasma parameters and resulting gain coefficient for the 10.9 nm laser line. The plasma is assumed to be created by a sequence of two 210 ps duration prepulses with intensities of 4.8×10^{10} Wcm^{-2} and 1.8×10^{12} Wcm^{-2} separated by 5.6 ns, and to be subsequently transiently heated with a 5 ps FWHM duration pulse with an intensity of 9.8×10^{13} Wcm^{-2} impinging at 30 deg grazing incidence. This pumping geometry, which is inherently a traveling wave, takes advantage of the refraction of the pump beam in the electron

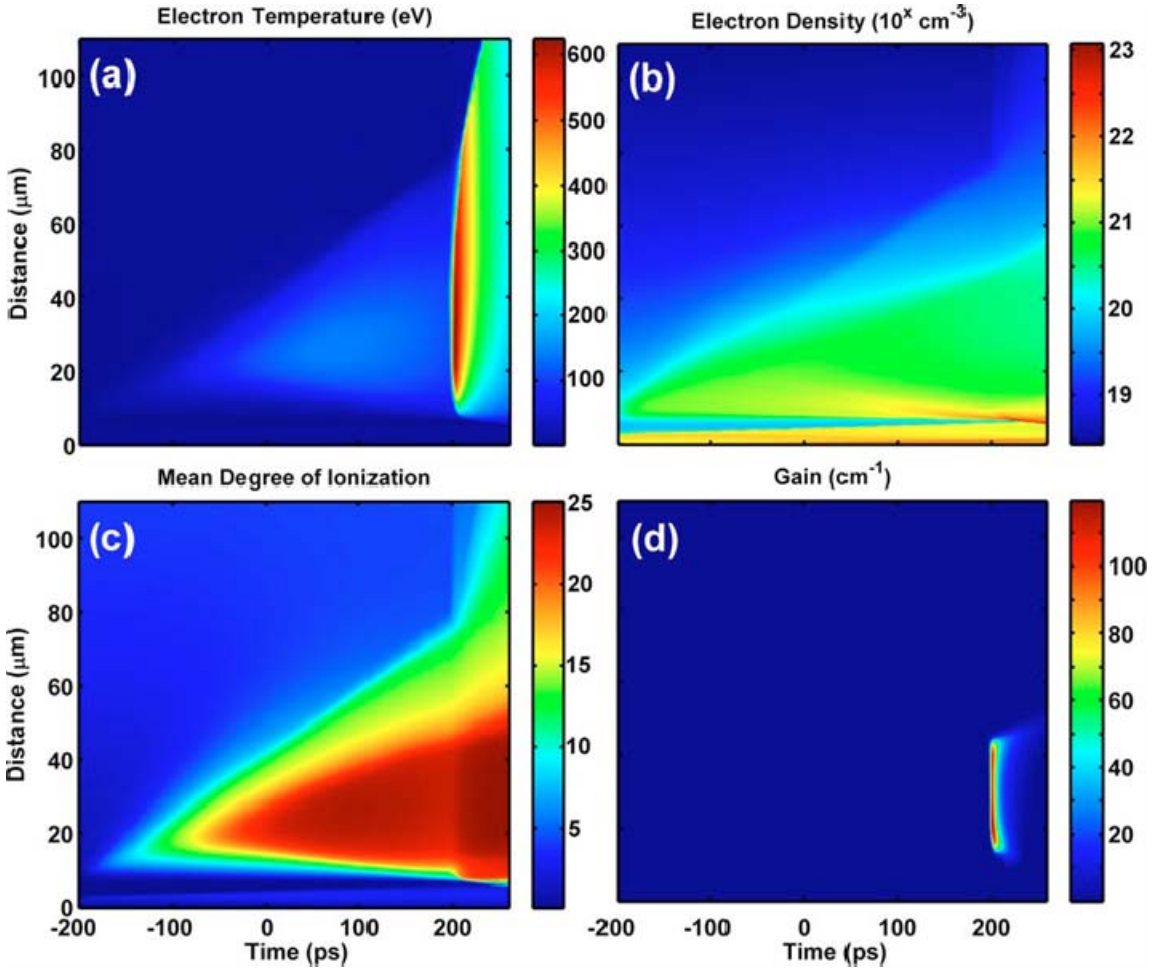

Figure 4.1: Simulated evolution of (a) electron temperature, (b) electron density, (c) mean degree of ionization, and (d) λ=10.9 nm gain coefficient for a Te plasma

density gradient of the pre-created plasma to efficiently deposit energy into a plasma density region with optimum conditions for amplification [4.3-4.6, 4.8-4.10, 4.14]. The first laser pulse is responsible for creating the ion density profile, and the second laser pulse heats the plasma, ionizing 40% of the ions into the nickel-like state over a relatively broad region [Fig. 4.1(c)]. A dip in the degree of ionization develops between the outer region where the prepulse energy is absorbed and the target region dominated by pressure ionization. The short pulse energy is coupled by refraction into a region where the electron density is ~$4x10^{20}$ cm^{-3} and rapidly increases the electron temperature to ~600 eV [Fig. 4.1(a)]. This is computed to generate a transient inversion resulting in a peak gain of ~120 cm^{-1} with a FWHM duration of ~9 ps [Fig. 4.1(d)]. A 3-D post-processor ray-tracing code [4.13] predicts a spatially integrated gain of 64 cm^{-1}. The experiments described below used similar excitation conditions to demonstrate a λ=10.9 nm tabletop nickel-like Te laser operating at a repetition rate of 1 Hz with an average power of ~1 μW.

4.2) Experimental Setup

The experiment was conducted by rapidly heating a 5-mm-wide solid Te slab target at the irradiation conditions described above using a chirped-pulse amplification Ti:sapphire laser system. Three stages of amplification were used to amplify λ =800 nm pulses to energies up to 5.5 J before compression. After the third amplification stage the stretched pulses have a duration of 210 ps. A beam splitter placed after the final amplification stage was used to redirect 40% of the energy into a prepulse arm used to create a plasma with relatively smooth density gradients. About 2% of the energy was

split to create an initial plasma that was subsequently ionized to the nickellike ionization stage by the second 210 ps duration pulse. The two prepulses, separated by 5.6 ns, were focused into a 30 μm x 5 mm FWHM line onto the target. The remaining 60% of the laser energy was compressed into a 5 ps FWHM pulse in a vacuum grating compressor constructed using dielectric diffraction gratings [4.15] and focused into an overlapping line of the same dimension. The plasma emission was filtered by a 0.3-μm-thick Al foil and a 0.3-μm-thick Zr foil both with parylene support and was directed onto a grazing incidence spectrometer consisting of a 1200 lines/mm variable-line-spaced grating and a back-illuminated CCD detector.

4.3) Experimental Results

Figure 4.2 shows the measured λ=10.9 nm laser intensity as a function of time delay between the peaks of the main prepulse and the short pulse. Strong soft x-ray lasing was observed to take place over a relatively narrow range of excitation delays centered at 200 ps. Lasing is observed to cease when the delay is increased to 400 ps. However, further increase of the delay results in weak lasing around 550 ps. This late laser pulse was predicted by the simulations. It occurs when Co-like ions recombine into Ni-like ions, indicating that the plasma is slightly over-ionized at the time of peak laser gain.

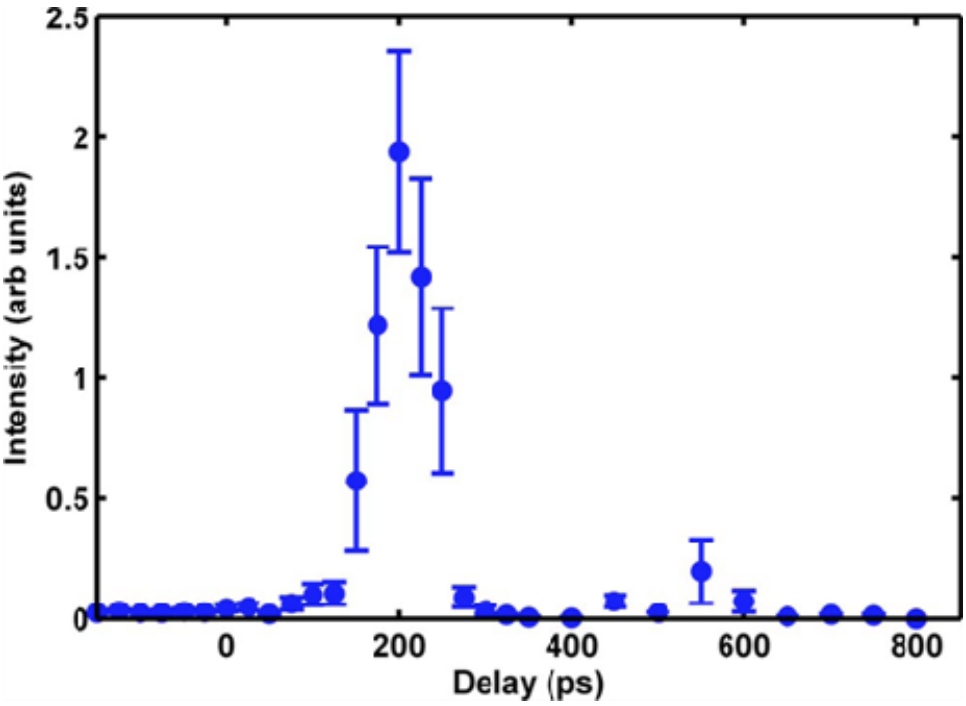

Figure 4.2: Measured λ=10.9 nm laser intensity as a function of delay between the prepulse and short pulse.

Figure 4.3(a) shows a series of on-axis single-shot spectra and their corresponding vertical integrations for plasmas of different lengths between L=1.8 and 5 mm. The total pump energy on the target was fixed at 3.4 J. For a target length of 1.8 mm the 10.9 nm laser line is very weak and has an intensity similar to that of other plasma lines. The soft x-ray laser intensity rapidly grows with target length to dominate the entire spectra, eventually reaching saturation. From these spectra it was determined that for the 5 mm target the soft x-ray laser beam divergence in the direction parallel to the target is 8.5±1 mrad. The measured soft x-ray laser intensity as a function of target length is shown in Fig. 4.3(b). The line is a fit of the data with an equation by Tallents et al. [4.16] that takes into account gain saturation. The fit shows a small signal gain of g_0=45.3 cm^{-1} and an

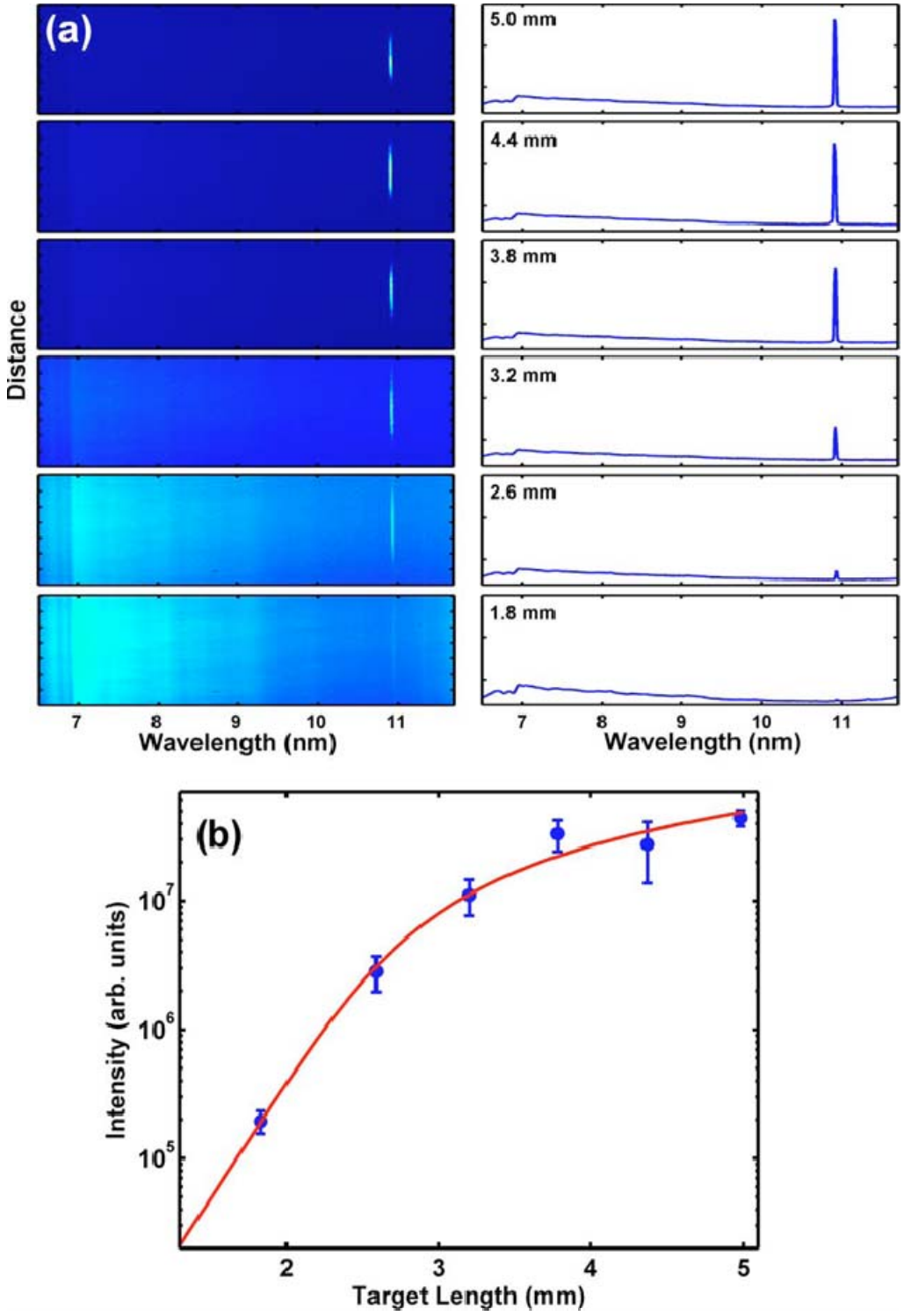

Figure 4.3: (a) On-axis single-shot spectra from the Te plasma for increasing plasma column lengths from 1.8 to 5 mm. Strong lasing is observed at 10.9 nm. (b) Measured laser line intensity as a function of plasma column length. Each data point is an average of eight laser shots, and error bars correspond to one standard deviation.

integrated gain length product of 14.1 at 5 mm. At about 3 mm, the intensity starts to show signs of saturation.

Results of the variation of the soft x-ray laser pulse energy at a laser repetition rate of 1 Hz are shown in Fig. 4.4. These data were obtained pumping a 6-mm-wide Te target with 4.2 J of total laser pump energy on target. The target was continually moved at a speed of 200 m per second to renew the surface irradiated by each shot. The soft x-ray laser average power obtained was ~1 μW. The shot-to-shot energy variation is characterized by a standard deviation of 36%. This large variation can be explained by the brittle nature of the tellurium target, which often fractures locally near the edges when irradiated with the high-energy pulses used in this experiment, affecting the subsequent laser shot. In comparison, in a similar experiment conducted with a Ag target that does not fracture we measured a λ=13.9 nm output pulse laser energy variation characterized by an 8% standard deviation. An increase in the speed at which the Te target is moved should decrease the shot-toshot fluctuation in soft x-ray laser pulse energy. The energy of the most intense laser pulses was estimated to be ~2 μJ from the CCD counts, taking into account the attenuation of the filters, the grating efficiency, and the quantum efficiency of the detector. Assuming a laser pulse duration of 4–5 ps and a near-field laser spot of ~15 μm diameter, both resulting from the 3-D postprocessor ray-trace simulation, the laser beam intensity is estimated to reach ~2.5 x 10^{11} W cm^{-2}. This exceeds the 0.6–1.4 x 10^{10} Wcm^{-2} computed saturation intensity of this line for the plasma conditions of the experiment.

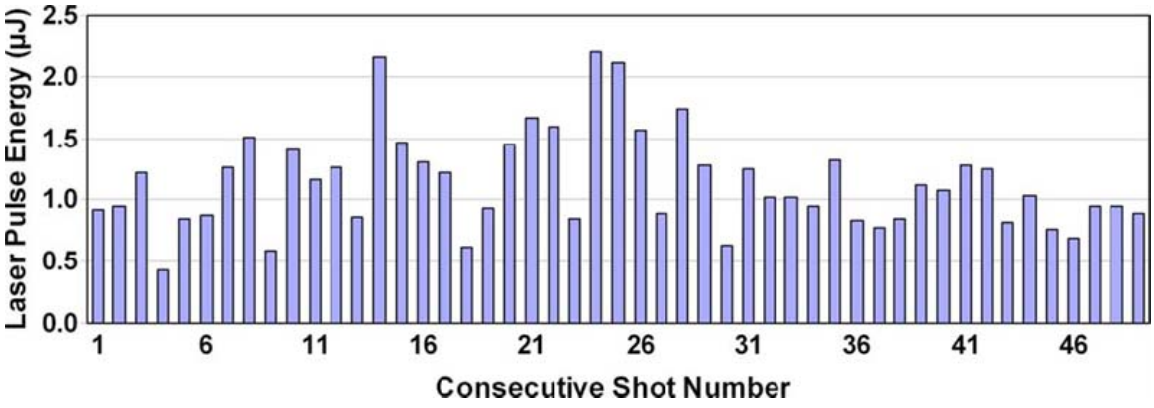

Figure 4.4: Sequence of λ=10.9 nm laser shots acquired at 1 Hz repetition rate achieving an average power of ~1 μW.

4.4 Conclusions

In summary, we have extended gain-saturated tabletop soft x-ray lasers down to 10.9 nm by transient excitation of a nickel-like Te plasma. To our knowledge, this is the shortest wavelength gain saturated tabletop laser reported to date. With an average power of ~1 μW and pulse energies of up to 2 μJ, this laser will enable applications of tabletop lasers at shorter wavelengths.

4.5) References

[4.1] B. R. Benware, C. D. Macchietto, C. H. Moreno, and J. J. Rocca, *"Demonstration of a High Average Power Tabletop Soft X-Ray Laser,"* Phys. Rev. Lett. **81**, 5804 (1998).

[4.2] S. Sebban, R. Haroutunian, P. Balcou, G. Grillon, A. Rousse, S. Kazamias, T. Marin, J. P. Rousseau, L. Notebaert, M. Pittman, J. P. Chambaret, A. Antonetti, D. Hulin, D. Ros, A. Klisnick, A. Carillon, P. Jaegle, G. Jamelot, and J. F. Wyart, *"Saturated Amplification of a Collisionally Pumped Optical-Field- Ionization Soft X-Ray Laser at 41.8 nm,"* Phys. Rev. Lett. **86**, 3004 (2001).

[4.3] B. M. Luther, Y. Wang, M. A. Larotonda, D. Alessi, M. Berrill, M. C. Marconi, J. J. Rocca, and V. N. Shlyaptsev, *"Saturated high-repetition-rate 18.9-nm tabletop laser in nickellike molybdenum,"* Opt. Lett. **30**, 165 (2005).

[4.4] Y. Wang, M. A. Larotonda, B. M. Luther, D. Alessi, M.Berrill, V. N. Shlyaptsev, and J. J. Rocca, *"Demonstration of high-repetition-rate tabletop soft-x-ray lasers with saturated output at wavelengths down to 13.9 nm and gain down to 10.9 nm,"* Phys. Rev. A **72**, 053807 (2005).

[4.5] J. J. Rocca, Y. Wang, M. A. Larotonda, B. M. Luther, M. Berrill, and D. Alessi, *"Saturated 13.2 nm high-repetition-rate laser in nickellike cadmium,"* Opt. Lett. **30**, 2581 (2005).

[4.6] D. Alessi, B. M. Luther, Y. Wang, M. A. Larotonda, M. Berrill, and J. J. Rocca, *"High repetition rate operation of saturated tabletop soft x-ray lasers in transitions of neon-like ions near 30 nm,"* Opt. Express **13**, 2093 (2005).

[4.7] M.-C. Chou, P.-H. Lin, C.-A. Lin, J.-Y. Lin, J. Wang, and S.-Y. Chen, *"Dramatic Enhancement of Optical-Field-Ionization Collisional-Excitation X-Ray Lasing by an Optically Preformed Plasma Waveguide,"* Phys. Rev. Lett. **99**, 063904 (2007).

[4.8] K. Cassou, S. Kazamias, D. Ros, F. Plé, G. Jamelot, A. Klisnick, O. Lundh, F. Lindau, A. Persson, C.-G.Wahlström, S. de Rossi, D. Joyeux, B. Zielbauer, D. Ursescu, and T. Kühl, *"Optimization toward a high-average-brightness soft-x-ray laser pumped at grazing incidence,"* Opt. Lett. **32**, 139 (2007).

[4.9] S. Kazamias, K. Cassou, D. Ros, F. Ple, G. Jamelot, A. Klisnick, O. Lundh, F. Lindau, A. Persson, C.-G. Wahlstrom, S. de Rossi, D. Joyeux, B. Zielbauer, D. Ursescu, and T. Kuhl, *"Characterization of a transient collisional Ni-like molybdenum soft-x-ray laser pumped in grazing incidence,"* Phys. Rev. A **77**, 033812 (2008).

[4.10] H. T. Kim, I. W. Choi, N. Hafz, J. H. Sung, T. J. Yu, K. H. Hong, T. M. Jeong, Y. C. Noh, D. K. Ko, K. A. Janulewicz, J. Tummler, P. V. Nickles, W. Sandner, and J. Lee, *"Demonstration of a saturated Ni-like Ag x-ray laser pumped by a single profiled laser pulse from a 10-Hz Ti : sapphire laser system,"* Phys. Rev. A **77**, 023807 (2008).

[4.11] G. Vaschenko, C. Brewer, F. Brizuela, Y. Wang, M. A. Larotonda, B. M. Luther, M. C. Marconi, J. J. Rocca, and C. S. Menoni, *"Sub-38 nm resolution tabletop microscopy with 13 nm wavelength laser light,"* Opt. Lett. **31**, 1214 (2006).

[4.12] H. Daido, S. Ninomiya, T. Imani, R. Kodama, M. Takagi, Y. Kato, K. Murai, J. Zhang, Y. You, and Y. Gu, *"Nickellike soft-x-ray lasing at the wavelengths between 14 and 7.9 nm,"* Opt. Lett. **21**, 958 (1996).

[4.13] M. Berrill, Ph.D Dissertation, Colorado State University, (2010)

[4.14] R. Keenan, J. Dunn, P. K. Patel, D. F. Price, R. F. Smith, and V. N. Shlyaptsev, "*High-repetition-rate grazing-incidence pumped x-ray laser operating at 18.9 nm,"* Phys. Rev. Lett. **94**, 103901 (2005).

[4.15] D. H. Martz, H. T. Nguyen, D. Patel, J. A. Britten, D. Alessi, E. Krous, Y. Wang, M. A. Larotonda, J. George, B. Knollenberg, B. M. Luther, J. J. Rocca, and C. S. Menoni, *"Large area high efficiency broad bandwidth 800 nm dielectric gratings for high energy laser pulse compression,"* Opt. Express **17**, 23809 (2009).

[4.16] G. J. Tallents, Y. Abou-Ali, M. Edwards, R. E. King, G.J. Pert, S. J. Pestehe, F. Strati, R. Keenan, C. L. S. Lewis, S. Topping, O. Guilbaud, A. Klisnick, D. Ros, R. Clarke, D. Neely, and M. Notley, *"Saturated and Short Pulse Duration X-Ray Lasers,"* in Eighth International Conference on X-ray Lasers, J. J. Rocca,J. Dunn, and S. Suckewer, eds., AIP Conference Proceedings Vol. **C641** (AIP, 2002), p. 291

CHAPTER 5

EFFICIENT EXCITATION OF GAIN-SATURATED SUB-9 NM WAVELENGTH TABLE-TOP SOFT X-RAY LASERS AND LASING DOWN TO 7.36 NM

This chapter discusses the efficient generation of sub-9-nm wavelength picosecond laser pulses of microjoule energy at 1-Hz repetition rate by a table-top laser. Gain-saturated lasing was obtained at 8.85-nm by collisional excitation of nickel-like lanthanum ions using a picosecond optical laser pulse of only 4-J energy to heat a pre-created plasma. Furthermore, isoelectronic scaling resulted in lasing at wavelengths as short as 7.36-nm. Simulations show that the collisionally broadened atomic transitions in these dense plasmas can support the amplification of sub-picosecond SXRL pulses.

This chapter was also submitted to Physical Review X in 2011.

Author List: David Alessi,[1,2] Yong Wang,[1,2] Bradley M. Luther,[1,2] Liang Yin,[1,2] Dale H. Martz,[1,2] Mark R. Woolston,[1,2] Yanwei Liu,[1,3] Mark Berrill,[1,2,4] and Jorge J. Rocca[1,2,5]

[1]*NSF Engineering Research Center for Extreme Ultraviolet Science and Technology*

[2]*Department of Electrical and Computer Engineering, Colorado State University, Fort Collins, CO 80523*

[3]*Department of Electrical Engineering and Computer Sciences, University of California Berkeley, Berkeley, CA*

[4]*Oak Ridge National Laboratory, Oak Ridge, TN 37830*

[5]*Department of Physics, Colorado State University, Fort Collins, CO 80523*

5.1) Introduction

The high demand for bright soft x-ray laser (SXRL) pulses greatly exceeds the beam time available at a few single-user free electron laser facilities [5.1, 5.2]. This motivates the development of more compact and widely accessible SXRLs for a broad range of experiments in small laboratory settings. Significant progress has been achieved in the past several years in the development of compact plasma-based soft x-ray lasers [5.3-5.10] (SXRL). However, repetitive operation of table-top SXRLs has been limited to wavelengths above 10.9 nm [5.10]. At lower wavelengths the large pump energy required has limited the repetition rate to typically a shot per hour [5.11-5.15]. Soft x-ray lasing at sub-10 nm wavelengths in lanthanide ions was first demonstrated using several hundred joules of optical laser pump energy [5.12, 5.13]. Lasing in nickel-like lanthanum at 8.85 nm was latter obtained using 18 J pulses from a chirped pulse amplification (CPA) laser to achieve transient excitation, but with a gain-length product ($g \times l = 7.7$) remained insufficient to reach gain-saturation [5.15]. Progress towards saturated lasing in this transition has been recently reported [5.16, 5.17]. In turn, lasing at 7.36 nm in nickel-like Sm was initially demonstrated using 130 J pump pulses [5.12] and latter gain-

saturation was reached using a ~40 J picosecond pump pulse added to a pre-pulse of similar energy [5.14]. Also recently the lasing threshold in this line was reached using 36 J of total optical pump pulse energy [5.18]. However, the practical realization of high repetition rate table-top lasers at sub-10 nm wavelengths requires obtaining gain-saturated lasing at significantly lower pump energies. We report the generation of gain-saturated picosecond SXRL pulses at 8.85 nm wavelength at 1 Hz repetition rate. The result was obtained using picosecond pump pulse with an unprecedentedly low energy of 4 J and a total optical pump energy of 7.5 J, that will make possible operation at high repetition rates. Furthermore, using the same pump energy we have also observed lasing at wavelengths down to 7.36 nm in transitions of higher Z nickel-like lanthanide ions, opening the prospect of practical gain-saturated table-top lasers at shorter wavelengths. Modeling suggests that these dense plasma amplifiers have the bandwidth necessary to sustain the amplification of sub-ps SXRL pulses.

We conducted hydrodynamic/atomic physics modeling and 3-dimensional ray trace simulations for an axially uniform plasma column of a constant width, 30 μm. This model is coupled with a complete atomic code that is capable of solving for the atomic populations of all ion species in the relevant energy levels using a fully transient solution, including full radiation transport. The results suggest gain-saturated amplification in the λ = 8.85 nm $4d^1S_0 \rightarrow 4p^1P_1$ line of nickel-like lanthanum can be achieved using a total pump energy of only 4 J. While the experimental realization can be expected to require larger pump energy to compensate for factors not considered in the model, such as processes that decrease absorption at high irradiation intensities [5.19], imperfections in the plasma column uniformity and target oxide layer, its magnitude is likely to remain in the range

that allows for high repetition rate SXRL operation. A peak gain of ~90 cm^{-1} with a duration of ~5 ps is computed to result from the irradiation of a solid lanthanum target with a sequence of a $3.3x10^{12}$ Wcm^{-2} pre-pulse 210 ps FWHM in duration followed by traveling wave excitation with a $2x10^{14}$ Wcm^{-2}, 3 ps FWHM duration pulse impinging a 35º grazing incidence. The short pulse is computed to rapidly heat the region of the pre-created plasma where the electron density is ~$6x10^{20}$ cm^{-3} to an electron temperature ~850 eV. Ray-trace simulations predict the SXRL pulse duration progressively shortens to reach 1.5-2 ps just before gain-saturation. As the pulse intensity continues to increase by an additional order of magnitude above saturation the laser pulse duration is computed to re-broaden to ~2.5 ps.

5.2) Experimental Setup

The SXRL results were obtained irradiating 1-2 mm thick solid slab targets with a sequence of two laser pulses from a λ = 800 nm Ti:sapphire CPA laser consisting of a normal incidence pre-pulse followed by a main picosecond pulse impinging at a grazing incidence angle of 35º with a traveling wave velocity of ~(1.04±0.03) c. The pump laser has four stages of amplification, of which the last two are pumped with the frequency doubled output of Nd-glass slab amplifiers designed to operate at repetition rates of up to 4 Hz [5.20]. The plasmas were created by normal incidence irradiation at I = $6x10^{12}$ Wcm^{-2} with a pre-pulse of 210 ps duration that is focused onto the target to form a ~30 μm × 6.4 mm FWHM line focus using the combination of a spherical and a cylindrical lens. The plasma created by this pre-pulse is allowed to expand to reduce the density gradient and is subsequently rapidly heated by irradiation at I = $6x10^{14}$ Wcm^{-2} with a 4 J

pulse of 1-3 ps duration shaped into a line-focus of the same dimension. The target surface was tilted with respect to the axis of the short pulse to define a grazing incidence angle of θ = 35° for efficient heating [5.3, 5.4]. At this angle of incidence refraction couples the pump beam energy into the plasma region where $n_e = 5.7\times10^{20}$ cm^{-3}. To assist in achieving efficient pumping we developed a new focusing geometry designed to create a plasma column of constant width along the target (Figure 5.1a). In the conventional implementations of grazing incidence pumping in which a parabolic or spherical mirror is used to focus the beam [5.3-5.5, 5.9, 5.10], the tilted target intercepts the short pulse pump beam at different distances from the beam waist. This creates a "butterfly" shape line-focus on target that

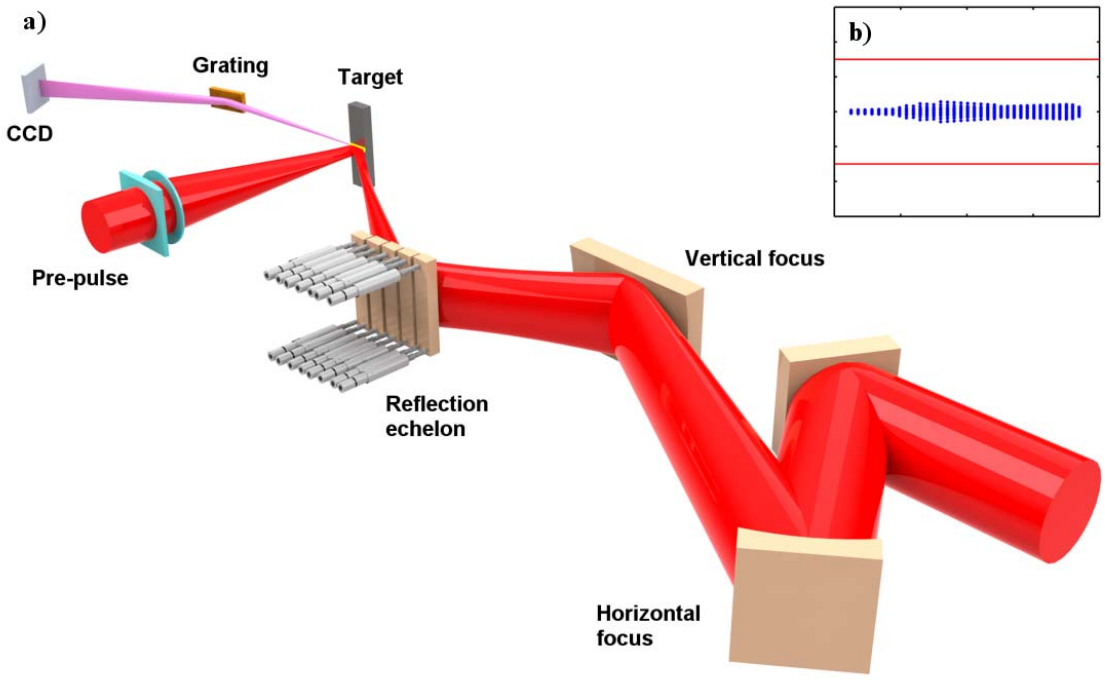

Figure 5.1: Schematic representation of the set up used in the sub-9 nm SXRL experiments. (a) A pair of cylindrical mirrors focuses the short pulse beam at 35º grazing incidence on target creating a line-focus of uniform width. A reflection echelon is used to obtain quasi-traveling wave excitation. (b) Raytrace simulation of the line-focus on target. All rays fall within the line width defined by diffraction (red lines).

for small f-number systems can deposit part of the pump energy outside the useful gain column, decreasing the gain. To overcome this limitation we focused the short pulse beam with a pair of cylindrical mirrors designed to create a line-focus of constant width along a target irradiated at grazing incidence. The beam first impinges on a cylindrical mirror of f = 6.5 m that is used to generate a 6.4 mm long line. The beam is subsequently made to impinge onto a second cylindrical mirror of f = 2.8 m that generates a 30 μm wide vertical focus. Each segment of the converging beam impinging on the vertical focus mirror has a unique focal length $f = R/(2\cos\theta)$ and a unique path length to the tilted target. The difference between path length and focal length is brought below the diffraction limit using an incidence angle of 54° on the vertical mirror (see raytrace simulations results in Fig. 5.1b).

Due to the short duration of the gain the mismatch between the propagation velocities of the pump pulse and the amplified pulse significantly reduces the amplification of the SXRL pulse. To overcome this limitation a reflection echelon [5.21, 5.22] composed of five mirror segments was used to obtain a quasi-traveling wave excitation velocity of ~(1.04±0.03) c. Measurements at 1-Hz repetition rate were obtained continuously moving the target at a speed of 200 μm/s to renew the surface after each shot. The output of the SXRLs was analyzed using a flat field spectrometer with a nominally 1200 lines/mm grating set at 3° grazing incidence and a back-illuminated CCD detector placed at 48 cm from the target. Zirconium filters with thickness up to 2.1 μm were used to avoid saturating the detector and to eliminate visible plasma light. The SXRL pulse energy was estimated from the CCD counts taking into account the

attenuation of the filters, the grating efficiency, and the quantum efficiency of the detector.

5.3) Experimental Results

Figure 5.2a shows a series of on-axis spectra as a function of plasma column length for a lanthanum plasma column created depositing 4 J of short pulse energy and a total of 7.5 J of optical pump energy on target at the irradiation conditions described above. Strong amplification is observed in the 8.85-nm $4d^1S_0 \rightarrow 4p^1P_1$ transition of Ni-like La. Figure 5.2b shows that the intensity grows by nearly four orders of magnitude as the plasma length increases from 1.7 mm to 6.2 mm. Saturation of the intensity is observed to have an onset at a plasma column length of ~4 mm. A fit of the data with an expression that takes into account gain saturation [5.23] yields a gain coefficient of 33 cm^{-1} and a gain-length product of 14.6. The energy of the most intense laser pulses was estimated to be 2.7 μJ from the CCD counts.

Gain-saturated operation was confirmed by measuring the SXRL flux at the exit of the amplifier. The near field profile of the 8.85 nm laser was recorded imaging the output of the plasma amplifier with a f = 25 cm near-normal incidence Mo-Y multilayer mirror onto a back-illuminated CCD detector. The mirror was measured at a synchrotron beam line to have a reflectivity of 25%. Fig. 5.3a shows the beam pattern at the amplifier exit consists of a spot with ~19 μm × 30 μm FWHM dimension in the direction perpendicular and parallel to the target respectively, centered at 14 μm from the target surface. This area defines a laser fluence of ~0.6 Jcm^{-2} for the most intense laser shots. Assuming the laser pulse duration of 2.5 ps from the simulations, the laser intensity at the

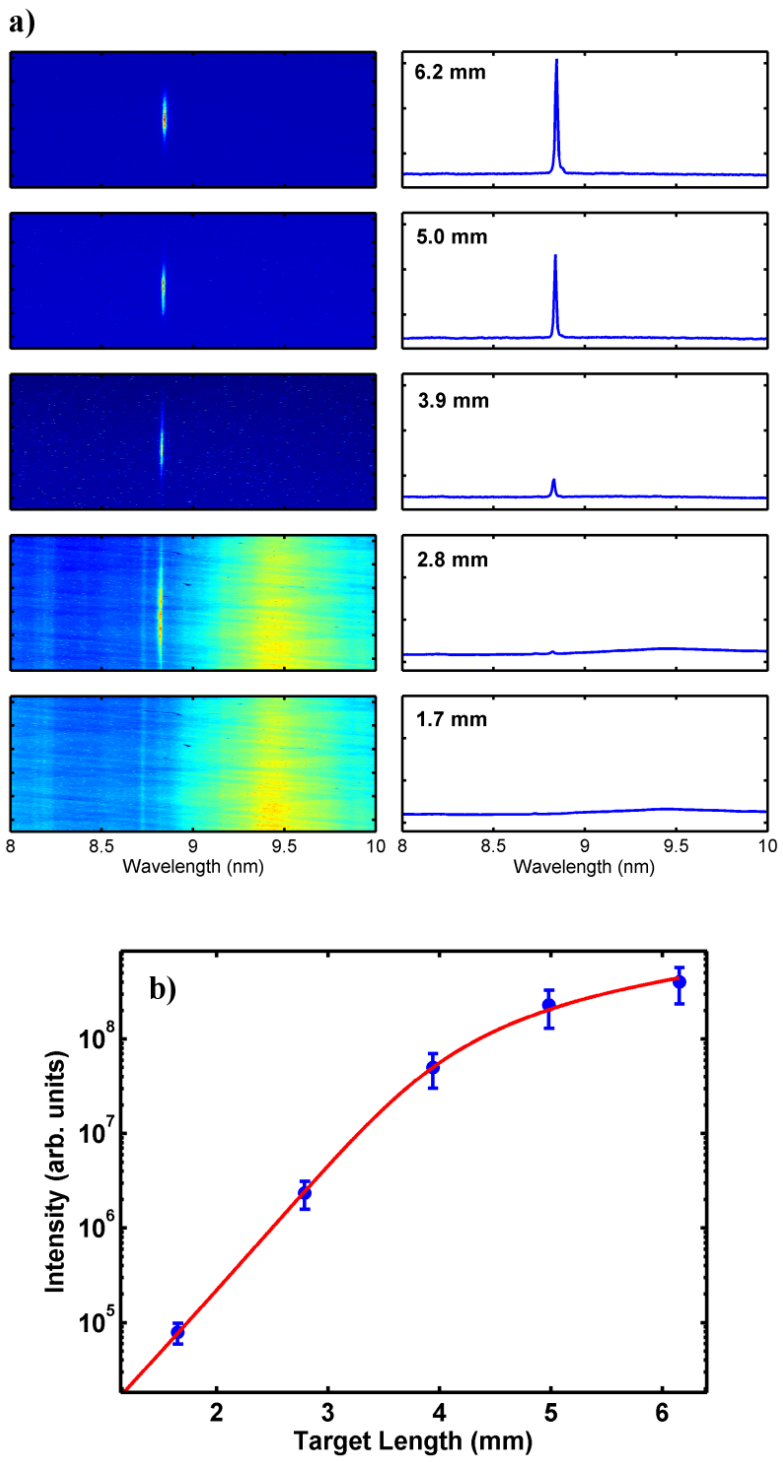

Figure 5.2: End-on spectra of a line focus lanthanum plasma column showing saturated amplification in the 8.85-nm line of Ni-like La (a). (b) Intensity of the 8.85-nm laser line as a function of plasma column length. The line is a fit of the data that yields a gain coefficient of 33-cm^{-1} and a gain-length product of 14.6.

amplifier exit is estimated to be 2.4×10^{11} Wcm^{-2}, which significantly exceeds the computed saturation intensity of $1.5\text{-}3 \times 10^{10}$ Wcm^{-2} calculated using a detailed atomic model with atomic rates from the Flexible Atomic Code [5.24]. The far field beam profile was recorded on a CCD by bending the beam with a 45° incidence angle narrow-band Mo-Y multilayer mirror that also served to filter background plasma light. Far field images acquired at 0.86-m from the amplifier exit, such as that illustrated in Fig. 5.3b, show the laser beam divergence is $(5.9 \pm 0.7) \times (4.7 \pm 0.7)$ $mrad^2$ in the directions perpendicular and parallel to the target surface respectively.

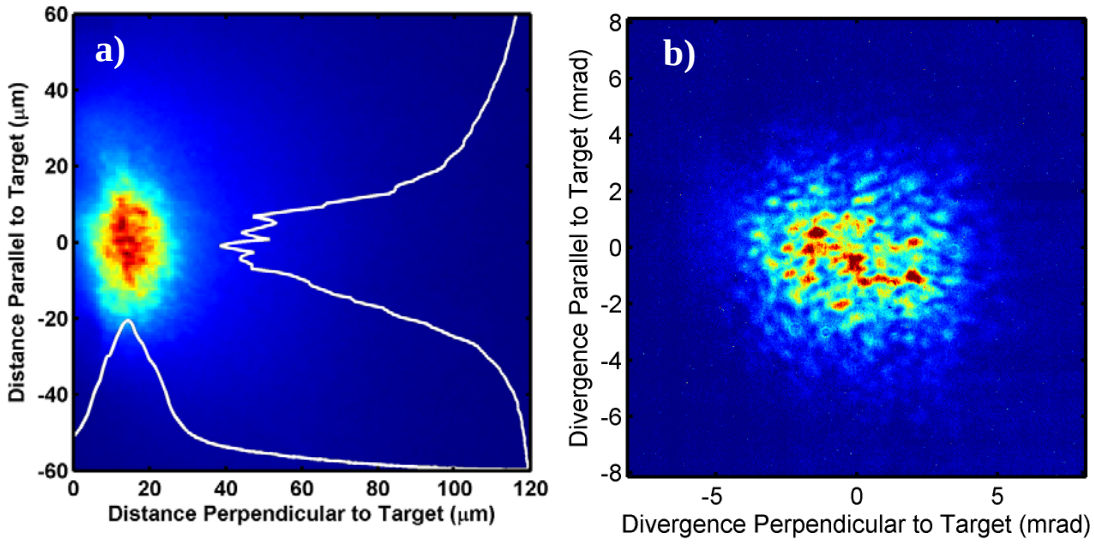

Figure 5.3: Characteristics of the λ = 8.85-nm lanthanum laser. (a) Measured near-field pattern. The center of the laser beam at the amplifier exit is at 14-μm from the target. (b) Measured far-field pattern at a distance of 0.83 m from the source.

Fig. 5.4b illustrates the λ=8.8 nm laser pulse intensity variations for 10 consecutive shots recorded at 1 Hz repetition rate moving the target 200 μm/s between shots. Fig. 5.4a shows maximum laser output is observed when the short pulse arrives to the target ~25 ps before the maximum of the 210 ps FWHM pre-pulse. This implies that more than half of the pre-pulse energy is not used in the laser excitation process. Therefore optimization of the pre-pulse should result in a further reduction of the total

pump energy required for saturated operation. The combination of these results with future advances in diode-pumped CPA pump lasers [5.25, 5.26] that have already reached 1 J energy output at 10 Hz repetition rate [5.25], promise to lead to the realization of high average power sub-9 nm lasers on a table-top (eg. 0.25 mW at 100 Hz).

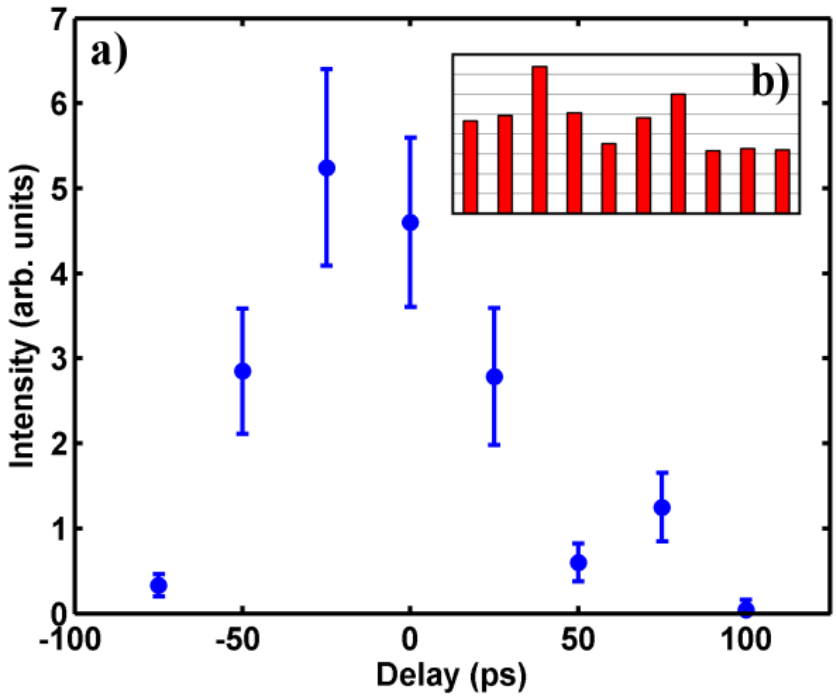

Figure 5.4: (a) Measured laser intensity as a function of delay between the peak of the pre-pulse and the short pulse. (b) Measured shot-to-shot intensity variation of the 8.85-nm laser operating at a 1-Hz repetition rate.

Another significant aspect of these amplifiers is the fact that collisional SXRL amplification at shorter wavelengths favors higher plasma densities, resulting in collisionally broaden lines that can support the amplification of sub-picosecond seed XRL pulses, a subject of current interest [5.27-5.29]. Model simulations indicate amplification at 8.85 nm occurs in a plasma region where the plasma density is 5-9x10^{20} cm^{-3} and the ion temperature ~150 eV. At the plasma conditions for peak gain the laser

line profile is defined by collisional broadening ($\Delta\nu_L$ = 1.7x10^{12} Hz) and Doppler contributions ($\Delta\nu_D$ = 2.8x10^{12} Hz) that define a Voigt linewidth of $\Delta\nu$ = 3.8x10^{12} Hz that can support the amplification of 200 fs pulses**.** The variation of the bandwidth and pulse duration of an injected high harmonic seed pulse as it propagates thought the lanthanum plasma amplifier was computed with a 3D ray-trace post processor that couples the amplification and ray propagation equations with a time and space depended atomic physics model that includes all relevant levels and stimulated emission. The ray trace code is capable of fully resolving the temporal duration and bandwidth of both the amplified stimulated emission and the amplified seed beam. Pulse broadening of a seed due to line-narrowing is included using the Fourier transform of the amplified bandwidth accounting for the group velocity delay caused by the gain profile. Fig. 5.5 shows the computed pulsewidth variation of an injected 8.85 nm, 30 fs duration high harmonic seed

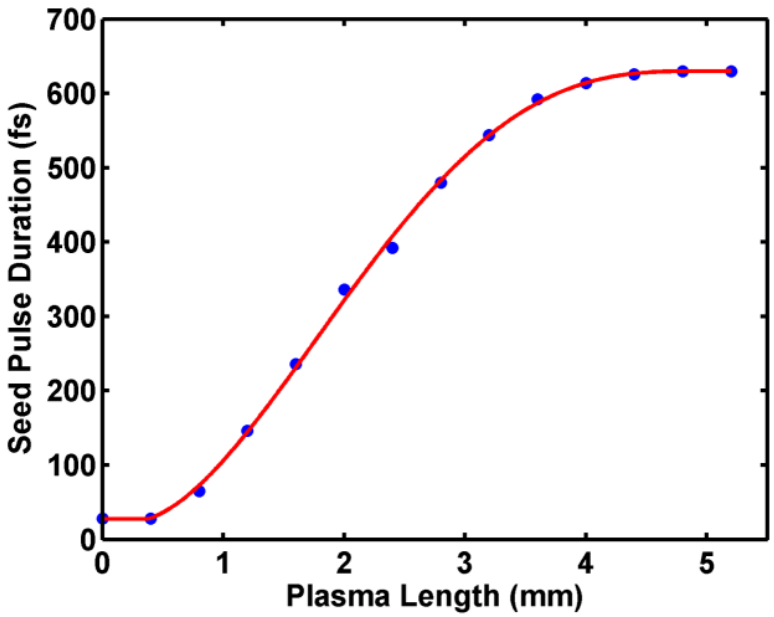

Figure 5.5: Computed variation of the pulse duration of an injected 30-fs high harmonic seed pulse as a function lanthanum plasma column length. The seed pulse duration is initially increased by linewidth narrowing and later by saturation broadening. The high harmonic seed pulse is assumed to have an energy of 0.1-nJ and the gain and plasma conditions are those resulting from the simulations described in the text.

pulse as it propagates thought the lanthanum plasma amplifier for plasma conditions that result in an ASE laser output energy similar to that obtained in the experiment. Simulations conducted for a range of different pumping parameters predict output pulse durations in the range of 500-700fs.

The demonstration of a gain-saturated table-top laser at λ = 8.85 nm with low pump energy also opens the prospect for bright high repetition rate plasma-based lasers at shorter wavelengths. In progress toward this goal we made use of isoelectronic scaling along the elements of the lanthanide series to obtain lasing in several shorter wavelength transitions. The spectra of Fig. 5.6 shows that the use of similar irradiation conditions resulted in lasing at 8.5 nm in Ni-like Ce, 8.2 nm in Ni-like Pr, and 7.9 nm in Ni-like Nd. Lasing was also observed at 7.36 nm in Ni-like Sm by reducing the main pump pulse duration to 1.1 ps. The laser emission at 8.5 nm in Ni-like Ce is very strong, with an output energy >1 μJ. From comparison with the 8.85 nm amplifier measurements the 8.5 nm laser is estimated to be operating at, or close to, gain saturation.

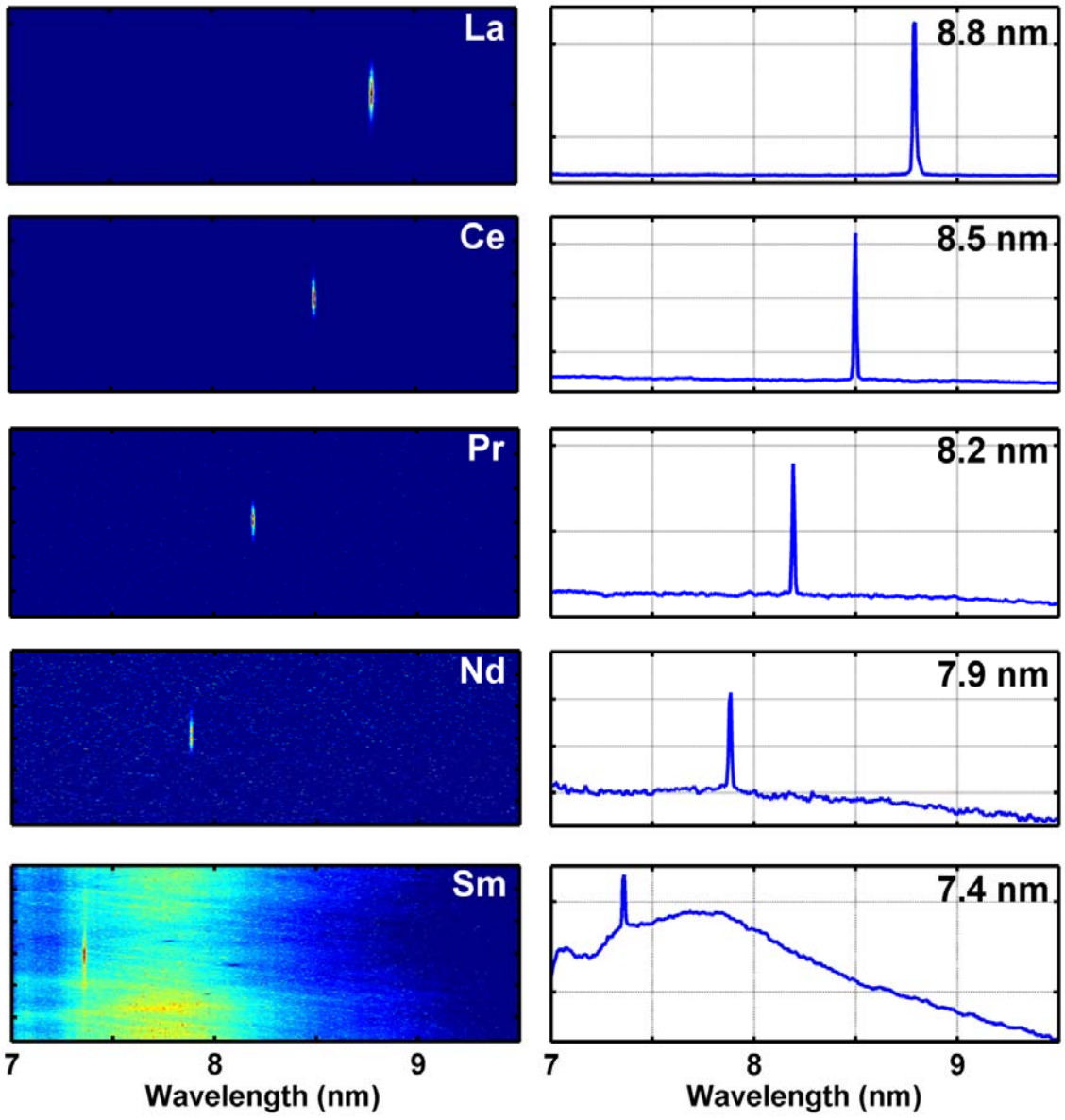

Figure 5.6: End-on spectra showing lasing at progressively shorter wavelengths in the $4d^1S_0 \rightarrow 4p^1P_1$ line of nickel-like lanthanide ions, down to 7.36-nm in nickel-like samarium

5.4) Conclusions

In summary, we have demonstrated the generation of bright gain-saturated sub-9 nm wavelengths with a table-top laser operating at 1 Hz repetition rate for the first time. Using a picosecond optical laser pump with 4 J energy we have also obtained laser amplification at wavelengths as short as 7.36 nm. The combination of these results with new advances in high repetition rate diode-pumped optical lasers promises to lead to the generation of high average power sub-10 nm wavelength laser beams on a table-top. The short wavelength, microjoule pulse energy, picosecond pulse duration, and repetitive operation of these lasers will enable new applications such as sequential imaging of ultrafast nano-scale dynamic phenomena to be realized on a table top.

5.6) References

[5.1] W. Ackermann *et al.* "Operation of a free-electron laser from the extreme ultraviolet to the water window," Nature Photonics **1**, 336-342 (2007)

[5.2] B. W. J. McNeil and N. R. Thompson, "X-ray free-electron lasers," Nature Photonics **4**, 814-821 (2010)

[5.3] R. Keenan, J. Dunn, P. K. Patel, D. F. Price, R. F. Smith, and V. N. Shlyaptsev, "High-Repetition-Rate Grazing-Incidence Pumped X-Ray Laser Operating at 18.9 nm," Phys. Rev. Lett. **94**, 103901 (2005)

[5.4] B. M. Luther, Y. Wang, M. A. Larotonda, D. Alessi, M. Berrill, M. C. Marconi, J. J. Rocca, and V. N. Shlyaptsev, "Saturated high-repetition-rate 18.9-nm tabletop laser in nickellike molybdenum," Optics Letters **30**, 165-167 (2005)

[5.5] Y. Wang, M. A. Larotonda, B. M. Luther, D. Alessi, M. Berrill, V. N. Shlyaptsev, and J. J. Rocca, "Demonstration of high-repetition-rate tabletop soft-x-ray lasers with saturated output at wavelengths down to 13.9 nm and gain down to 10.9 nm," Phys. Rev. A **72**, 053807 (2005)

[5.6] T. Mocek, C.M. McKenna, B. Cros, S. Sebban, D.J. Spence, G. Maynard, I. Bettaibi, V. Vorontsov, A.J. Gonsavles, S.M. Hooker, "Dramatic enhancement of XUV laser output using a multimode gas-filled capillary waveguide," Phys. Rev. A **71**, 013804 (2005)

[5.7] H. T. Kim, I. W. Choi, N. Hafz, J. H. Sung, T. J. Yu, K. H. Hong, T. M. Jeong, Y. C. Noh, D. K. Ko, K. A. Janulewicz, J. Tummler, P. V. Nickles, W. Sandner, and J. Lee, "Demonstration of a saturated Ni-like Ag x-ray laser pumped by a single profiled laser pulse from a 10-Hz Ti:sapphire laser system," Phys. Rev. A **77**, 023807 (2008)

[5.8] M. Nishikino, N. Hasegawa, T. Kawachi, H. Yamatani, K. Sukegawa , K. Nagashima, "Characterization of a high brilliance soft x-ray laser at 13.9 nm by use of an oscillator-amplifier configuration," Appl. Optics **47**, 1129, (2008)

[5.9] M. Grunig, C. Imesch, F. Staub, J.E. Balmer, "Saturated X-ray lasing in Ni-like Sn at 11.9 nm using the GRIP sheme," Optics Comm. **282**, 267-271 (2009)

[5.10] D. Alessi, D. H. Martz, Y. Wang, M. Berrill, B. M. Luther, and J. J. Rocca, "Gain-saturated 10.9 nm tabletop laser operating at 1 Hz repetition rate," Optics Letters **35**, 414-416 (2010)

[5.11] B.J.Mac Gowan, L.B.da Silva, D.J. Fields, C.J. Keane, J.A. Koch, R.A. London, D.J. Matthews, S. Maxon, A.L. Osterheld, J.H. Scofiled, G. Shinkaveg, J.E. Trebes,

R.S Walling, “Short Wavelenght Laser Research at Lawrence Livermore National Laboratory,” Phys. Fluids B **4**, 2326 (1992)

[5.12] H. Daido, Y.Kato, K. Murai, S.Ninomiya, R. Kodame, G.Yuan, Y. Oshikane, M.Takagi, H.Takabe and F. Koike “Efficient soft x-ray lasing at 6-8 nm in nickel-like lanthanides,” Phys.Rev. Lett. **75**, 1074 (1995)

[5.13] H. Daido, S. Ninomiya, T. Imani, R. Kodama, M. Takagi, Y. Kato, K. Murai, J. Zhang, Y. You, Y. Gu, “Nickellike soft-x-ray lasing at the wavelengths between 14 and 7.9 nm,” Optics Letters **21**, 958-960 (1996)

[5.14] J. Zhang, A. G. MacPhee, J. Lin, E. Wolfrum, R. Smith, C. Danson, M. H. Key, C. L. S. Lewis, D. Neely, J. Nilsen, G. J. Pert, G. J. Tallents, J. S. Wark, “A Saturated X-ray Laser Beam at 7 Nanometers,” Science **276**, 1097 (1997)

[5.15] Tetsuya Kawachi, Akira Sasaki, Momoko Tanaka, Maki Kishimoto, Noboru Hasegawa, Keisuke Nagashima, Masato Koike, Hiroyuki Daido, and Yoshiaki Kato, “Observation of strong soft-x-ray amplification at 8.8 nm in the transient collisional-excitation scheme,” Phys. Rev. A **69**, 033805 (2004)

[5.16] J.E. Balmer, C. Imesch, and F. Staub, 12th International Conference on X-Ray Lasers, X-Ray Lasers 2010, Guanju, Korea.

[5.17] J. J. Rocca, et. al, 12th International Conference on X-Ray Lasers, X-Ray Lasers 2010, Guanju, Korea

[5.18] D. Zimmer, D. Ros, O. Guilbaud, J. Habib, S. Kazamias, B. Zielbauer, V. Bagnoud, B. Ecker, D. C. Hochhaus, B. Aurand, P. Neumayer, and T. Kuehl, “Short-wavelength soft-x-ray laser pumped in double-pulse single-beam non-normal incidence,” Phys. Rev. A **82**, 013803 (2010)

[5.19] R. E. King, G. J. Pert, S. P. McCabe, P. A. Simms, A. G. MacPhee, C. L. S. Lewis, R. Keenan, R. M. N. O’Rourke, G. J. Tallents, S. J. Pestehe, F. Strati, D. Neely, and R. Allott, “Saturated x-ray lasers at 196 and 73 Å pumped by a picosecond traveling-wave excitation,” Phys. Rev A **64**, 053810 (2001)

[5.20] D. Martz, D. Alessi, B.M. Luther, Y. Wang, D. Kemp, M. Berrill, and J.J. Rocca, “High Energy 13.9 nm Table-top Soft X-ray Laser at 2.5 Hz Repetition Rate Excited by a Slab-pumped Ti:sapphire Laser,” Optics Letters **35**, 1632 (2010)

[5.21] J. Dunn, Y. Li, A.L. Osterheld, J. Nilsen, J. R. Hunter and V.N. Shlyaptsev, “Gain saturation regime for tabletop, Ni-like ion transient X -ray lasers,” Phys. Rev. Lett., **84** 4834 (2000)

[5.22] J. R. Crespo, et al., Proc. SPIE, Int. Soc. Opt. Eng. , 2010, 258, (1993)

[5.23] G. J. Tallents, Y. Abou-Ali, M. Edwards, R. E. King, G. J. Pert, S. J. Pestehe, F. Strati, R. Keenan, C. L. S. Lewis, S. Topping, O. Guilbaud, A. Klisnick, D. Ros, R. Clarke, D. Neely, and M. Notley, "Saturated and Short Pulse Duration X-Ray Lasers," in X-Ray Lasers 2002: 8th International Conference on X-ray Lasers, J. J. Rocca, J. Dunn, and S. Suckewer, eds., AIP Conference Proceedings Vol. **C641** (AIP, 2002), p. 291

[5.24] Ming Feng Gu, "The Flexible Atomic Code," Atomic Processes in Plasmas: 14th APS Topical Conference on Atomic Processes in Plasmas, James S. Cohen, Stephane F. Mazevet, and David P. Kilcrease, eds., AIP Conference Proceedings Vol. **730** (AIP, 2004) p. 127-136

[5.25] F. Furch, B. Reagan, B. Luther, A. Curtis, S. Meehan, and J.J. Rocca, "Demonstration of an all-diode-pumped soft x-ray laser," Optics Letters **34**, 3352 (2009)

[5.26] J. Tümmler, R. Jung, H. Stiel, P. V. Nickles, and W. Sandner, "High-repetition-rate chirped-pulse-amplification thin-disk laser system with joule-level pulse energy," Optics Letters, **34**, 1378-1380 (2009)

[5.27] P. Zeitoun, G. Faivre, S. Sebban, T. Mocek, A. Hallou, M. Fajardo, D. Aubert, Ph. Balcou, F. Burgy, D. Douillet, S. Kazamias, G. de Lachèze-Murel, T. Lefrou, S. le Pape, P. Mercère, H. Merdji, A. S. Morlens, J. P. Rousseau and C. Valentin, "A high-intensity highly coherent soft X-ray femtosecond laser seeded by a high harmonic beam," Nature **431**, 426–429 (2004)

[5.28] Y. Wang, E. Granados, F. Pedaci, D. Alessi, B. Luther, M. Berrill and J. J. Rocca, "Phase-coherent, injection-seeded, table-top soft-X-ray lasers at 18.9 nm and 13.9 nm," Nature Photonics **2**, 94-98 (2008)

[5.29] C.M. Kim, K. A. Janulewicz, H.T. Kim, J. Lee, " Amplification of a high harmonic pulse in an active medium of a plasma-based soft x-ray laser", Phys. Rev. **A**, 80, 053811, (2009)

CHAPTER 6

SUMMARY

The work in this dissertation has resulted in significant progress towards high average power and high pulse energy table-top soft X-ray lasers at sub-11 nm wavelengths as well as an increase in the diversity of soft X-ray laser wavelengths available utilizing transitions near 30 nm. Applying the grazing incidence pumping geometry to neon-like plasmas resulted in the demonstration of microwatt average power laser-pumped neon-like ion lasers. This occurred in transitions near 30 nm in titanium with lasing also demonstrated in vanadium and chromium. Gain-saturated table-top soft x-ray lasers were also extended down to 10.9 nm by transient excitation of nickel-like ions in a tellurium plasma, producing an average power of ~1 μW and pulse energies of up to 2 μJ. The first demonstration of bright gain-saturated sub-9-nm wavelengths with a table-top laser operating at 1-Hz repetition rate was also realized. Operation of the 8.8 nm transisiton in nickel-like lanthanum resulted in a maximum energy per pulse of 2.7 μJ. Using this picosecond optical laser pump with unprecedentedly low laser energy resulted in amplification at wavelengths as short as 7.36-nm. These advancements in SXR lasers were made possible due to the development of a high energy Nd:glass slab laser for pumping a Ti:Sapphire laser. With this upgrade, the Ti:sapphire laser produces 12 J uncompressed laser pulses at 1 Hz. This short wavelength, microjoule pulse energy,

picosecond pulse duration, and repetitive operation of these lasers will enable new applications such as sequential imaging of ultrafast nano-scale dynamic phenomena to be realized on a table top.

APPENDIX 1

RELATED WORK

Previous chapters discuss the development of a Ti:Sapphire laser system as well as gain-saturated table-top repetitive soft X-ray (SXR) lasers with wavelengths near 30 nm and 9-11 nm with lasing down to 7.4 nm. The work done in this thesis contributed to the development and characterization of gain-saturated table-top repetitive SXR lasers with wavelengths from 13 to 19 nm, improved SXR beam properties by injection seeding with high harmonic generated (HHG) pulses, and imaging applications. All these results are discussed in the following publications:

1) Development and characterization of repetitive SXR lasers from 11 nm to 19 nm

- M.A. Larotonda, B.M. Luther, Y. Wang, Y. Liu, D. Alessi, M. Berrill, A. Dummer, F. Brizuela, C.S. Menoni, M.C. Marconi, V.N. Shlyaptsev, J. Dunn, and J.J. Rocca, *"Characteristics of a Saturated 18.9-nm Tabletop Laser Operating at 5-Hz Repetition Rate,"* IEEE Journal of selected topics in Quantum Electronics **10**, 1363 (2004)
- B.M. Luther, Y. Wang, M.A. Larotonda, D. Alessi, M. Berrill, M.C. Marconi, J.J. Rocca, and V.N. Shlyaptsev, *"Saturated high-repetition-rate 18.9-nm tabletop laser in nickellike molybdenum,"* Optics Letters **30**, 165 (2005)

- B.M. Luther, Y. Wang, M. Berrill, D. Alessi, M.C. Marconi, M.A. Larotonda, and J.J. Rocca, "*Highly Ionized Ar Plasma Waveguides Generated by a Fast Capillary Discharge,"* IEEE Transactions on Plasma Science **33**, 582 (2005)
- Y. Wang, M.A. Larotonda, B.M. Luther, D. Alessi, M. Berrill, V.N. Shlyaptsev, and J.J. Rocca, "*Demonstration of high-repetition-rate tabletop soft-x-ray lasers with saturated output at wavelengths down to 13.9 nm and gain down to 10.9 nm,"* Physical Review A **72**, 053807 (2005)
- J.J. Rocca, Y. Wang, M.A. Larotonda, B.M. Luther, M. Berrill, and D. Alessi, *"Saturated 13.2 nm high-repetition-rate laser in nickellike cadmium,"* Optics Letters **30**, 2581 (2005)
- B.M. Luther, Y. Wang, M.A. Larotonda, D. Alessi, M. Berrill, J.J. Rocca, J. Dunn, R. Keenan, and V.N. Shlyaptsev, *"High Repetition Rate Collisional Soft X-Ray Lasers Based on Grazing Incidence Pumping,"* IEEE Journal of Quantum Electronics **42**, 4 (2006)
- A. Weith, M.A. Larotonda, Y. Wang, B.M. Luther, D. Alessi, M.C. Marconi, J.J. Rocca, and J. Dunn, *"Continuous high repetition rate operation of collisional soft x-ray lasers using solid targets,"* Optics Letters **31**, 1994 (2006)
- D. H. Martz, D. Alessi, B. M. Luther, Y. Wang, D. Kemp, M. Berrill and J. J. Rocca, *"High Energy 13.9 nm Table-top Soft X-ray Laser at 2.5 Hz Repetition Rate Excited by a Slab-pumped Ti:sapphire Laser,"* Optics Letters **35**, 1632 (2010)

2) Demonstration and characterization of injection-seeded SXR lasers at 13 nm and 19 nm

- Y. Wang, E. Granados, F. Pedaci, D. Alessi, B. Luther, M. Berrill, and J.J. Rocca, *"Phase-coherent, injection-seeded, table-top soft-x-ray lasers at 18.9 nm and 13.9 nm,"* Nature Photonics **2**, 94 (2008)
- M. Berrill, D. Alessi, Y. Wang, S. R. Domingue, D. H. Martz, B. M. Luther, Y. Liu and J. J. Rocca, *"Improved beam characteristics of solid-target soft x-ray laser amplifiers by injection-seeding with high harmonics,"* Optics Letters **35**, 2317 (2010)
- L. M. Meng, D. Alessi, O. Guilbaud, Y. Wang, M. Berrill, B. M. Luther, S. R. Domingue, D. H. Martz, D. Joyeux, S. De Rossi, J.J. Rocca, and A. Klisnick, *"Temporal coherence and spectral linewidth of an injection-seeded transient collisional soft x-ray laser,"* Optics Express **19**, 12087 (2011)

3) Table-top nano-scale microscopy with a 13.2 nm SXR laser

- F. Brizuela, S. Carbajo, A. Sakdinawat, D. Alessi, D. Martz, Y. Wang, B. Luther, K. A. Goldberg, I. Mochi, D. T. Attwood, B. La Fontaine, J. J. Rocca, and C. S. Menoni, *"Extreme Ultraviolet Laser-based Table-Top Aerial Image Metrology of Lithographic Masks,"* Optics Express **18**, 14467 (2010)

4) Development of dielectric gratings for a Ti:sapphire laser system compressor

- D. H. Martz, H. T. Nguyen, D. Patel, J. A. Britten, D. Alessi, E. Krous, Y. Wang, M. A. Larotonda, J. George, B. Knollenberg, B. M. Luther, J. J. Rocca and C. S.

Menoni, *"Large area high efficiency broad bandwidth 800 nm dielectric gratings for high energy laser pulse compression."* Optics Express **17**, 23809-23816 (2009)